

FINITE ELEMENT ANALYSIS OF
LARGE STRAINS IN SOILS

by

RODRIGO MOLINA FERNANDEZ

Ingeniero de Caminos, Canales y Puertos
Escuela Tecnica Superior de I.C.C.P. Madrid
(1970)

Submitted in partial fulfillment
of the requirements for the degree of

Master of Science

at the

Massachusetts Institute of Technology

(September 1971)

Signature of Author
Department of Civil Engineering, (August 30, 1971)

Certified by
Thesis Supervisor

Accepted by
Chairman, Departmental Committee on Graduate Students

Archives

1



ABSTRACT

FINITE ELEMENT ANALYSIS OF
LARGE STRAINS IN SOILS

by

RODRIGO MOLINA FERNANDEZ

Submitted to the Department of Civil Engineering on August 30, 1971, in partial fulfillment of the requirements for the degree of Master of Science in Civil Engineering.

Some problems of behavior of soils under given boundary conditions involve large deformations and strains, but finite element analyses of soil problems have traditionally considered only infinitesimal strain analysis.

Suitable large strain formulations in cartesian coordinates for an incremental procedure are studied. One of the formulations is based on the general tensorial formulation when applied to cartesian coordinates. The fact that the constitutive equations are not easy to obtain for soils makes this formulation impractical. A second formulation is based in Biot's incremental deformation formulation, and, because physics and geometry are separated, the constitutive equations can be easily found.

Two types of constitutive laws are used. One is the perfectly plastic formulation for a Tresca Material, the other one is obtained from a hyperbolic approximation of the experimental stress-strain curve for the given soil. An interpolation procedure is used to obtain the constitutive equations of an anisotropic material from active and passive tests.

Finite Element programs are developed, one for each constitutive equation, for the solution of plane strain problems. An incremental procedure with a mid-point integration scheme is used.

Results from test runs are inconclusive. Good results are obtained in simple problems, and some improvement over an "infinitesimal strain" approach is observed in one case. Some major problems are encountered, however, especially lack of equilibrium between stresses and nodal forces, instability of the solution after

failure, impossibility of using unloading procedures, and deviation from the correct solution, especially after failure.

The lack of equilibrium between stresses and forces can be traced to the midpoint integration procedure and a post yielding modification of stresses to keep them in the yield surface. The other problems are thought to be mainly caused by the imperfect constitutive equations.

Thesis Supervisor:
Title:

John T. Christian
Associate Professor
of Civil Engineering

ACKNOWLEDGMENTS

The author is especially indebted to Professor John T. Christian, his faculty adviser and thesis supervisor, without whose direction, encouragement and dedication this thesis would not have been done.

Special thanks are due to Professor Charles C. Ladd, Professor J.J. Connor, Dr. Alfred J. Hagmann, Miss Deborah Walther and Mr. W. Allan Marr for helpful discussions.

Miss Margaret Clark and Miss Sharon Niles typed the manuscript. Mrs. Lelia Passos drafted the figures. Their skilled efforts are very much appreciated.

The thesis research was a part of a research program sponsored by the National Aeronautics and Space Administration.

CONTENTS

	Page
TITLE PAGE	1
ABSTRACT	2
ACKNOWLEDGMENTS	4
TABLE OF CONTENTS	5
LIST OF TABLES	8
LIST OF FIGURES	9
CHAPTER 1 INTRODUCTION	11
CHAPTER 2 THE LARGE STRAIN FORMULATION	16
2.1 Introduction and Background	16
2.2 Tensorial Formulation	17
2.2.1 Large Strains	17
2.2.2 Stresses	19
2.2.3 Equilibrium	21
2.2.4 Incremental Procedure	23
2.2.5 Constitutive Relations	25
2.2.6 Stress Transformation	26
2.3 Felippa's Formulation (1966)	27
2.4 Biot's Formulation	29
CHAPTER 3 CONSTITUTIVE EQUATIONS	38
3.1 Introduction	38
3.2 Soil as an Elasto-Plastic Material	38
3.3 Pseudo Plastic Stress-Strain Laws	40
3.4 Elastic Perfectly Plastic Tresca Material	41
3.5 Hyperbolic Stress-Strain Relation	43

3.5.1	Hyperbolic Approximation	43
3.5.2	σ_3 Dependency	45
3.5.3	Tangent Modulus	46
3.5.4	Unloading Stress-Strain Law	48
3.5.5	Post Yielding Behavior	49
3.5.6	Election of Elastic Parameters	49
3.5.7	Anisotropy	50
3.5.8	Experimental Determination of Parameters	52
3.5.9	Plotting of Anisotropically Consolidated Test Results	57
3.5.10	Formulation	58
CHAPTER 4	FINITE ELEMENT PROGRAMS	64
4.1	Finite Element Analysis	64
4.1.1	Introduction to the Displacement Method	65
4.1.2	Element	66
4.1.3	Stiffness Matrix	68
4.2	Incremental Procedure	70
4.3	Post Yielding Stress	72
4.4	Computer Programs	74
CHAPTER 5	TEST RUNS	75
5.1	Compression Test	75
5.2	Side Wall	77
5.3	Footing on Layer of Undrained Clay	80
5.4	Simple Shear	83
5.5	Model Footing	85
CHAPTER 6	SUMMARY, CONCLUSIONS AND RECOMMENDATIONS	103
REFERENCES		109

APPENDIX A	LIST OF SYMBOLS AND NOTATIONS	113
APPENDIX B	BIOT'S FORMULATION	123
	B.1 Strains	123
	B.2 Incremental Stresses	128
	B.3 Constitutive Equations	133
	B.4 Equilibrium	134
APPENDIX C	DERIVATION OF THE STIFFNESS MATRIX	141
APPENDIX D	ADJUSTMENT OF STRESSES TO YIELD SURFACE	149
APPENDIX E	USER'S MANUAL	153
APPENDIX F	PROGRAM DESCRIPTION, MAIN AND SUBROUTINES	170
APPENDIX G	THE UNIT SQUARE	179

TABLES

Table		Page
5.1	Results of the Unit Cube Runs	101
5.2	Stress-Strain Parameters	102
E.1	User's Manual Table	169

FIGURES

Figure		Page
2.1	Positive Sign Convention in Two Dimensions	36
2.2	Force Vector in the Definition of Lagrange and Kirchhoff	37
3.1	Elastic and Plastic Material	59
3.2	Hyperbolic Stress-Strain Curve	60
3.3	Transformed Hyperbolic Stress-Strain Curve	61
3.4	Variation of Initial Tangent Modulus with σ_3	61
3.5	Mohr-Coulombe Failure Criterion	62
3.6	Dense Sands and Overconsolidated Clays	62
3.7	Anisotropic Undrained Tests in N.C. Clay	63
3.8	Equivalent Hyperbolic Approximation	63
5.1	Side Wall Active, Stress Distribution at Failure, $S_u = 1.75 T/m^2$	88
5.2	Side Wall Active, From K_0 to K_a	88
5.3	Side Wall Active, Smooth Bottom, Stress Distribution in the Wall when all Elements are in Failure $S_u = 2.6 T/m^2$	89
5.4	Standard Mesh for Footing on Layer	90
5.5	Element Type Influence	91
5.6	Mesh and Increment Influence	92

5.7	Integration Procedure Influence	93
5.8	Simple Shear	94
5.9	Simple Shear, Normal Stress Distribution in the Upper Face of the Sample at Ten Percent Strain	95
5.10	Simple Shear Yielded Zones	96
5.11	Simple Shear, Stress-Strain Curves for Boston Blue Clay	97
5.12	Stress-Strain Parameters for Boston Blue Clay	98
5.13	Model Footing, Settlement Curves	99
5.14	Model Footing on Clay, First Part of Settlement Curves	100
B.1	Pure Strain	137
B.2	Load Translation, Rotation and Pure Strain	138
B.3	Representation of the Initial Stresses S_{xx} , S_{yy} , S_{xy} and the Final Stresses with respect to the two Sets of Axes	139
B.4	Components of Force in an Infinitesimal Element	140
C.1	Natural Triangular Coordinates	148
D.1	Adjustment of Stresses	152

Chapter 1

INTRODUCTION

The object of the research is to develop analytical techniques for the prediction of displacement and stress fields on soils submitted to forces, such that an appreciable change in geometry is obtained during loading. The physical properties of the material have to be readily obtainable from standard testing techniques, and the constitutive equations must be simple enough to be formulated mathematically.

The influence of the changes in geometry may be important in the analysis of stress distribution and deformation of test specimens, in the analysis of field testing devices, and in post-failure behavior of foundations.

The work is divided into three phases:

- 1) Formulation of the problem.
- 2) Development of appropriate numerical techniques to solve the differential field equations, namely finite element computer programs.
- 3) Testing of the programs.

Two types of non-linearity are involved in the formulation of a large displacement problem in soils:

- a) Non linear constitutive relations. This is a physical non-linearity that is indeed a property of all soils even at very low values of strain. Because of the

complicated particulate structure of soils and the influence of physical and chemical interaction between particles, constitutive laws are not only non-linear but extremely variable from soil to soil and even dependent on location in the soil layers. The formulation of a mathematical model, simple enough to be operational becomes an enormous task. Scores of such models have been suggested and used. All of them obtain the parameters from the results of standard tests, mainly triaxial cell tests and plane strain tests. The results of these tests have been traditionally given as stress-strain curves where the values of strain are obtained from the displacements, dividing the total displacement by the original height, and the values of the stresses are corrected to take into account the change in cross-sectional area, so the actual stress at each moment is obtained. It will be seen below how this definition of the constitutive law affects the formulation of the problem.

b) Geometric non-linearity: This is caused by the change in geometry throughout the problem.

The effect of geometric non-linearity appears in many different problems, sometimes under different labels. It is, for example, the basis of buckling and stability analysis and the cause of increased torsional stiffness of prismatic bars under high tractions.

There are two main approaches to the formulation of problems involving non-linearity:

- a) A general approach by the use of a tensorial formulation.
- b) A problem-oriented approach using geometric concepts and "physical" properties of the material.

The first one is in a sense more comprehensive and very beautiful, the second is, however, more practical, easier to understand, and immediately applicable to real problems. The tensorial formulation does not have a direct physical representation and has been often misinterpreted and misused.

In both of them, the geometric non-linearity appears at two levels:

- a) A non-linear relation between strain and actual displacements.
- b) The equilibrium and boundary conditions have to be satisfied in the deformed position.

The geometric non-linearity and the material non-linearity will be the object of Chapters 2 and 3, respectively.

Two methods of analysis have been used to solve the non-linear problems:

- a) Direct iteration, in which the final state is determined by the iterative solution of the system of non-linear equations.

- b) Incremental analysis, in which the final state is reached after a certain number of "linearized" steps.

Both procedures can be used when dealing with small strains and conservative constitutive laws, because the final result is not path dependent. Even in the case of small displacements and non-conservative constitutive laws the iterative procedure can be used if an equivalent conservative constitutive law is found. But in the case of a large strain non-conservative material problem the final result is totally path dependent and an incremental procedure has to be used. This is, of course, the case for large strain in soils. This incremental procedure, although more time-consuming, gives information about every step, and both load-deformation relations and a general history of the loading or unloading is obtained.

Finally the problem is reduced to the solution of a differential field equation. In this case that will be the Euler equation of the functional that gives the total potential energy, which has to be minimized to obtain equilibrium in each step. Actually what is normally done is to equate the first variation of the total strain energy to zero which is an equivalent equation (Elsgolc, 1961). This makes it possible to solve a problem in which the strain energy function is not defined, using the principle

of virtual work.

The finite element method was chosen to solve this equation because of its versatility and flexibility. A superficial description of the several methods and a more thorough description of the particular portions that deal with the large displacement parts and the integration procedure are contained in Chapter 4.

Chapter 5 is dedicated to the study of the results of the testing of the method; and Chapter 6 to conclusions and recommendations.

Appendices, including the development of the formulation and the documentation of the computer programs, are provided.

Chapter 2

THE LARGE STRAIN FORMULATION

2.1 INTRODUCTION AND BACKGROUND

A large strain formulation for an incremental procedure with a finite element method is the object of this chapter. A general tensorial formulation and an "incremental deformation" formulation will be discussed.

In the literature there are several examples of finite element programs to handle large displacements or large strains, see Martin (1965). Most of the work has been done for plates, shells, and columns, and for stability analysis. In general, the formulations are very specialized, are made to meet the problem at hand, are often too complicated, and are many times restricted to large rotations and small deformation of the elements.

An attempt to formulate the problem in a general tensorial form was made in 1966 by Felippa. Felippa's formulation for the incremental solution was the first formulation used in this work, but the investigation of the lack of equilibrium in some of the simple tests led to the conclusion that some of the assumptions made by Felippa were wrong.

2.2 TENSORIAL FORMULATION *

2.2.1 Large Strains

It is very important to define correctly the meaning of strain when dealing with finite elasticity. In general, strain is a measure of unitary deformation, but there are various ways of expressing this deformation. A simple example will show this very clearly. In a traction test, the ratio of the final length of the sample l to the initial length l_0 is:

$$\Delta = \frac{l}{l_0} \quad (2-1)$$

Strain can be defined as

$$\text{a) } \frac{l - l_0}{l_0} = (\Delta - 1) \quad \text{Cauchy} \quad (2-2)$$

$$\text{b) } \frac{l - l_0}{l} = \left(1 - \frac{1}{\Delta}\right) \quad \text{Swainger} \quad (2-3)$$

$$\text{c) } \frac{1}{2} \left(\frac{l}{l_0} \frac{l}{l_0} - 1 \right) = \frac{1}{2} (\Delta^2 - 1) \quad \text{Green} \quad (2-4)$$

$$\text{d) } \frac{1}{2} \left(1 - \frac{l_0}{l} \frac{l_0}{l} \right) = \frac{1}{2} \left(1 - \frac{1}{\Delta^2} \right) \quad \text{Almansi} \quad (2-5)$$

$$\text{e) } \int_{l_0}^l \frac{dL}{L} = \ln L \Big|_{l_0}^l = \ln \frac{l}{l_0} = \ln \Delta \quad \text{Hencky} \quad (2-6)$$

where L is the instantaneous length.

* The continuum mechanics sign convention is used in this work except where otherwise specified.

If the rod length doubles, $\Delta = 2$, the values of the strains are:

$$\begin{aligned} \text{a) } &= 100\% & \text{b) } &= 50\% & \text{c) } &= 150\% \\ \text{d) } &= 37.5\% & \text{e) } &= 66\% \end{aligned}$$

There is an infinite number of possible strains; a general equation is given by Karni and Reiner (1962). Only the Cauchy, Green, and Almansi strain tensors are of interest here.

The Cauchy strain tensor is

$$\epsilon_{ij} = \frac{1}{2} \left(\frac{\partial u_i}{\partial a_j} + \frac{\partial u_j}{\partial a_i} \right) \quad (2-7)$$

The Green strain tensor is: *

$$E_{ij} = \frac{1}{2} \left(\frac{\partial u_i}{\partial a_j} + \frac{\partial u_j}{\partial a_i} + \frac{\partial u_k}{\partial a_i} \frac{\partial u_k}{\partial a_j} \right) \quad (2-8)$$

The Almansi strain tensor is:

$$e_{ij} = \frac{1}{2} \left(\frac{\partial u_i}{\partial x_j} + \frac{\partial u_j}{\partial x_i} - \frac{\partial u_k}{\partial x_i} \frac{\partial u_k}{\partial x_j} \right) \quad (2-9)$$

where u_i is the displacement field, a_i are the coordinates of the points of the undeformed body, and x_i and the coordinates of the points of the deformed body, everything referred to the same Cartesian frame.

The Cauchy strain tensor gives the well known expressions for the infinitesimal strain.

* The Einstein summation convention is used except where specifically suppressed.

Both Green and Almansi tensors are obtained by expressing the change in the square of the length of a segment. The Green tensor is obtained when it is expressed as a function of the undeformed geometry, and the Almansi tensor when it is expressed as a function of the deformed geometry. The derivations can be found in general, well known texts. (Fung, 1965; Green and Zerna, 1954; Prager, 1961).

2.2.2 Stresses

The concept of stress is unique as opposed to the concept of strain. Rigorously, it has to be defined as a tensorial field such that its contraction with the normal vector of a differential area gives the actual force acting in such area. This definition, however, should not obscure the simple, well known interpretation. This tensor, named after Euler, will be expressed as σ_{ij} .

There are many other tensors defined to give some required forces on some given differential areas. They are called stress tensors by extension, but the forces that they give in an area are not the real ones acting there. These tensors are defined for convenience in developing a theory.

Two of these additional stress tensors are very useful for the basic finite elasticity theory. The Eulerian stress tensor (σ_{ij}) is defined in the actual geometry, that is, in the deformed geometry. But the deformed geometry is not known "a priori", and it is convenient to relate

everything to the undeformed geometry. It is possible to define a tensor such that it will give a differential force corresponding to a differential area in the undeformed position that will be equal to the actual differential force acting in the deformed differential area. This is called the Lagrangian stress tensor.

Figure 2.2 shows the situation for a two dimensional case.

$$dT_{0i}^{(L)} = dT_i \quad (2-10)$$

where T_i and T_{0i} are components of force in the deformed and the undeformed geometry, respectively, and (L) stands for Lagrangian.

If v_{0j} and v_j are the unitarian normal vectors to the differential surface, before and after deformation, respectively, and dS_0 , dS are the corresponding areas of the differential surface, then:

$$dT_i = \sigma_{ji} v_j dS \quad (2-11)$$

by definition of σ_{ji} ,

$$dT_{0i}^{(L)} = T_{ji} v_j dS_0 = dT_i \quad (2-12)$$

T_{ji} is the Lagrangian stress tensor and it is defined by this equation (2-12).

The relation between both tensors (Fung, 1965), is:

$$T_{ji} = \frac{\rho_0}{\rho} \frac{\partial a_j}{\partial x_m} \sigma_{mi} \quad (2-13)$$

where ρ_0 and ρ are the densities before and after deformation.

Although σ_{mi} is symmetric, T_{ji} is not, as the Equation (2-13) shows. Because of lack of symmetry, this is very inconvenient to use in formulating constitutive relations. A different tensor is then defined such that it will give on a differential area before deformation a differential force dT_{0i} , such that:

$$dT_{0i}^{(K)} = \frac{\partial a_i}{\partial x_j} dT_j \quad (2-14)$$

where dT_j is the actual force in the differential area after deformation. (K) stands for Kirchhoff, after whom this tensor is named.

The relation between Kirchhoff's tensor s_{ij} and σ_{ij} (the actual value of stress in deformed position [Eulerian]) is (Fung, 1965):

$$s_{ji} = \frac{\rho_0}{\rho} \frac{\partial a_i}{\partial x_\alpha} \frac{\partial a_j}{\partial x_\beta} \sigma_{\beta\alpha} \quad (2-15)$$

and this is a symmetric tensor.

It is important to realize that the only way to know what these tensors represent is through the definition.

2.2.3 Equilibrium

Equilibrium has to be established in the deformed

position, but equivalent expressions for equilibrium can be found in the undeformed position as a function of T_{ij} or S_{ij} (Fung, 1965),

$$\text{Eulerian} \quad \rho F_i + \frac{\partial \sigma_{ji}}{\partial x_j} = 0 \quad , \quad \sigma_{ji} v_j = T_i \quad (2-16)$$

$$\text{Lagrangian} \quad \rho_0 F_{0i} + \frac{\partial T_{ji}}{\partial a_j} = 0 \quad , \quad T_{ji} v_{0j} = T_{0i}^* \quad (2-17)$$

$$\text{Kirchhoff} \quad \rho_0 F_{0i} + \frac{\partial}{\partial a_j} (S_{ik} \frac{\partial x_i}{\partial a_k}) = 0, \quad (2-18)$$

$$S_{jl} \frac{\partial x_i}{\partial a_l} v_{0j} = T_{0i}^*$$

where $F_{0i} = F_i$ are the body forces per unit mass, T_i are the surface tractions referred to the deformed area, and T_{0i}^* are the surface tractions referred to the undeformed area, but keeping the direction they have in the deformed position.

Equivalent virtual work equations can be derived for the three tensors (Fung, 1965). (*)

Virtual work for the Eulerian and Lagrangian stress tensors is, respectively:

$$\int_V \sigma_{ji} \frac{\partial \delta u_i}{\partial x_j} dV - \int_V \rho F_i \delta u_i dV - \int_S T_i \delta u_i dS \quad (2-19)$$

$$\int_{V_0} T_{ji} \frac{\partial \delta u_i}{\partial a_j} dV_0 - \int_{V_0} \rho_0 F_{0i} \delta u_i dV_0 - \int_{S_0} T_{0i}^* \delta u_i dS_0 \quad (2-20)$$

For the Kirchhoff stress tensor:

* The derivation by Fung is based in the strain energy function, but it is valid for virtual work.

$$\int_{V_0} S_{ji} \delta E_{ji} dV_0 - \int_{V_0} \rho_0 F_{0i} \delta u_i dV_0 - \int_{S_0} T_{0i}^* \delta u_i dS_0 \quad (2-21)$$

where

$$\delta E_{ji} = \frac{\partial E_{ji}}{\partial \left(\frac{\partial u_k}{\partial a_\ell} \right)} \frac{\partial \delta u_k}{\partial a_\ell} \quad (2-22)$$

Virtual work must be 0, then equilibrium is obtained.

2.2.4 Incremental Procedure

For an initial state where strains are 0 and stresses have some finite value, there is a stress tensor, of Eulerian type, that is not identical to 0. Such a tensor will be called σ_{0ij} . A corresponding set of surface tractions will also exist T_{0i}^v such that:

$$\sigma_{0ij}^v v_{0i} = T_{0i}^v \quad (2-23)$$

For these to be in equilibrium:

$$0 = \int_{V_0} \sigma_{0ji} \frac{\partial \delta u_i}{\partial a_j} dV_0 - \int_{V_0} \rho_0 F_{0i} \delta u_i dV_0 - \int_{S_0} T_{0i}^v \delta u_i dS_0 \quad (2-24)$$

If a set of surface tractions is now applied to the body such that the total surface traction in the deformed position is T^v , the corresponding Eulerian stress tensor will be σ_{ij} , and T_i^v and S_{ij} will be the Lagrangian

and Kirchhoff tensors.

Equilibrium conditions in the undeformed position will be the Equations (2-20) and (2-21) for the Lagrangian and Kirchhoff tensors respectively.

If:

- a) the body forces remain constant,
- b) the surface tractions are conservative, that is they keep a constant direction; then:

$$\int_V dT_{0i}^* dS_0 = \int_V dT_i dS \quad (2-25)$$

- c) and ΔS_{ij} and ΔT_{ij} are defined as:

$$\Delta S_{ij} = S_{ij} - \sigma_{0ij} \quad (2-26)$$

$$\Delta T_{ij} = T_{ij} - \sigma_{0ij} \quad (2-27)$$

then, from Equations (2-20) and (2-24):

$$\int_{V_0} \Delta T_{ji} \frac{\partial \delta u_i}{\partial a_j} dV_0 - \int_{S_0} [T_{0i}^* - T_{0i}] \delta u_i dS_0 = 0 \quad (2-28)$$

which can be expressed as:

$$\int_{V_0} \Delta T_{ji} \frac{\partial \delta u_i}{\partial a_j} dV_0 - \int_{S_0} \Delta T_{0i} \delta u_i dS_0 = 0 \quad (2-29)$$

where

$$\Delta T_{0i} = T_{0i}^* - T_{0i} \quad (2-30)$$

this value, because the surface tractions are conservative, is the real value of the increment of surface tractions

referred to the undeformed position.

In a similar way, realizing that (Fung, 1965)

$$\delta E_{ji} = \frac{1}{2} \left(\delta_{jk} \delta_{il} + \delta_{ik} \delta_{jl} + \frac{\partial u_k}{\partial a_i} \delta_{jl} + \frac{\partial u_l}{\partial a_j} \delta_{ik} \right) \frac{\partial \delta u_k}{\partial a_l} \quad (2-31)$$

and that $\sigma_{0ij} = \sigma_{0ji}$ and $S_{ij} = S_{ji}$

$$\int_{V_0} \left(\sigma_{0ji} \frac{1}{2} \left(\frac{\partial u_k}{\partial a_i} \delta_{jl} + \frac{\partial u_l}{\partial a_j} \delta_{ik} \right) \frac{\partial \delta u_k}{\partial a_l} + \Delta S_{ji} \delta E_{ji} \right) dV_0 - \int_{S_0} \Delta T_{0i} \delta u_i dS_0 \quad (2-32)$$

where

$$\begin{aligned} \delta_{ij} &= 1 && \text{if } i = j \\ &= 0 && \text{if } i \neq j \end{aligned} \quad (\text{Kronecker delta})$$

2.2.5 Constitutive Relations

To be able to solve the problem, the relations between ΔT_{ij} and $\frac{\partial \delta u_k}{\partial a_l}$ and between ΔS_{ij} and $\frac{\partial \delta u_k}{\partial a_l}$ have to be known.

Because Equations (2-29) and (2-32) describe the same phenomenon, the constitutive relations have to provide for the differences, mainly the fact that in (2-29), the geometric influence of σ_{0ij} is not explicit as it is in (2-32); therefore, the relation between ΔT_{ij} and $\frac{\partial \delta u_k}{\partial a_l}$ will depend on σ_{0ij} , not only physically, but also geometrically. At the same time, ΔT_{ij} is not symmetric, which makes the constitutive relations more complicated.

The relation between ΔS_{ij} and $\frac{\partial \delta u_k}{\partial a_l}$ presents some problems, mainly because ΔS_{ij} does not have any physical meaning. This is made clearer by realizing that the Kirchhoff stress tensor (S_{ij}) represents also the actual state of stress referred to the undeformed geometry and to the convected frame. A convected frame is defined in such a way that the covariant coordinates of a point with respect to this convected frame remain constant throughout the deformation (Green and Zerna, 1956). This definition involves the use of curvilinear coordinates, even if the original frame is cartesian, and can not be expressed as a rotation of the original frame only. Because σ_{0ij} and S^{ij} (it is a contravariant tensor) are referred to different frames, ΔS_{ij} does not have any physical meaning and it is not certain that a constitutive relation for ΔS_{ij} would depend physically on σ_{0ij} only.

It is difficult in any case to find the constitutive laws from the simple tests that are the only meaningful measures of soil properties, because of this lack of physical meaning of the incremental stress tensors.

2.2.6 Stress Transformation

If a constitutive law could be found and the field equations solved so that for a given set of applied forces, the corresponding field of displacements was obtained, the constitutive equations and the definition of the strain

in each case would give at the end the stress tensor field. Depending on what formulation has been used, the stress tensor would be the Lagrangian or Kirchhoff's.

To be able to do the next step, the Eulerian stress tensor has to be found. Again, the conversion equations are given by the definition of the different stress tensors (Fung, 1965).

$$\sigma_{ji} = \frac{\rho}{\rho_0} \frac{\partial x_i}{\partial a_p} T_{pj} = \frac{\rho}{\rho_0} \frac{\partial x_i}{\partial a_\alpha} \frac{\partial x_j}{\partial a_\beta} S_{\beta\alpha} \quad (2-33)$$

These can be expanded as functions of $\frac{\partial u_i}{\partial a_j}$. If the exterior forces are given as surface tractions, a transformation from T_{oi}^* to T_i has to be done. This is not necessary in the case of a finite element analysis where all exterior forces are given as nodal forces.

2.3 FELIPPA'S FORMULATION (1966)

This formulation is the one that has been followed above with the Kirchhoff stress tensor.

A simplification is made and Equation (2-32) becomes:

$$\int_{V_0} (\sigma_{0ji} \delta \eta_{ji} + \Delta S_{ji} \delta \epsilon_{ji}) dV_0 - \int_{S_0} \Delta T_{0i}^v \delta u_i dS_0 \quad (2-34)$$

where:

$$\delta E_{ji} = \delta \eta_{ji} + \delta \epsilon_{ji} \quad (2-35)$$

$$\delta \eta_{ji} = \frac{1}{2} \left(\frac{\partial u_k}{\partial a_i} \delta_{jl} + \frac{\partial u_l}{\partial a_j} \delta_{ik} \right) \frac{\partial \delta u_k}{\partial a_l} \quad (2-36)$$

$$\delta \varepsilon_{ji} = \frac{1}{2} (\delta_{jk} \delta_{il} + \delta_{ik} \delta_{jl}) \frac{\partial \delta u_k}{\partial a_l} \quad (2-37)$$

That is:

$$\Delta S_{ji} \delta \eta_{ji} = 0 \quad (2-38)$$

This is based on the assumption that $\Delta S_{ji} \delta \eta_{ji}$ is a third order infinitesimal, that is, that ΔS_{ji} is an infinitesimal with respect to σ_{0ij} .

The constitutive equations are:

$$\Delta S_{ij} = C_{ijkl} \varepsilon_{kl} \quad (2-39)$$

Some comments have been made already about the difficulty of obtaining C_{ijkl} because of the lack of physical meaning of ΔS_{ij} . The worst assumption, however, was made when, instead of using the transformation Equation (2-23) to obtain σ_{ij} from S_{ij} , the following one was used:

$$\begin{aligned} \sigma_{ij} = S_{ij} (1 - \varepsilon_{kk}) + \frac{1}{2} S_{ik} (\varepsilon_{jk} + 2\omega_{jk}) \\ + \frac{1}{2} S_{jk} (\varepsilon_{ik} + 2\omega_{ik}) \end{aligned} \quad (2-40)$$

where

$$\omega_{ij} = \frac{1}{2} \left(\frac{\partial u_i}{\partial a_j} - \frac{\partial u_j}{\partial a_i} \right) \quad (2-41)$$

This transformation would be valid if S_{ij} , instead of being the Kirchhoff stress tensor, were the expression for T_{ij} referred to the cartesian axes rotated on an angle ω counterclockwise.

The reason behind using this transformation is

that for very small strains in the body but large rotations (a common case in structures), the tensor S_{ij} is very similar to the values of T_{ij} referred to the rotated axes.

As it will be shown in Chapter 5, Felippa's formulation led to lack of equilibrium in a simple problem, because the simplifications and assumptions were not done consistently throughout the formulation, in such a way that when some of these assumptions were violated, the results were not only wrong, but inconsistent among themselves.

A solution would have been to use the correct transformation equations. However, the insecurity about the constitutive relation remained. Furthermore, once it was decided to assume that ΔS_{ij} had to be an infinitesimal with respect to σ_{0ij} , then a more consistent and, if possible, more "physically" based formulation was sought.

2.4 BIOT'S FORMULATION

This formulation was developed by Biot(1965) for incremental deformations of initially stressed mediums. Everything is based on physical and geometrical considerations.

The main assumption is that the incremental stress is an infinitesimal with respect to the initial stress.

The derivation of the formulation for a plane strain case is given in Appendix B; an outline of this derivation is included here.

The formulation is based on the separation of physics from geometry. The deformation of a continuum gives to a small region around a material point:

- 1) a translation
- 2) a rigid body rotation
- 3) a pure strain, that is, the strain caused by a deformation such that it is possible to find three orthogonal directions that remain orthogonal after the deformation.

It is well known that for these three directions to exist, $\epsilon_{ij} = \epsilon_{ji}$, when ϵ_{ij} are the components of the pure strain.

After some geometric considerations, the expressions for ϵ_{ij} , for plane strain, to the second order are:

$$\begin{aligned}\epsilon_{11} &= e_{xx} + e_{xy}\omega + \frac{1}{2}\omega^2 \\ \epsilon_{22} &= e_{yy} - e_{xy}\omega + \frac{1}{2}\omega^2 \\ \epsilon_{12} &= e_{xy} + \frac{1}{2}(e_{yy} - e_{xx})\omega\end{aligned}\tag{2-42}$$

where:

$$\begin{aligned}e_{xx} &= \frac{\partial u}{\partial x} \\ e_{yy} &= \frac{\partial v}{\partial y} \\ e_{xy} &= e_{yx} = \frac{1}{2} \left(\frac{\partial v}{\partial x} + \frac{\partial u}{\partial y} \right) \\ \omega &= \frac{1}{2} \left(\frac{\partial v}{\partial x} - \frac{\partial u}{\partial y} \right)\end{aligned}\tag{2-43}$$

where u and v are the displacement field components with respect to the original cartesian frame x,y and where ϵ_{11} , ϵ_{22} , ϵ_{12} are referred to axes 1,2 rotated an angle θ counterclockwise from x and y respectively (Figure B.2).

The stress in the body before deformation is S_{xx} , $S_{xy} = S_{yx}$, S_{yy} referred to the x,y axes; after deformation it becomes:

$$\begin{aligned}\sigma'_{xy} &= S_{xy} + s'_{xy} \\ \sigma'_{xx} &= S_{xx} + s'_{xx} \\ \sigma'_{yy} &= S_{yy} + s'_{yy}\end{aligned}\tag{2-44}$$

s'_{xx} , s'_{xy} , s'_{yy} are the total incremental stress referred to the axes x,y . But, they do not depend only on the strain, but also on the rotation, in such a way that if there is no strain but only a rigid body rotation, $s' \neq 0$.

If the stress after deformation is referred to the rotated axes 1,2 then:

$$\begin{aligned}\sigma'_{11} &= S_{xx} + s'_{11} \\ \sigma'_{22} &= S_{yy} + s'_{22} \\ \sigma'_{12} &= \sigma'_{21} = S_{xy} + s'_{12}\end{aligned}\tag{2-45}$$

s'_{11} etc., depend only on the pure strain, because in a rigid body rotation they are 0; see Figure B.3.

From geometric considerations and assuming that

the incremental stress and the rotation are quantities of the first order

$$\begin{aligned}
 s'_{xx} &= s'_{11} - 2S_{xy}\omega \\
 s'_{yy} &= s'_{22} + 2S_{xy}\omega \\
 s'_{xy} &= s'_{12} + (S_{xx} - S_{yy})\omega
 \end{aligned}
 \tag{2-46}$$

Equilibrium is established in the deformed position and equilibrium equations in S_{xy} and s'_{12} , etc., are found (Biot, 1965).

In order to obtain an equivalent variational or virtual work principle the components of the stress have to be referred to the undeformed areas and the rotated axes.

To the first order

$$\begin{aligned}
 T_{11} &= S_{xx} + t_{11} = \sigma'_{11} + S_{xx}e_{yy} - S_{xy}e_{xy} \\
 T_{22} &= S_{yy} + t_{22} = \sigma'_{22} + S_{yy}e_{xx} - S_{xy}e_{xy} \\
 T_{12} &= S_{xy} + t_{12} = \sigma'_{12} + \frac{1}{2}S_{xy}(e_{xx} + e_{yy}) \\
 &\quad - \frac{1}{2}(S_{xx} + S_{yy})e_{xy}
 \end{aligned}
 \tag{2-47}$$

Now the principle of virtual work is:

$$\int_{V_0} T_{ij} \delta \epsilon_{ij} dV_0 = \int_{V_0} \rho X_i(\xi_\ell) \delta u_i dV_0 + \int_{S_0} f_i \delta u_i dS_0
 \tag{2-48}$$

if body forces $X_i(\xi_\ell) = 0$

Because of the equilibrium of the initial state:

$$\int_{V_0} s_{ij} \delta e_{ij} dV_0 = \int_{S_0} s_{ij} v_{0j} \delta u_i dS_0 \quad (2-49)$$

and, keeping only second order terms:

$$\int_{V_0} (t_{ij} \delta e_{ij} + s_{ij} \delta \eta_{ij}) dV_0 = \int_{S_0} \Delta f_i \delta u_i dS_0 \quad (2-50)$$

where

$$\eta_{ij} = \frac{1}{2}(e_{il} \omega_{lj} + e_{jl} \omega_{li} + \omega_{il} \omega_{jl}) \quad (2-51)$$

and $t_{ij} \delta \eta_{ij}$ is a third order term.

So far in this formulation, only second order terms have been kept in order to establish the virtual work with all the second order terms. The theory is then a linear theory, but it is consistent throughout the formulation.

Furthermore, t_{ij} is the real increment of stress due to the strain; this is because t_{ij} is what has to be added to the initial stress to get the final stress when both are referred to the same axes and geometry.

It can be said then, that for an elastic increment

$$t_{ij} = C_{ijkl} \epsilon_{kl} \quad (2-52)$$

To the first order (2-52) becomes

$$t_{ij} = C_{ijkl} e_{kl} \quad (2-53)$$

where C_{ijkl} are the same constants that relate stress and strain in infinitesimal elasticity; in an isotropic case, they can be reduced to combinations of two parameters.

To obtain these parameters from standard testing procedures, it has to be remembered that $e_{k\ell}$ would be the incremental Cauchy strain; this is the incremental deformation referred to the geometry just before the increment. In the same way, t_{ij} is the real increment of stress referred each moment to the geometry just before deformation. The last step is to recover the value of σ'_{xy} , σ'_{xx} , σ'_{yy} , that is the stress in the body after deformation referred to the x,y frame.

From the virtual work equation, once f_i are known the displacement field can be obtained and from it, through the constitutive equations, t_{ij} . The value of t_{ij} will be exact to the first order only, so the transformation equations from T_{ij} to σ'_{xy} , etc., have to be exact to the first order only.

The first order transformation equations are

$$\begin{aligned}\sigma'_{xx} &= T_{11} - S_{xx}e_{22} + S_{xy}(e_{12} - 2\omega) & (2-54) \\ \sigma'_{yy} &= T_{22} - S_{yy}e_{11} + S_{xy}(e_{12} + 2\omega) \\ \sigma'_{xy} &= T_{12} - \frac{1}{2}S_{xy}(e_{11} + e_{22}) + S_{xx}\frac{1}{2}(e_{12} + 2\omega) \\ &\quad + S_{yy}\frac{1}{2}(e_{12} - 2\omega)\end{aligned}$$

These are the transformation equations used by Felippa, if instead of S_{xy} , T_{12} , etc., is used. That gives some second order terms.

In summary, Biot's formulation is consistent; it does not require the assumption of rotations being of a

larger order than strains, and it uses a constitutive equation defined between physical quantities, where geometric characteristics do not have influence and which can be easily related to the standard tests.

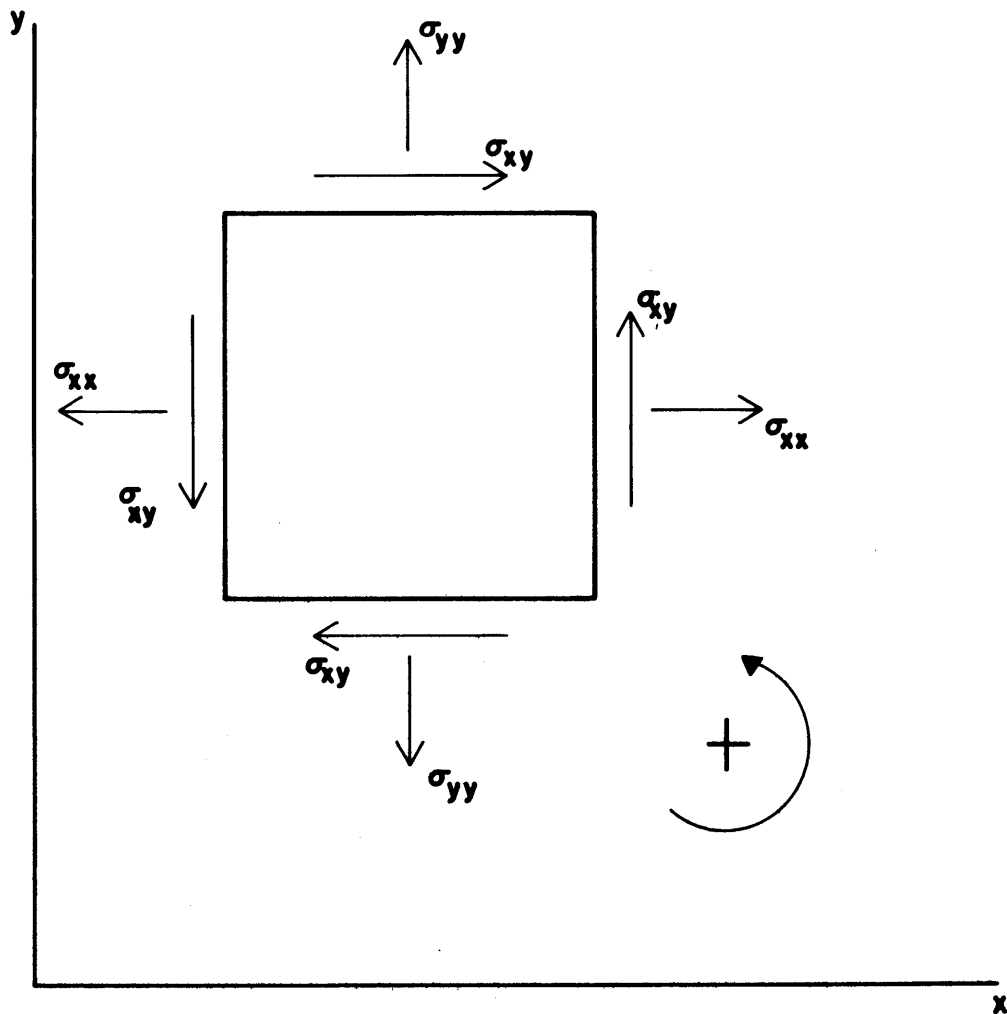


FIGURE 2.1 : POSITIVE SIGN CONVENTION IN TWO DIMENSIONS

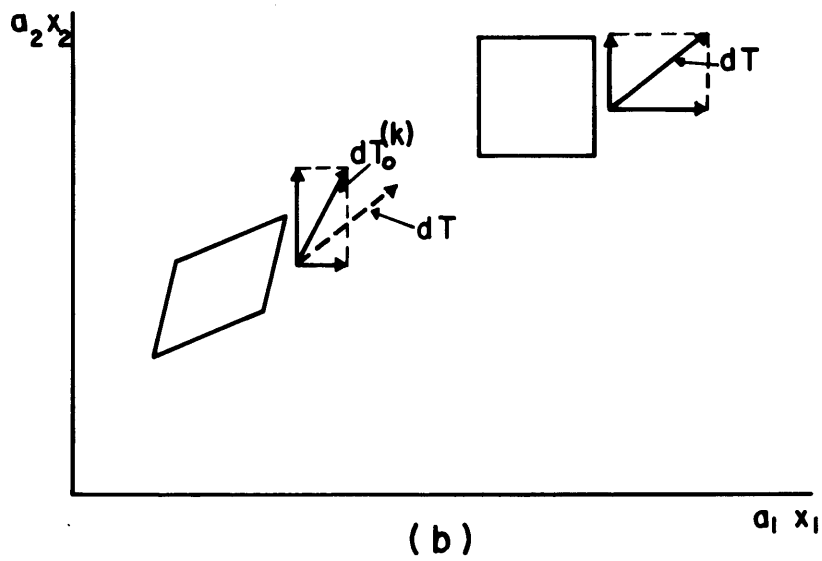
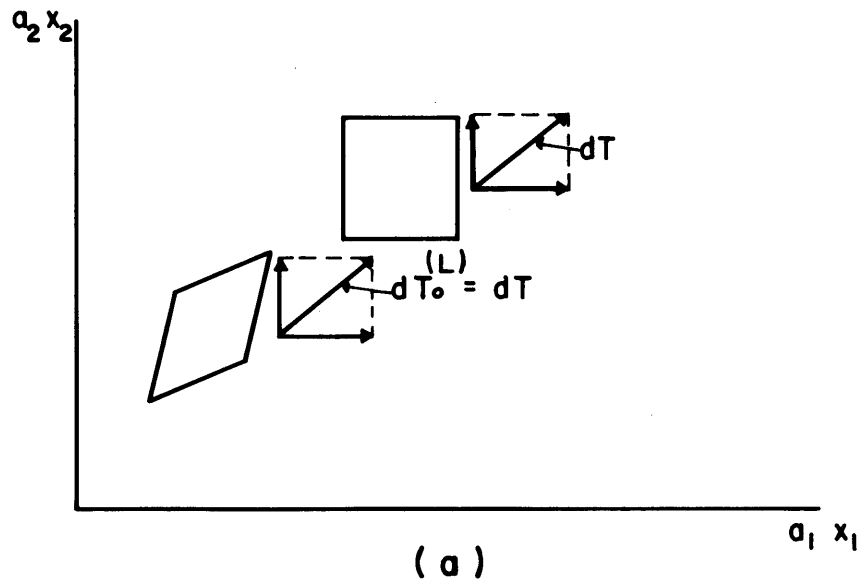


FIGURE 2.2 : FORCE VECTORS IN THE DEFINITION OF : a) LAGRANGE AND b) KIRCHHOFF

Chapter 3

CONSTITUTIVE EQUATIONS

3.1 INTRODUCTION

When loads are applied to a body, three basic kinds of response can be expected:

a) Elastic The deformation is instantaneously dependent on only the load and independent of how the load was applied. Essentially, the body has a natural state that is free of stress and strain, to which it returns when unloaded. (Fig. 3.1,a)

b) Plastic The state of deformation is stress path dependent; different loads can give the same deformation and vice versa. (Fig. 3.1,b)

c) Viscous The deformations are time dependent.

Mixed responses are common, as for instance, elasto-plastic and viscoelastic responses. Soils show all three kinds of behavior. No attempt will be made here to treat time dependent effects. A literature survey, formulation, and some solutions are presented by B. J. Watt (1969).

3.2 SOIL AS AN ELASTO-PLASTIC MATERIAL

The widespread use of linear elastic theory to treat problems in soils has been caused by the possibility of obtaining analytical solutions. Even with the use of

computers, many problems have been solved taking the soil as a linear, bilinear or non-linear elastic material (for references, see Hagmann, 1971).

However, the soil is elastic only at very low strains and stresses. Residual deformation after very small cyclic loads are noticeable. Soils, then, are plastic materials.

The application of the plasticity theory to soils centers on the determination of the yield function. A large amount of research has been done in this field lately; see Hagmann for a review (1971). The first yield functions used to obtain a formulation valid for perfectly plastic materials were the well known Tresca and von Mises yield criteria (Christian, 1966). The generalized Mohr- Coulomb failure law, and the stress hardening theory have also been used (Hagmann, 1971) in an effort to simulate more closely the real behavior of soils.

The use of plasticity theories has been possible because of the availability of high speed computers, through techniques such as finite differences (Ang and Harper, 1964), and finite elements (Zienkiewicz and Y.K. Cheung, 1967).

A different approach to the problem has also been made possible because of these techniques, especially with the use of finite elements and incremental procedures. The method defines two elastic laws, one for loading and another

for unloading, thus obtaining a pseudo-plastic behavior or a deformation plasticity. The unloading law is usually linearly elastic, and the same law is used for loading until the maximum previous load is reached. (Fig. 3.1,b) The loading law can be non-linear, and a failure criterion can be defined such that, once the yield surface has been reached, the law gives a finite, but very large, value of strain for small increments of stress.

This approach has the advantage over a rigorous plastic law that it is easier to formulate and easier to use in a finite element program.

This kind of approach has been used several times, with different mathematical models to define the non-linear, elastic, loading law (Wong, 1971), (Duncan and Chang, 1970), (Desai, 1971).

3.3 PSEUDO PLASTIC STRESS-STRAIN LAWS

In the incremental procedures, each increment is supposed to be isotropically elastic; one of the two parameters that define the isotropically elastic constitutive law is usually constant throughout the complete problem, namely, either the Poisson's Ratio or the Bulk Modulus, depending on the selection of parameters. The other is obtained as the tangent, or the local secant, of a given stress-strain curve.

The stress-strain curve is obtained from plane strain or triaxial tests. The experimental data is plotted

and a curve is fitted through it. Kondner (1963), Kondner and Zelasco (1963) suggested a hyperbolic approximation; this approximation has been used by Duncan and Chang (1970) in a finite element analysis. Wong (1971) suggested a polynomial least square method, and Desai (1971) a spline curve defined by the experimental points. From the normalized curve, a set of curves can be found for different values of the stress level.

The hyperbolic approximation is good for many normally consolidated clays and loose sands. It can be used for overconsolidated clays and dense sands to approximate the first part of the curve until the peak of the curve is reached. The second part has to be approximated by a straight line. It is not always possible to approximate the test results by a hyperbola, and in such cases, one of the other two methods can be used. The hyperbolic method is simpler, however, and is the one chosen here.

The other constitutive law used in this study is the simple elasto-plastic relations derived in the perfect plasticity theory from the Tresca yield criterion.

3.4 ELASTIC PERFECTLY PLASTIC TRESCA MATERIAL

The Tresca yield criterion for plane strain is defined by:

$$f = \left(\frac{\sigma_{xx} - \sigma_{yy}}{2} \right)^2 + \sigma_{xy}^2 - k^2 = 0 \quad (3-1)$$

physically it means that at some value, k , of the maximum shear stress the material will yield, independently of the value of the normal stresses.

This is a valid assumption in soils only in an undrained and saturated condition, where the effective stresses* are independent of the total stress, and only depend on the consolidation stress. The value of the maximum shear stress at failure is then constant in a total stress analysis.

The behavior of the soil inside the yielding surface will be considered linearly elastic and isotropic.

The constitutive law for plane strain is

(Timoshenko and Goodier, 1951):

$$\begin{aligned}\sigma_{xx} &= \frac{E}{(1+\nu)(1-2\nu)} [(1-\nu)\epsilon_{xx} + \nu\epsilon_{yy}] \\ \sigma_{yy} &= \frac{E}{(1+\nu)(1-2\nu)} [(1-\nu)\epsilon_{yy} + \nu\epsilon_{xx}] \\ \sigma_{yx} &= \frac{E}{(1+\nu)} \epsilon_{yx}\end{aligned}\quad (3-2)$$

If, instead of E , Young's modulus, and ν , Poisson's ratio, the chosen parameters are G , shear modulus, and B , bulk modulus, the law becomes, in a matrix form:

$$\begin{bmatrix} \sigma_{xx} \\ \sigma_{yy} \\ \sigma_{yx} \end{bmatrix} = \begin{bmatrix} B + (4/3)G & B - (2/3)G & 0 \\ B - (2/3)G & B + (4/3)G & 0 \\ 0 & 0 & 2G \end{bmatrix} \begin{bmatrix} \epsilon_{xx} \\ \epsilon_{yy} \\ \epsilon_{xy} \end{bmatrix}\quad (3-3)$$

* For the effective stress definition and similar basic concepts in soil mechanics, see any text book [Lambe and Whitman(1968), Terzaghi (1943)]

The derivation of the perfectly-plastic Tresca material formulation can be found in Harper (1963), Whitman (1964), or Christian (1966), and it will not be included here.

The formulation in an incremental form is for plane strain:

$$\begin{aligned}
 \Delta\sigma_{xx} &= \left[\frac{4G+3B}{3} - \frac{G}{k^2} \left(\frac{\sigma_{xx}-\sigma_{yy}}{2} \right)^2 \right] \Delta\epsilon_{xx} \\
 &+ \left[\frac{-2G+3B}{3} + \frac{G}{k^2} \left(\frac{\sigma_{xx}-\sigma_{yy}}{2} \right)^2 \right] \Delta\epsilon_{yy} \\
 &+ \left[-\frac{G\sigma_{xy}}{k^2} - \frac{\sigma_{xx}-\sigma_{yy}}{2} \right] 2\Delta\epsilon_{xy} \\
 \Delta\sigma_{yy} &= \left[\frac{-2G+3B}{3} + \frac{G}{k^2} \left(\frac{\sigma_{xx}-\sigma_{yy}}{2} \right)^2 \right] \Delta\epsilon_{xx} \\
 &+ \left[\frac{4G+3B}{3} - \frac{G}{k^2} \left(\frac{\sigma_{xx}-\sigma_{yy}}{2} \right)^2 \right] \Delta\epsilon_{yy} \\
 &+ \left[\frac{G\sigma_{xy}}{k^2} - \frac{\sigma_{xx}-\sigma_{yy}}{2} \right] 2\Delta\epsilon_{xy} \\
 \Delta\sigma_{xy} &= \left[-\frac{G}{k^2} \sigma_{xy} \left(\frac{\sigma_{xx}-\sigma_{yy}}{2} \right) \right] \Delta\epsilon_{xx} \\
 &+ \left[\frac{G}{k^2} \sigma_{xy} \left(\frac{\sigma_{xx}-\sigma_{yy}}{2} \right) \right] \Delta\epsilon_{yy} \\
 &+ \left[G \left(1 - \frac{\sigma_{xy}^2}{k^2} \right) \right] 2\Delta\epsilon_{xy}
 \end{aligned} \tag{3-4}$$

3.5 HYPERBOLIC STRESS-STRAIN RELATION

3.5.1 Hyperbolic Approximation

Kondner (1963) and Kondner and Zelasko (1963) have shown that many stress-strain curves of sands and clays can

be approximated by a hyperbola. The proposed equation was:

$$\sigma_1 - \sigma_3 = \frac{\epsilon}{a+b\epsilon} \quad (3-5)$$

where σ_1^* and σ_3 are the major and minor principal stresses, ϵ is the axial strain, and a and b constants. This curve is based on the results of compression triaxial tests, where σ_3 remains constant throughout the test. The main phenomenon involved in the test is a shear failure, so the hyperbolic relation could be written alternatively:

$$\tau = \frac{\gamma}{a'+b'\gamma} \quad (3-6)$$

where τ is the maximum shear stress, γ the maximum engineering shear strain and a' and b' constants.

In a plot τ vs. γ (Fig. 3.2), the value of a' is the inverse of the initial tangent to the curve, $\frac{1}{a'} = G_i$, and b' is the inverse of the value of τ that defines the horizontal asymptote to the curve,

$$\frac{1}{b'} = \tau_{ult}$$

An easy way to find a' and b' would be to plot the curves in transformed axes: γ/τ vs. γ as suggested by Kondner (Fig. 3.3). From Equation (3-6)

$$\frac{\gamma}{\tau} = a' + b'\gamma \quad (3-7)$$

* The sign convention in section 3.5 will be the standard for soil mechanics, that is, compression positive.

a' is the initial value of $\frac{\gamma}{\tau}$ for $\gamma=0$ and b' the slope of the resulting straight line. It does happen that $\tau_{ult} = \frac{1}{b'}$ is bigger than the strength of the soil, so it can be said then

$$\tau_f = R_f \tau_{ult} \quad (3-8)$$

where τ_f is the value of the maximum shear stress at failure; R_f is called the failure ratio. Its value has been found to be, for different soils, between 0.75 and 1.00 (Duncan and Chang, 1970).

3.5.2 σ_3 Dependency

Both parameters $G_i = \frac{1}{a'}$, (initial shear modulus) and $\tau_{ult} = \frac{1}{b'}$, depend on σ_3 . If the relations between G_i and σ_3 can be found, a family of hyperbolae with σ_3 as parameter will be derived.

Janbu (1963) recommended a relationship

$$E_i = k p_a \left(\frac{\sigma_3}{p_a} \right)^n \quad (3-9)$$

for the initial value of the tangent Young's modulus; where p_a is the atmospheric pressure and K and n constants. Of course, for a given Poisson's ratio: $G = k_1 E$, therefore, a similar equation can be applied to G_i

$$G_i = K' p_a \left(\frac{\sigma_3}{p_a} \right)^{n'} \quad (3-10)$$

A plot of G_i vs. σ_3 in log log scale gives the values of K' as the value of G_i for $\sigma_3 = 1$, and n' as the value of the

slope of the straight line, (Fig. 3.4)*. This equation can be transformed into

$$G_i = K' \sigma_3 \quad (3-11)$$

for $n' = 1$. This is the basis for the normalized representation of test results, and the result will be useful when the data for the problem is scarce.

The Janbu equation does not hold for total stress analysis of undrained cases where the stress-strain curves depend only on the value of the consolidation stress.

The Mohr-Coulomb failure criterion provides the relationship between τ_f (and τ_{ult} , therefore) and σ_3 .

$$\tau_f = \frac{c \cos \phi + \sigma_3 \sin \phi}{1 - \sin \phi} \quad (3-12)$$

where c is the cohesion intercept and ϕ the friction angle (Fig. 3.5).

3.5.3 Tangent Modulus

Duncan and Chang (1970), from Equations (3-5), (3-9), and the equations equivalent to Equations (3-8) and (3-12), that is:

$$(\sigma_1 - \sigma_3)_f = R_f (\sigma_1 - \sigma_3)_{ult} \quad (3-13)$$

* A term is dropped to develop this; from Equation (3-10): $\log G_i = \log K' + n' \log \sigma_3 + \log p_a (1 - n')$, so $(1 - n') \log p_a$ is considered 0. This is exact if the dimensions of σ_3 are such that $p_a \approx 1$.

and

$$(\sigma_1 - \sigma_3)_f = \frac{2c \cos\phi + 2\sigma_3 \sin\phi}{1 - \sin\phi} \quad (3-14)$$

obtain an expression for the tangent Young's modulus as a function of σ_3 and σ_1 :

$$E_t = \left(1 - \frac{R_f(1-\sin\phi)(\sigma_1 - \sigma_3)}{2c\cos\phi + 2\sigma_3\sin\phi} \right)^2 K_{p_a} \left(\frac{\sigma_3}{p_a} \right)^n \quad (3-15)$$

A similar expression can be derived from Equations (3-10), (3-6), (3-8) and (3-12).

From (3-6) and (3-8):

$$\tau = \frac{\gamma}{\left(\frac{1}{G_i} + \frac{\gamma R_f}{\tau_f} \right)} \quad (3-16)$$

The tangent shear modulus is defined as:

$$G_t = \frac{\partial \tau}{\partial \gamma} \quad (3-17)$$

so

$$G_t = \frac{\left(\frac{1}{G_i} + \frac{\gamma R_f}{\tau_f} \right) - \frac{\gamma R_f}{\tau_f}}{\left(\frac{1}{G_i} + \frac{\gamma R_f}{\tau_f} \right)^2} = \frac{1/G_i}{\left(\frac{1}{G_i} + \frac{\gamma R_f}{\tau_f} \right)^2} \quad (3-18)$$

but from (3-16)

$$\gamma = \frac{\tau}{G_i \left(1 - \frac{R_f}{\tau_f} \tau \right)} \quad (3-19)$$

and then (3-9) becomes, after some transformations

$$G_t = G_i \left(1 - \frac{R_f \tau}{\tau_f} \right)^2 \quad (3-20)$$

If the values of G_i and τ_f from Equations (3-10) and (3-12)

are introduced in (3-20),

$$G_t = K' p_a \left(\frac{\sigma_3}{p_a} \right)^{n'} \left(1 - R_f \frac{\tau(1-\sin\phi)}{c \cos\phi + \sigma_3 \sin\phi} \right)^2 \quad (3-21)$$

Observe that after substituting τ for its value

$$\tau = \frac{\sigma_1 - \sigma_3}{2}$$

(3-21) has the same form as (3-15).^{*} This makes it very simple to change the computer programs to define the elastic constitutive equations as a function of E and ν instead of G and B .

3.5.4 Unloading Stress-Strain Law

The hyperbolic law gives the values of the incremental modulus for loading; during unloading and reloading, the material can be considered linearly elastic. The value of the unloading-reloading Young's modulus has been suggested by Duncan and Chang to vary with σ_3 in the same fashion as E_i does. The value of K would be different, bigger usually, but the same value of n would be used. In a similar fashion as Equation (3-10)

$$G_u = K_u p_a \left(\frac{\sigma_3}{p_a} \right)^{n'} \quad (3-22)$$

* Equation [3-15] is good for triaxial test results; if the results are from plane strain tests, E_t has to be multiplied by $(1-\nu^2)$ to get the actual value of E_t ; this follows from the existence of an intermediate principal stress $\Delta\sigma_2 \neq 0$ in plane strain tests while $\Delta\sigma_2 = 0$ in triaxial tests.

3.5.5 Post-Yielding Behavior

When the hyperbolic approximation is used, the yield surface is not the curve given by the τ_{ult} , but by the smaller value τ_f . After yielding, the stress-strain relation has to be defined. In many cases, especially for over-consolidated clays and dense sands, there is a decrease in τ with γ increasing (Fig. 3.6). Because negative elastic parameters cannot be used, it is impossible for an incremental procedure to model such behavior, except by using strain softening plasticity theory. The best approximation that can be made in a pseudo-plastic approach is a straight line with a very small slope; zero slope is not possible because of numerical instabilities. The value of the slope will be the value of the ultimate E or G, whichever is used.

3.5.6 Election of Elastic Parameters

In a pseudo-plastic approach, the non-linear loading law gives one of the two elastic parameters needed to describe the isotropic, linearly elastic behavior, usually the Young's modulus; the other one, usually the Poisson's ratio, is given a constant value. However, when the elements, in a finite element method, reach yielding values, the small value of E causes some inconveniences. Sometimes, the element becomes so "soft" that a negative area is obtained, (D'Appolonia, 1968).

A way to overcome this is to fix the value of the bulk modulus, and to use the hyperbolic approximation to

obtain the shear modulus. This choice has some physical meaning. First, the stress-strain curves are obtained in tests where the main phenomenon is shear, and, second, the isotropic compressibility of a soil (the bulk modulus measures its inverse) cannot decrease with shear as much as the shear modulus does. Certainly, to give it a constant value, for a given σ_3 , is a better approximation than to make it decrease as much as the shear modulus.

The dependence of the bulk modulus on σ_3 can be expressed in the same way that the dependence of E_i , G_i or G_u :

$$B = K_B p_a \left(\frac{\sigma_3}{p_a} \right)^{n'} \quad (3-23)$$

3.5.7 Anisotropy

So far, the soil has been considered as homogeneous, isotropic material; both assumptions are not true. The non-homogeneity is handled through the finite element method, assigning different material properties over different zones.

Anisotropy in soils can be shown by running isotropically consolidated active and passive plane strain tests. The anisotropy in these tests is a characteristic of the soil, independent of the stresses, and probably caused by the way it was deposited. A second type of anisotropy can be caused in soils because of anisotropic consolidation, or an anisotropic state of stress in the soil (Ladd, 1964); this anisotropy appears mainly in undrained shear. A third

case of "anisotropy" can be obtained if triaxial compression and extension tests are used instead of plane strain active and passive tests. It is caused by the influence of σ_2 (Ladd, 1964). It is not a property of the soil as such, and if the problem being solved is a plain strain problem, the triaxial tests are going to give the wrong information. Plain strain tests should be preferred. Of course, in order to take into account both classes of anisotropy, the tests should be anisotropically consolidated if undrained.

To take into account the anisotropy of the soil without having to determine the five elastic constants necessary to characterize a layered material, an interpolation procedure is used after an idea of Duncan and Dunlop (1969). The values of G_t are found for both active and passive tests. These give, then, the corresponding values of G_t when the maximum principal stress, σ_1 , is vertical and horizontal, respectively. When σ_1 forms an angle θ with the vertical direction, then

$$G_{t\theta} = G_{th} - (G_{th} - G_{tv}) \cos^4 \theta \quad (3-24)$$

G_{tv} is obtained for $\theta = 0$, and G_{th} for $\theta = \frac{\pi}{2}$; $\cos^4 \theta$ is symmetric.

Duncan and Dunlop used a $\sin^2 \theta$ interpolation function, and, when the results were not very satisfactory, a $0.2 \sin^2 2\theta$ modification. However, $\cos^4 \theta$ has been shown by Christian (1970) to be theoretically based, thus giving good

results.

The Mohr-Coulombe failure criterion is considered a non directional property of the soil, and no anisotropy is considered in its parameters. However, in undrained cases a pseudo failure criterion in total stresses is considered, with $\phi = 0$ and $c = S_u$ then, anisotropy appears as a result of anisotropic consolidation. In such cases, S_u is determined in the standard passive and active tests and the same interpolation Equation (3-24) is used with c instead of with G_t .

3.5.8 Experimental Determination of Parameters

A summary of how the parameters are obtained in the different analyses is presented here.

a) Drained cases

The procedure is the same for all different soils. Two sets of tests have to be made: a set of drained plane strain active tests and a set of drained plane strain passive tests. If plane strain tests are not feasible, triaxial tests can be made; a set of drained compression tests, loading, and a set of drained extension tests, loading.

Volume changes have to be measured in order to obtain the horizontal displacement, and to determine from horizontal and vertical displacements the maximum shear strain γ .

Every set must be of at least three tests to obtain the variation rate exponent, n' , and the modulus number, K' ,

of Equation (3-10). If only one test is available, n' can be assumed to be 1. If only compression or active tests are run, isotropy has to be assumed.

To obtain a stress-strain curve valid for an incremental procedure, both stress and strain have to be the actual values. The actual value of the stress is obtained as a standard testing procedure, when the correction due to the change in cross-sectional area is made. Strain, however, is customarily referred to the initial length of the specimen; it has to be corrected in such a way that each increment of strain is the increment of length divided by the actual length of the specimen before that increment. In many cases, this correction has no practical importance.

From the curves of maximum shear stress vs. maximum shear strain, K' , n' , and R_f can be obtained, as shown before, for both active and passive cases. ϕ and c can be obtained from any two of the tests as usual. An unload-reload cycle can be made in one of the tests to obtain values of K_u .

Values of K_B (bulk modulus) for $\sigma_3 = 1$ can be obtained from isotropic consolidation or from the value of K' (initial shear modulus for $\sigma_3 = 1$), assuming a reasonable value of ν and using the well known relation:

$$B = \frac{2(1+\nu)}{3(1-2\nu)} G \quad (3-25)$$

b) Undrained cases

Analysis of undrained cases is made in total

stresses. Therefore only two tests are necessary: one undrained active and one undrained passive plain strain test, or one triaxial undrained compression test and another one in extension. γ is readily obtainable from the axial strain in both cases, because the volume remains constant. Stress and strain have to be defined as in drained cases; the unloading and reloading value of G can be obtained from an unloading-reloading cycle. Bulk modulus is infinite in theory, though, in practice, the value has to be chosen so it will not create numerical problems when it is matched with the final value of G (see Chapter V).

As has been said before, the stress-strain curve for undrained analysis in total stresses is unique, and independent of the value of σ_3 , for each point in the soil mass. Therefore, from the two tests two values of G_1 and $c = S_u$, as well as G_u for unloading and reloading, can be obtained; ϕ is 0.

The stress-strain curve for undrained cases, which is unique in each element, varies from element to element, depending on the consolidation stress in each one. The procedure to obtain the local stress-strain curves from tests varies, depending on the type of clay.

1) overconsolidated clays

The profile has to be divided in horizontal layers of constant consolidation stress, overconsolidated ratio and coefficient of lateral stress at rest K_0 . Tests

have to be made for each layer. Tests should be anisotropically consolidated to obtain better results.

2) normally consolidated clays

In a profile in which K_0 remains fairly constant, only two tests are necessary to obtain the stress-strain curves, if the clay is normally consolidated. In a N.C. clay, $K_0 < 1$. Therefore, the consolidation is anisotropic, and the tests should be anisotropically consolidated. The results of the tests have to be normalized, dividing the stresses by the vertical consolidation stress. The corresponding stress-strain curve for any element can be found by multiplying the G_i and c parameters, of the normalized curve, by the corresponding vertical stress acting in the element (Ladd, 1964, b).

When the available data for saturated N.C. clays is from isotropically consolidated tests, an approximation can be done. This is a good approximation only for clays that do not show a big difference in the shapes of their plots $\frac{\sigma_1 + \sigma_3}{2}$ vs. $\frac{\sigma_1 - \sigma_3}{2}$ between undrained shear after isotropic consolidation and undrained shear after anisotropic consolidation (Ladd, 1964, b).

The approximation is based in the equation by Skempton and Bishop (1954):

$$\frac{c}{\sigma_{1c}} = \frac{[K_0 + A_f(1 - K_0)] \sin \phi}{1 + (2A_f - 1) \sin \phi} \quad (3-26)$$

where σ_{1c} is the vertical consolidation stress and A_f the value at failure of Skempton's parameter A defined as:

$$A = \frac{\Delta u - \Delta \sigma_3}{\Delta \sigma_1 - \Delta \sigma_3} \quad (3-27)$$

where $\Delta \sigma_1$ and $\Delta \sigma_3$ are the increments of the principal total stresses, and Δu the increment of the pore pressure.

If in Equation (3-26) $K_0 = 1$, isotropic consolidation, then:

$$\frac{c}{\sigma_c} = \frac{\sin \phi}{1 + (2A_f - 1) \sin \phi} \quad (3-28)$$

where σ_c is the value of the isotropic consolidation stress. Therefore, if for a given σ_{1c} a value of c is obtained, the equivalent value of σ_c that will give the same c is:

$$\begin{aligned} \sigma_c &= \frac{[1 + (2A_f - 1) \sin \phi]}{\sin \phi} \sigma_{1c} \frac{[K_0 + A_f(1 - K_0)] \sin \phi}{[1 + (2A_f - 1) \sin \phi]} \\ &= \sigma_{1c} [K_0 + A_f(1 - K_0)] \end{aligned} \quad (3-29)$$

Equation (3-29) gives the equivalent σ_c for a given σ_{1c} , K_0 and A_f for the active test, or compression test; for the passive, or extension test, (3-29) becomes

$$\sigma_c = \sigma_{1c} \left[\frac{1}{K_0} + A_f \left(1 - \frac{1}{K_0} \right) \right] \quad (3-30)$$

If the data from the isotropic tests is now normalized by dividing τ by σ_c , then the values of c , and similarly G_i , for a given point, can be found by multiplying the normalized values by the σ_c values given by Equations (3-28) and (3-29) respectively. σ_{1c} is again the vertical consolidation stress.

3.5.9 Plotting of Anisotropically Consolidated Test Results

The hyperbolic approximation was derived for stress-strain curves from isotropically consolidated tests. They pass through the origin of the stress-strain plot. However, if a soil is anisotropically consolidated, only anisotropically consolidated tests will give reliable values of c and G_i , in both active and passive undrained tests, values that will take into account the actual soil anisotropy.

The typical τ vs. γ curves from undrained anisotropically consolidated tests in N.C. clay could be the curves in Figure 3.7; if the passive test curve is rotated 180° around the origin of the stress-strain plot, a single curve is obtained (dotted in Fig. 3.7). If this curve is divided into two new curves at the intersection with the γ axis, the τ axis is translated to this point, and the lower curve is rotated 180° again, then, two curves are obtained to represent the active and passive tests that can be approximated by hyperbolae (Fig. 3.7). Of course, the part of the curve that changed from the passive to the active curve will have a different curvature than the hyperbola, but in most cases, that part is almost a straight line. The translation of τ can be made because the strain is only considered incrementally in the large strain theory, and the curve is identified by the value of τ , which has not

changed.

3.5.10 Formulation

The tangent value of G , G_t and the corresponding value of B , bulk modulus, both dependent on the stress level, will give, when introduced in Equations (3-3), the desired isotropic linearly elastic incremental constitutive equations.

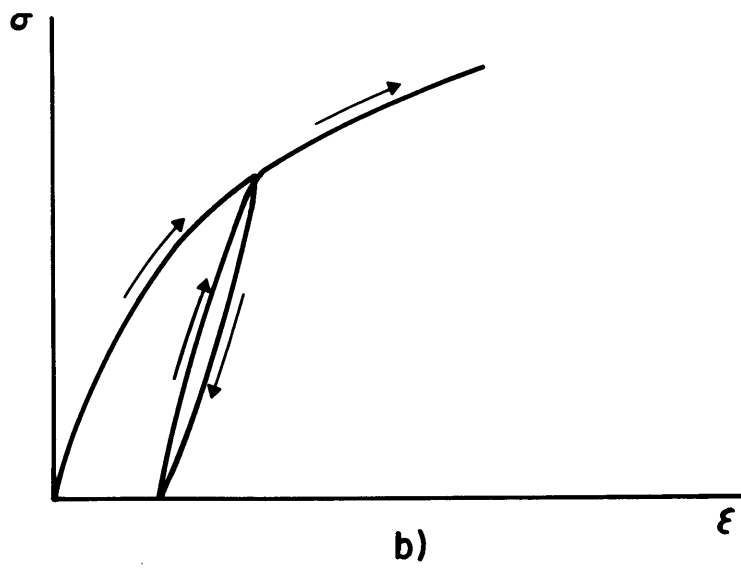
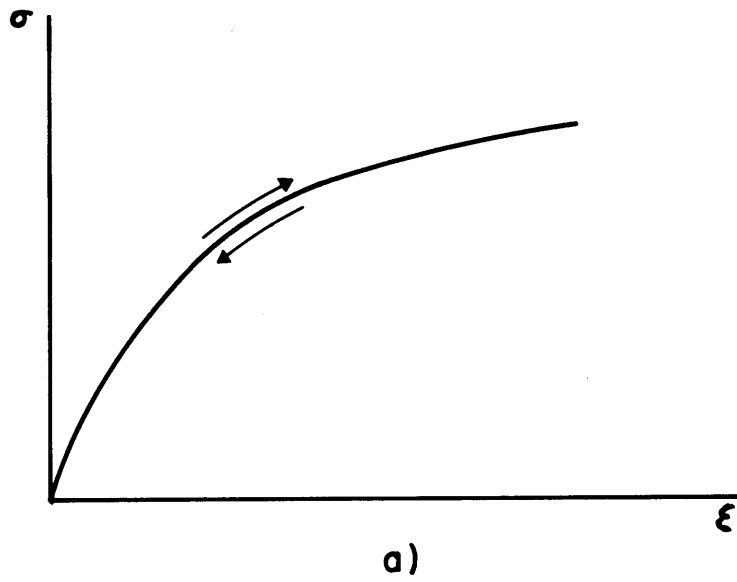


FIGURE 3.1 : ELASTIC a) AND PLASTIC b) MATERIAL

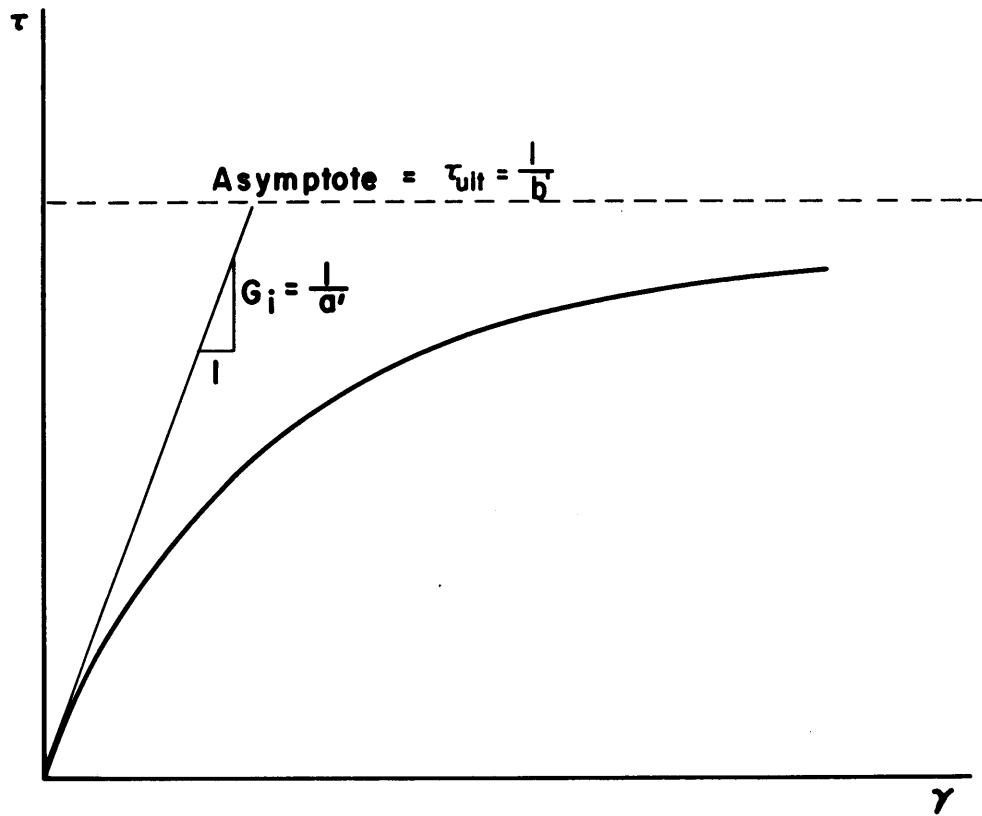


FIGURE 3.2 : HYPERBOLIC STRESS - STRAIN CURVE

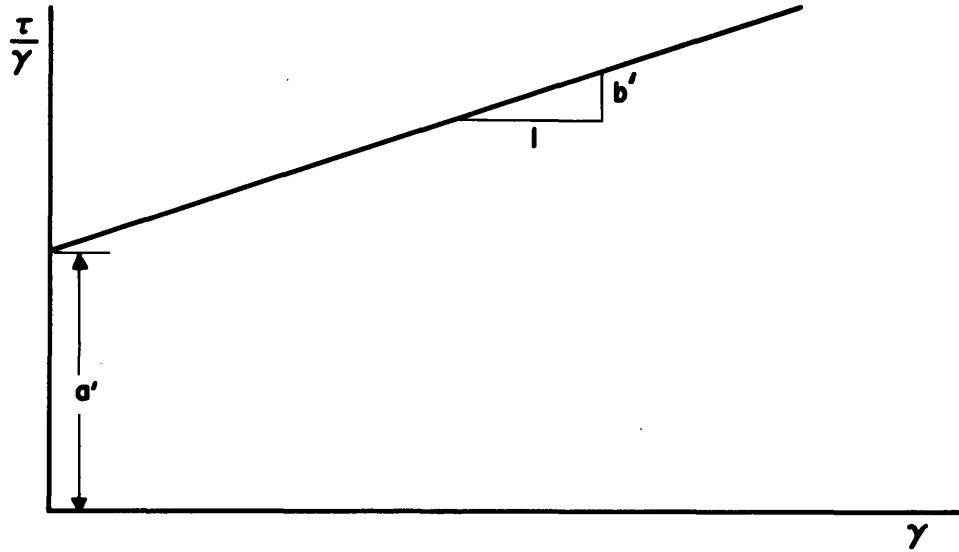


FIGURE 3.3: TRANSFORMED HYPERBOLIC STRESS-STRAIN CURVE

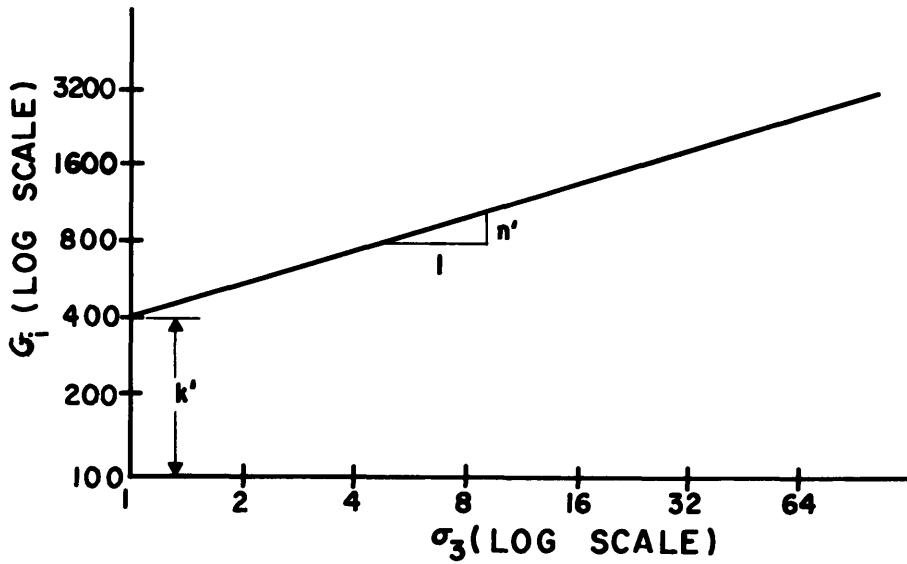


FIGURE 3.4 : VARIATION OF INITIAL TANGENT MODULUS WITH σ_3

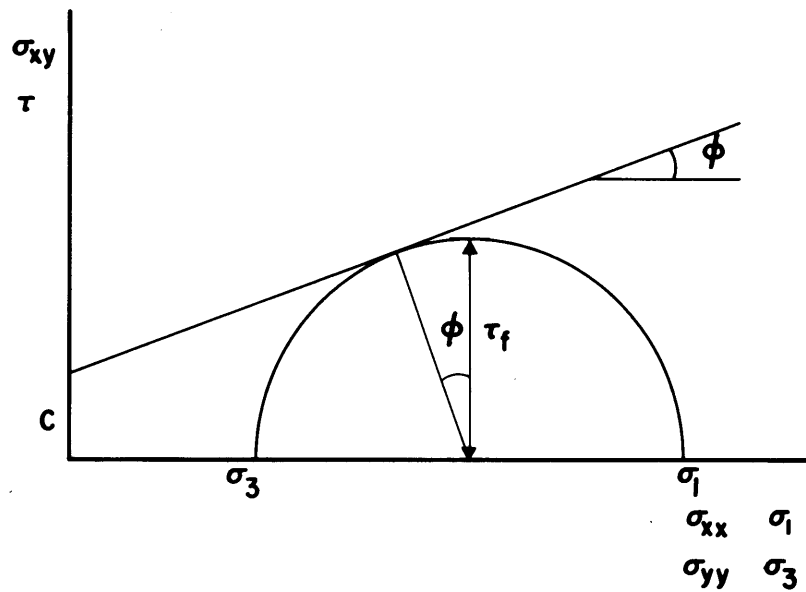


FIGURE 3.5 : MOHR COULOMB FAILURE CRITERION

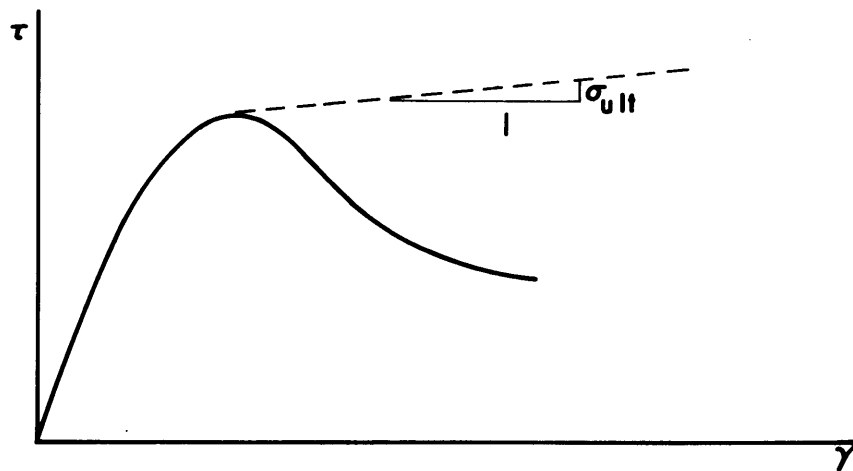
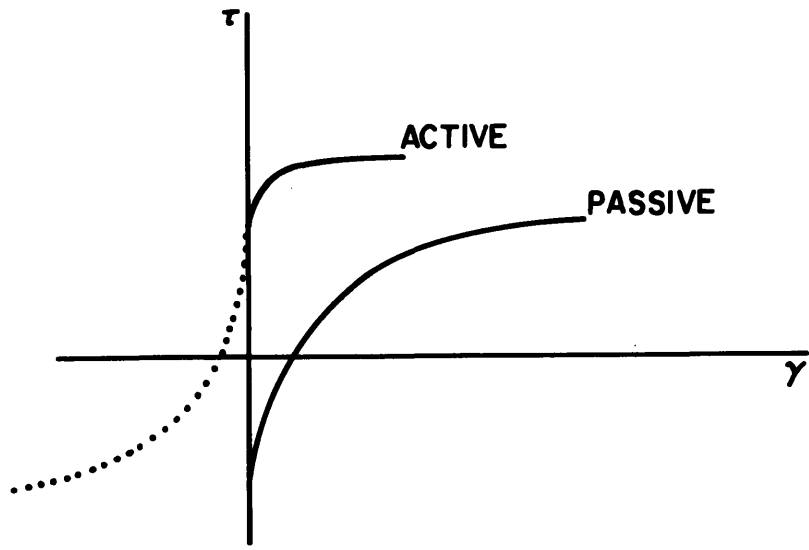
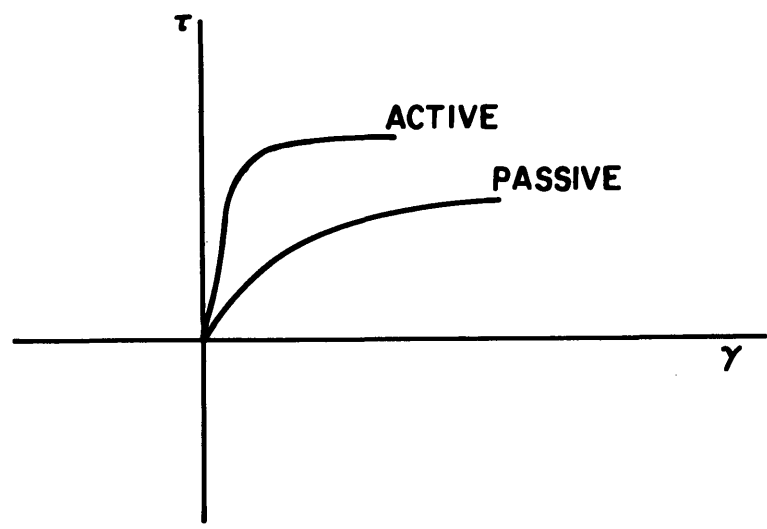


FIGURE 3.6 : DENSE SANDS AND OVER-CONSOLIDATED CLAYS



**FIGURE 3.7 : ANISOTROPIC UNDRAINED TESTS
IN N.C. CLAY**



**FIGURE 3.8 : EQUIVALENT HYPERBOLIC
APPROXIMATION**

Chapter 4

FINITE ELEMENT PROGRAMS

4.1 FINITE ELEMENT ANALYSIS

This powerful tool of numerical analysis was developed originally to find the solutions of field equations for two dimensional structural members. Because of its origin, the method was developed as a generalization of matrix methods in structural analysis. Later, however, the method was described more generally as a numerical technique to solve the "quasi-harmonic function", and its use was extended to many problems in engineering (Zienkiewicz and Cheung, 1967, Oden, 1969).

The finite element method has many advantages compared to equivalent numerical approaches. Because of its versatility and flexibility, it is possible to treat very different problems at many different levels of accuracy. The method can handle any geometric or material properties and any kind of boundary condition. It can also treat composite materials and anisotropy. Together with an incremental procedure the finite element method can treat changing geometry; furthermore, its analogy with structural analysis gives the method a physical nature, always valuable when dealing with real problems.

The literature about the finite element method is

abundant. Zienkiewicz and Cheung (1967) treat the method and give a selected bibliography in each chapter. The method is already well known and no treatment of it will be given here, except for those parts that pertain to large strain analysis, mainly the generation of the stiffness matrix and the integration procedure.

4.1.1 Introduction to the Displacement Method

The continuum is divided into a finite number of elements interconnected at a finite number of joints or nodal points and continuous across their mutual boundaries. In each element, the values of the displacements, strains, stresses, temperatures, and geometrical properties are constrained to belong to a finite class of interpolating functions, such that:

- a) the displacement field is continuous and can be made to satisfy boundary conditions,
- b) such functions can be determined by the values that they have at the nodal points.

The virtual work equation, or the analogous variational principle, that is applicable to the whole continuum can be applied to each element. The finite element approximation will be better for a larger number of elements and/or for a higher class displacement function (Felippa, 1965, Chapter II).

The stiffness of each element is then developed

from the variational principle, and obtained as a system of equations with forces and displacements at the nodes as unknowns. The element stiffness is added to the general stiffness, the sum of the forces in each node must be equal to the external forces acting on the nodes and the displacement of each node is unique.

A system of equations, linear or not, represents the variational principle in the continuum. From a solution for the displacements at the nodes, the values of the strains and stresses can be backfigured with the interpolating functions for each element and the constitutive equations.

In an incremental procedure the equations are linear. The geometry of the continuum and the constitutive equations for each nodal point or element are updated after each increment. The true value of stress is recovered if a large strain analysis is being done.

4.1.2 Element

For the plane strain case, the element is two dimensional. Possible two dimensional elements simple enough to be practical are the rectangle with four nodes and eight degrees of freedom; the triangle with six nodes and twelve degrees of freedom; and the triangle with three nodes and six degrees of freedom. The rectangle would be of no use after the first increment, because it would no longer

be a rectangle. The six node triangle, with three nodes in the vertices and three at the midpoints of the sides, is a very efficient element. The displacement function is a complete second order polynomial and, therefore, it satisfies all the requirements for the deformation field (Felippa, 1965, II.1.2); however, the updating of coordinates would transform the six nodes triangle into a hexagon or a curvilinear triangle, with second degree polynomial equations for the sides. This kind of element would be very difficult to treat.

The three nodes triangle was adopted. It defines the displacement as a first order complete polynomial, and therefore, the strain, stress and constitutive equations are constant throughout the element.

To improve the efficiency of the analysis, the triangular elements are grouped in sets of four to form a quadrilateral with five nodes. The stiffness of each triangle adds up to form the stiffness of the quadrilateral. The center node is independent of any other element outside the quadrilateral, so a static condensation can be done, and the stiffness of the quadrilateral found as a function of only the four outside nodes (Wilson, 1965). The value of the strain and stress for the quadrilateral element is then taken as the average of the values for the four triangular elements.

4.1.3 Stiffness Matrix

The element stiffness is obtained from Equations (2-50) or (B-49) applied to each element. Because all forces are applied as nodal forces instead of as surface tractions, the second member of the equation becomes the simple product of forces at the nodes times the corresponding displacements, in the direction of the forces.

A matricial notation is introduced now for convenience (matrices are denoted by square brackets []).

If [F] is the 6x1 matrix of the incremental force components at the nodes and [δU] the 6x1 matrix of the virtual displacement components at the nodes,

$$\int_{S_0} \Delta f_i \delta u_i dS_0 = [F]' [\delta U] \quad (4-1)$$

where [F]' is the transpose of [F].

The left hand side of the virtual work equation (B-49) is:

$$\int_{V_0} (e_{kl} C_{ijkl} \delta e_{ij} + S_{ij} \delta \eta_{ij}) dV_0 \quad (4-2)$$

In matrix form, Equation (4-2) becomes

$$A \left([U]' [B]' [C] [B] [\delta U] + [U]' [D]' [S] [D] [\delta U] \right) \quad (4-3)$$

Where A is the area of the element, [U]' is the transpose of [U], the incremental displacement matrix, and [B] is a matrix such that:

$$\begin{aligned} [B][\delta U] &= [\delta e] \\ [U]'[B]' &= [e]' \end{aligned} \quad (4-4)$$

where $[e]'$ and $[\delta e]$ are the matrix expression for e_{ij} and δe_{ij} respectively. In (4-3), $[C]$ and $[S]$ are the matrix forms of C_{ijkl} and S_{ij} respectively, and $[D]$ is defined as a matrix such that (Appendix C):

$$[U]'[D][S][D][\delta U] = S_{ij}\delta\eta_{ij} \quad (4-5)$$

If, in (4-3)

$$\begin{aligned} A[B]'[C][B] &= [K_c] \\ A[D]'[S][D] &= [K_g] \end{aligned} \quad (4-6)$$

and if Equations (4-3) and (4-1) are combined

$$[U]'([K_c]+[K_g])[\delta U] = [F]'[\delta U] \quad (4-7)$$

Equation (4-7) has to be true for any set of virtual displacements, then:

$$[U]'([K_c]+[K_g]) = [F]' \quad (4-8)$$

The stiffness matrix for the element is then:

$$[K] = ([K_c]+[K_g]) \quad (4-9)$$

where $[K_c]$ is the normal stiffness matrix for infinitesimal strain analysis, and $[K_g]$ reflects the geometric influence, and is called the "geometric stiffness". Matrix $[K]$ is symmetric. If a quadrilateral element is used, the $[K]$ matrices of the four triangles are added up to obtain the $[K]$ of the quadrilateral where the static condensation may

be done. The statically condensed quadrilateral stiffnesses add up to form the overall stiffness matrix, which is banded and symmetric.

4.2 INCREMENTAL PROCEDURE

The solution of the system of linear equations

$$[\underline{U}]' [\underline{K}] = [\underline{E}]' \quad (4-10)$$

or

$$[\underline{K}] [\underline{U}] = [\underline{E}]$$

where $[\underline{K}]$ is the overall stiffness matrix, and $[\underline{U}]$ and $[\underline{E}]$ the incremental displacement field and incremental exterior forces, give all the unknown incremental forces and displacements, if the problem is well formulated. The state of stress, the new geometry and the new constitutive parameters are then found, and the problem is again formulated and solved in a similar fashion. The procedure described above is a single step procedure. It requires very small increments to obtain a good result.

A common solution in numerical analysis to obtain higher accuracy with large increments is to iterate several times, using each time the values of the parameters from the preceding iteration; iterations are usually made until the consecutive iterations differ by less than a given amount. This can be done in infinitesimal analysis, if the secant elastic parameters are used instead of the

tangential parameters, because the only nonlinearity is the constitutive equations nonlinearity. However, when large strains are involved, the change in geometry has to be taken into account, because it will influence the stiffness matrix as much as will the change in tangential constitutive equations throughout the increment. This is a difficult task, and furthermore, the convergence of the iterative process can not be proven.

A midpoint integration procedure was used. It makes the error a second order error, instead of first order as it would be for a single step per increment procedure (Felippa 1965, IV. 1.5).

The stiffness matrix is calculated at the beginning of the increment, with this stiffness the geometry and state of stress of the body is found for half an increment, the stiffness corresponding to that middle point state is then calculated. This middle point stiffness is used now as the stiffness for the whole increment. The solution, incremental displacements and forces, is now added to the initial state to give the final state for the increment. If, instead of finding the final state, another middle point is calculated and the cycle repeated, additional accuracy may be obtained (see Chapter V), but convergence, again, is not assured.

The incremental strains, to the first order, that

are backfigured from the displacements, are used to calculate the stresses (Equation (2-53)), and also to transform the stresses referred to the old geometry and rotated axes to the stresses referred to the new geometry and original axes (Equation (2-54)). If the middle point integration is done, the stresses that are in equilibrium with the forces, are the stresses obtained from strains that are referred to the middle point geometry, using the constitutive laws of that middle point. The stresses are also referred to that middle geometry. This is a consequence of using the middle point stiffness, which is equivalent to the establishment of equilibrium in the middle point geometry, with everything referred to that geometry, as can be deduced from the derivation of Biot's incremental formulation (Chapter II and Appendix B). To obtain the components of the stress referred to the new geometry and original axes, the strains in the transformation Equation (2-54) have to be calculated from the displacements that would have to be imposed on the body to obtain the final geometry from the middle point geometry.

4.3 POST YIELDING STRESS

The Tresca material constitutive equations have a sharp change when the yield occurs and the formulation changes. If the yielding occurs in the middle of an increment, the use of the elastic formulation increases

the stiffness of the finite element model, so an iteration is made and the increment repeated with the perfectly plastic formulation. In the hyperbolic stress-strain relation, the change is very smooth, so no iteration is made.

For both formulations, after yielding the stresses do not remain on the yield surface, in the Tresca material formulation because of the finite size of each increment, and in the hyperbolic stress-strain relation because the value of the post yielding shear modulus (G_{ul}) is not 0. If the value of the stresses are not corrected back to the yield surface, they will increasingly diverge, and the error will be significant.

The correction is made at the end of each increment; the maximum shear stress τ is brought back perpendicular to the pseudo yield surface, defined in each case by the value of τ corresponding to the yielding state of stress (formulation and figure in Appendix D). The angle θ that the principal compressive stress forms with the vertical is kept constant during the correction.

The approximation leads to faulty equilibrium between stresses and forces; therefore, the value of the calculated τ should be less than 10% larger than the corresponding yielding value of τ . This limits the size of the increments in order to obtain equilibrium.

4.4 COMPUTER PROGRAMS

Two computer programs were written, both for plane strain analysis, one with the Tresca material formulation and the other with the hyperbolic stress-strain relation formulation. A different logic is used, but many of the subroutines and variable names are common. They are written in Fortran IV language, level G, to be used with a storage capacity of 450K bytes in double precision. External temporary storage is required, but the stiffness matrix is assembled and solved in block , in core. The storage has been reduced to a minimum by recalculating the necessary matrices instead of storing these matrices, except in rare occasions. This resulted in a more economical procedure for the small size meshes of the test runs and the particular pricing of time, core usage and input-output operations in the IBM 360-65/40 ASP/MVT System at the Information Processing Center in MIT, where the runs were made.

Appendix E gives the User's Manual and Appendix F gives the description of the main program and the subroutines.

Chapter 5

TEST RUNS

The behavior of the program is discussed in this chapter. Two types of test runs were made:

- a) simple examples to help in the debugging of the program and to verify equilibrium and failure
- b) models of experimental cases.

5.1 COMPRESSION TEST

The problem in two dimensions is reduced to the vertical compression of a square section of unit sides. The square will deform into a rectangle; the vertical stress will be equal to the applied force divided by the width; the other stresses must be zero. If an elastic material is used, such that the relation between the incremental strains and stresses is a linear relation independent of the stress or strain level, it can be seen that (Appendix G):

$$\begin{aligned} u &= XP \\ v &= (1 + \frac{Y}{X} XP) - 1 \end{aligned} \quad (5-1)$$

where u is the total increment of width, v the total increment of height, P the vertical force, and:

$$\begin{aligned} X &= -\frac{1}{E} (v + v^2) \\ Y &= \frac{1}{E} (1 - v^2) \end{aligned} \quad (5-2)$$

where E and ν are Young's modulus and Poisson's ratio respectively. Test runs were made for values of E and ν such that the bulk modulus B was 100 and the shear modulus G was 2. Table 5.1 presents the results of tests made with FELSP and with a mesh formed by one element. σ_x and σ_{xz} were 0 all the time. FELSH was checked and the results were the same as that for FELSP. A run was made with eight elements and the results were symmetrical and identical with the correspondent run with one element.

The results in Table 5.1 were obtained with Biot's formulation, where the geometric stiffness matrix becomes zero, because there is no rotation. The same problem was run with Felippa's formulation, and the results were wrong by ten to twenty percent. Hence, the tensorial formulation was reconsidered and Biot's formulation adopted. Also, from previous runs on the same problem, it was found that the best procedure to obtain the stresses with the midpoint integration is the procedure explained in Chapter 4.

Table 5.1 includes two kinds of information

a) Displacement values

It can be seen that the midpoint integration is very effective in obtaining good results with a small number of increments.

b) Equilibrium

The values of σ_z should be in equilibrium with P. A cause of lack of equilibrium is the fact that the incremental strains are not infinitesimal. The main effect is observed, in this case, in the transformation of stress Equations (2-54). The values of the stresses referred to the rotated axes and the old geometry are in equilibrium with the forces; however, when the strains are not infinitesimal, the transformation equations (2-54) are not exact and an error is introduced in the value of stresses referred to the general axes and new geometry; lack of equilibrium results then. The performance of Equation (2-54) is improved by using Felippa's version, Equation (2-40). The effect of this error is isolated by a single step procedure where no midpoint integration is done, (0 iterations). However, from Table 5.1, it can be seen that the equilibrium is very good for zero iterations; the cause for the lack of equilibrium in the other cases has to be the midpoint integration. Again the stress transformation must be the cause; now the strains used in Equations (2-54) are also obtained in an approximate way.

5.2 SIDE WALL

This is another simple case where the main phenomenon involved is shear, if a smooth bottom and an undrained case are considered.

The solution for the theoretical Rankine active

case is (Lambe and Whitman, 1969):

$$\sigma_x = -[\gamma_t Z - 2S_u] \quad (5-3)$$

The height of the wall is six meters and $\gamma_t = 1.8 \text{ T/m}^2$. K_0 was chosen as 0.5.

A first run with FELSH and with $S_u = 1.75$ gave the results shown in Figures 5.1 and 5.2. Figure 5.1 is obtained from the stresses in the elements next to the wall, in the first increment after all the elements were in failure. The theoretical resultant force acting in the wall is, from the integration of Equation (5-3), -11.4 T . From the stresses shown in Figure 5.1, the resultant force is -10.4 T . In Figure 5.2 the incremental force is plotted against the wall displacement. As it can be seen the failure occurs at $\Delta F = +6.8\text{T}$; that means that total force is -9.4T , because the initial force under K_0 conditions will be -16.2T .

Figure 5.3 gives the stress distribution in the wall, after failure, for four different cases, all of them with $S_u = 2.6\text{T/m}^2$. From these four runs and some others, it was found that the values given by stresses and by forces in the wall differ only by about 0.2 percent when forty increments were used and by about 5 percent when ten increments were used. In the case of the run with $S_u = 1.75 \text{ T/m}^2$, the lack of equilibrium was about 10

percent, as has been seen above.

Three aspects can be considered.

1) Failure

Figure 5.2 shows that there is no increase in the thrust of the fill over the wall once the active condition was reached, as the theory predicts. If the problem is run with FELSH, a slight increase in ΔF is obtained because of the shear modulus.

2) Values of σ_x at failure.

It can be seen that the solutions for $S_u = 2.6 \text{ T/m}^2$ are better, in general, and that a larger number of increments gives better results, and that quadrilateral elements give better values than triangular elements. The reason behind obtaining better values for a higher S_u is that, for $S_u = 1.75 \text{ T/m}^2$, the lower part of the wall is in failure under K_0 conditions, from the program's stand point. Because of that, the correct solution is never obtained. The fact that the use of FELSH (Fig. 5.3) gives the same kind of behavior has a similar origin; the shear modulus will be very low for the lower part of the wall in the hyperbolic approximation.

3) Equilibrium among forces and stresses

The use of higher S_u , such that no element is initially in failure, gives better results. The use of more increments clearly improves the equilibrium. Because

strains are really small in this case, the lack of equilibrium cannot be caused by the transformation equations as in the case of the unit cube. The cause is the reduction of post failure stresses to the yield surface. When more increments are used, the modification is smaller and the equilibrium is better. This is checked by verifying that before any element fails, equilibrium is satisfied in all runs.

5.3 FOOTING ON LAYER OF UNDRAINED CLAY

This case was taken from Christian, 1966. The depth of the layer is 140 feet, the loaded surface has a width of 120 feet. Although the soil is considered undrained, the Poisson's ratio is taken as 0.2 and B is 1660 T/ft^2 , while G is 1250 T/ft^2 . The value of S_u is taken as 1.75 T/ft^2 . The standard finite element mesh that was used is given in Figure 5.4. When triangular elements were used, each quadrilateral was divided into two triangles. From the value of S_u and the width, the bearing capacity (Lambe and Whitman, 1969) is:

$$\text{Bearing capacity} = 5.14 S_u = 9 \text{ T/ft}^2 \quad (5-4)$$

Figure 5.5 gives the settlement of the center of the footing for triangular elements and quadrilateral elements, both with FELSP and FELSH. The values of B and G used in FELSP are used in FELSH as initial values. Three main results are obtained from the comparison.

First, the hyperbolic stress-strain relation gives a smoother curve than the plastic relation. Second, the prediction of failure improves when the hyperbolic approximation is used. Finally, the quadrilateral element is softer than the triangular element.

All the test runs in Figure 5.5 were run with one iteration and twenty increments, with the standard mesh.

Figure 5.6 shows the influence of increasing the number of elements and the number of increments. The elements are triangular and FELSP was used.

It can be seen that increasing the number of elements gives a better prediction for the bearing capacity. However, the result is very irregular and unstable. A large heave is observed in increment 20 although the load is increased. The run with more increments gives the same value for the bearing capacity, but a much smoother behavior after failure. This suggests that the modification of stresses to stay in the yielding surface may be one of the causes of lack of smoothness and instability.

Figure 5.7 shows the influence of the midpoint integration; again the result improves when the midpoint integration is used. The other curve shows the result obtained when elements that yield during the increment

are considered as yielded throughout the increment instead of elastic as usual. The program requires more time for the softer procedure, because extra iterations have to be done, but the results improve.

FELSP with quadrilateral elements and twenty increments is used to obtain the results of Figure 5.7.

All the runs represented in Figures 5.5, 5.6 and 5.7 were made without taking into account the fact that unloading stress-strain laws are different than loading stress-strain laws. Many attempts were made to obtain results using the general procedure, all of them unsuccessful. The signs of both shear strains and stress were considered as a measure of loading and unloading. The increment was repeated with the correct stress-strain law; usually, the program entered in a closed iteration cycle, if the cycle was then broken, the results were unreliable, and sometimes a high instability was obtained.

The main problems were obtained when some elements were in failure; in general, the elements in failure were the ones that changed sign. The modification of stresses seemed a possible cause of trouble; however, an increase in increments and elements had no positive influence. Furthermore, if the modification of stresses was not done, the result was more unreliable and instable.

Similar problems were encountered when displacements were imposed, instead of forces.

The same kind of problems were found in the other examples when the unloading law was considered; therefore, all the results in this chapter are obtained for materials that in FELSP remain plastic once they have yielded, and in FELSH behave as non-linear elastic solids.

5.4 SIMPLE SHEAR

This case is based in experimental results reported by Duncan and Dunlop (1969). FELSH is used, the soil parameters are obtained from the reported results of plane strain tests in San Francisco Bay Mud. Table 5.2 gives the parameters that were obtained and used in the modeling of the simple shear test. K_0 is about 0.45. The consolidation stress was taken as 1 Kg/cm^2 ; the tests were made at consolidation stresses ranging from 0.9 to 1.34 Kg/cm^2 . The tests were made in the simple shear apparatus developed at Cambridge, England; the dimensions of the sample are 6x2 cm.

Figure 5.8 presents the comparison among experimental and computed values of the horizontal shear stress in the center of the sample. All the results are from runs with a mesh of forty-eight square and equidimensional elements, one iteration and ten increments.

Runs with four times more elements in the mesh and four times more increments give the same results as the run with ten increments and forty-eight elements, as far as shearing stress in the center of the sample is concerned.

In Figure 5.8, it can be seen that the use of large strain theory and modification of coordinates gives better results than the use of the classical infinitesimal strain approach. The other curve in Figure 5.8 is obtained when the initial values of K' are increased from 10.42 and 62.5 Kg/cm^2 to 20 and 80 Kg/cm^2 respectively. It shows how dependent is the result on the initial values. The fact that all computed curves tend to be stiffer at failure than the corresponding experimental curves can be caused by the use of an ultimate shear modulus greater than zero, when in many cases the clays are actually strain softening.

Figure 5.9 presents the distribution of stresses in the upper face of the sample at ten percent strain. It can be seen that the experimental decrease in vertical force is represented in the computer modeling. The influence of the number of elements is here important, smoothing the distribution of forces. It can also be seen that equilibrium among stresses and forces is fairly good.

Finally, Figure 5.10 gives the plastified zones for both runs with forty-eight and one hundred-ninety-two

elements. The results are perfectly symmetric about the center of the sample, so only one half is represented.

The value of B , Table 5.2, is a low value; runs were made with a higher value ($21,000 \text{ Kg/cm}^2$) and strange results were obtained. The value of the normal stresses became positive after two increments. If the modification of coordinates was passed over, the result was correct; it was verified that only the modification of coordinates was causing this problem, when the bulk modulus was very big.

5.5 MODEL FOOTING

Some model footing cases were run in Boston Blue Clay by Kinner (1970). The parameters of the used clay are obtained from results of plane strain tests; tests A.6 and P.4. The Figures 5.11 and 5.12 show how the parameters are obtained.

K_0 is 0.53, K_B is 1000, the ultimate value of G/σ_{ic} is 0.27; the soil is consolidated at 3.83 kg/cm^2 . Although the problem is an undrained case with $\nu = 0.5$, K_B is chosen small to avoid numerical instabilities.

Two runs were made, one with a mesh of two hundred forty-eight elements and twenty increments, the other with a mesh of forty-two elements and eighty increments. The normalized results of the settlement versus the force per unit area are presented in Figure

5.13. Figure 5.14 gives the results in the initial part of the curve.

The results are bad. First, there is a tremendous lack of equilibrium among stresses and forces on the footing. Second, the program does not identify the failure load. Finally, the settlement versus force per unit area curve before failure is not predicted when the finer mesh and less increments are used; the prediction is a little better for the run with a coarse mesh and more increments (Figure 5.14).

The lack of equilibrium increases with the number of increments, instead of decreasing as in other cases.

The fact that the active curve in Figure 5.11 can not very well be model by a hyperbola, and the fact that there is a residual G_{ult} as opposed to the strain softening obtained in test A.6, may be what causes the runs not to fail.

A conclusion that can be obtained from these runs is that an increase in increments with coarse meshes is a better way to gain accuracy than an increase in the number of elements with small numbers of increments.

It can also be seen that the solution for the stresses is better than the solution for the forces, because the stresses are modified to remain on the yield

surface, while the forces are not.

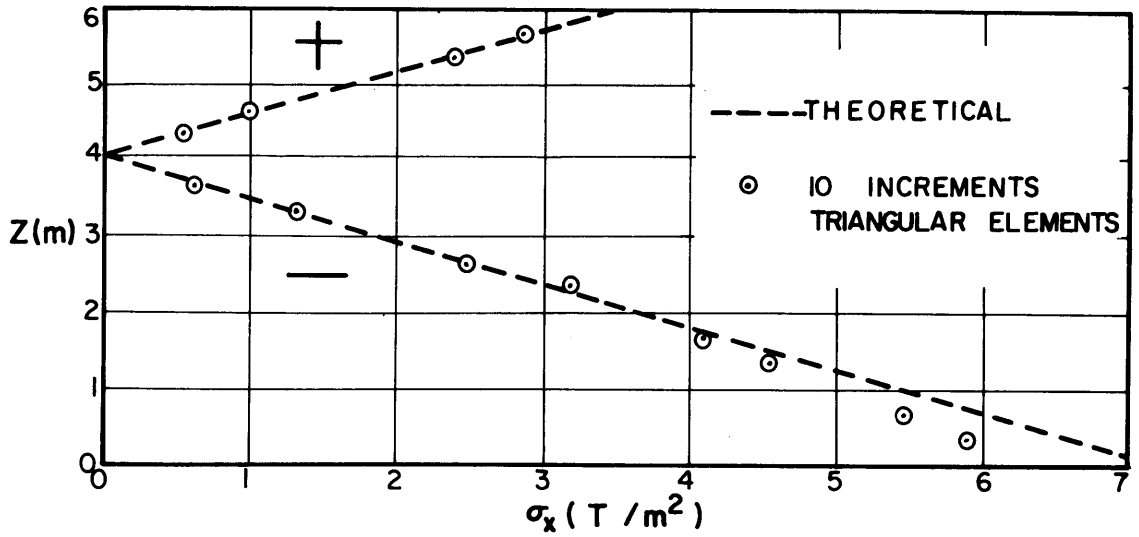


FIGURE 5.1: SIDE WALL ACTIVE ,STRESS DISTRIBUTION AT FAILURE , $S_u = 1.75 T/m^2$

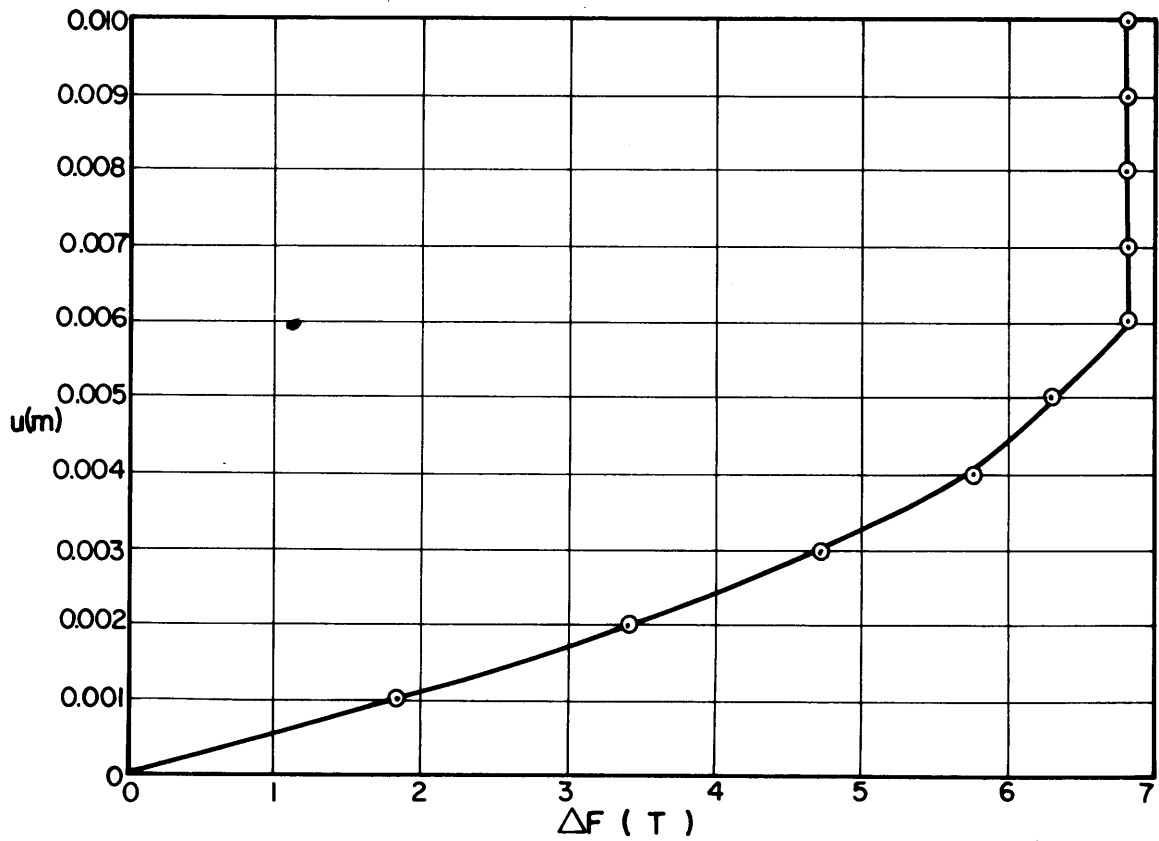


FIGURE 5.2: SIDE WALL ACTIVE ,FROM K_0 TO K_0

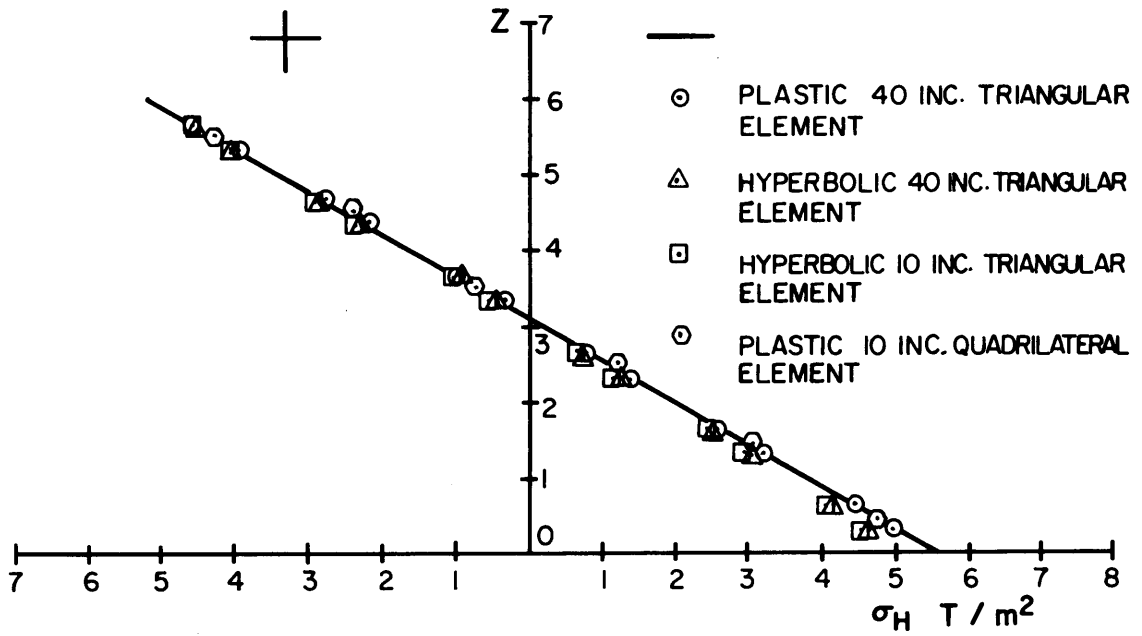


FIGURE 5.3: SIDE WALL , ACTIVE , SMOOTH BOTTOM ,
 STRESS DISTRIBUTION IN THE WALL
 WHEN ALL ELEMENTS ARE IN FAILURE
 $S_u = 2.6 T / m^2$

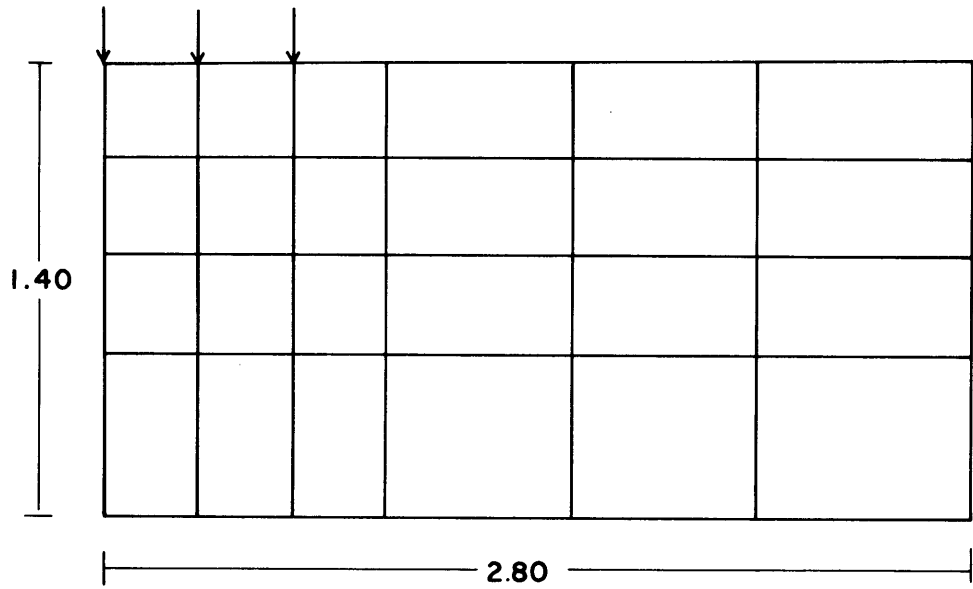


FIGURE 5.4: STANDARD MESH FOR FOOTING ON LAYER

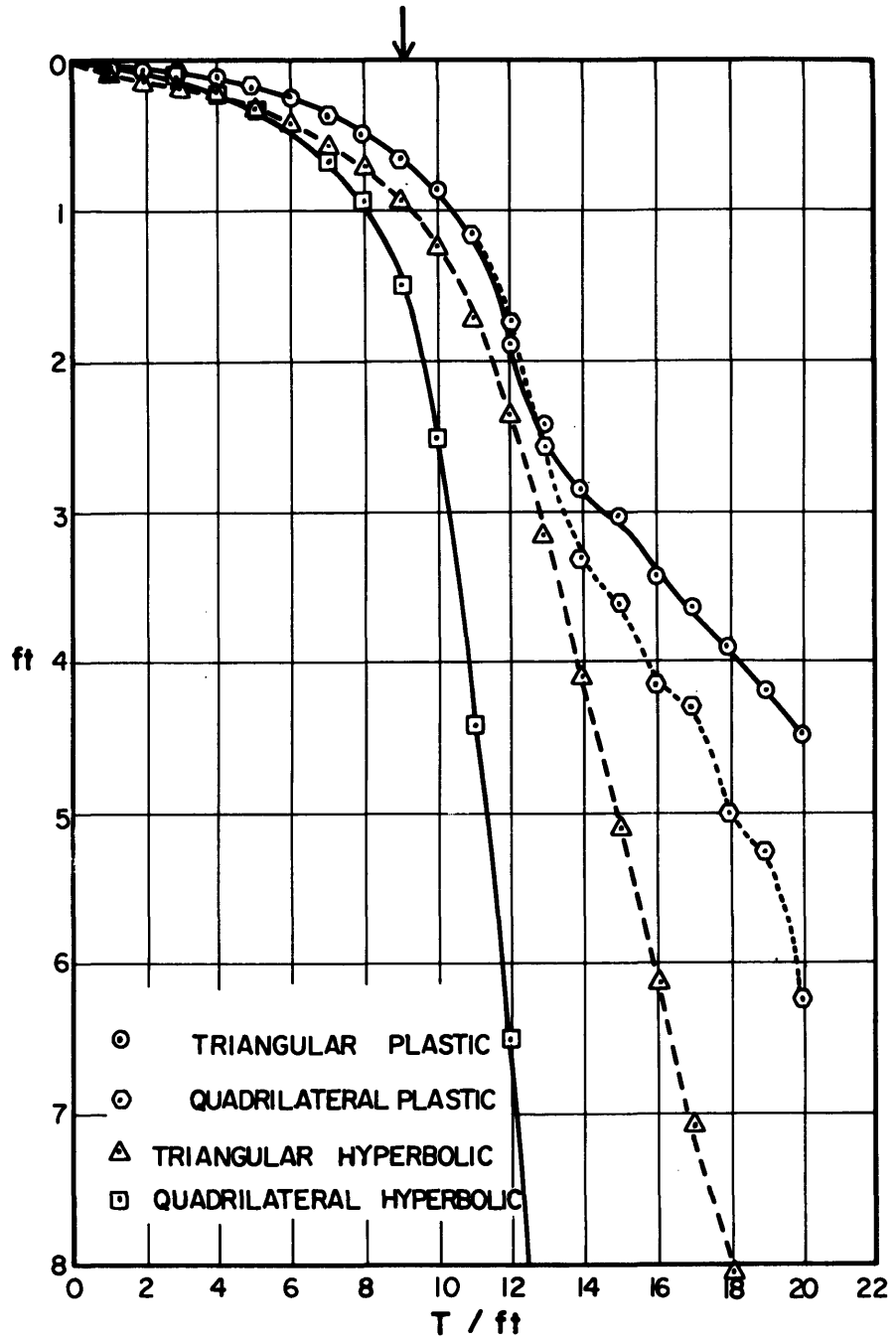


FIGURE 5.5 : ELEMENT TYPE INFLUENCE

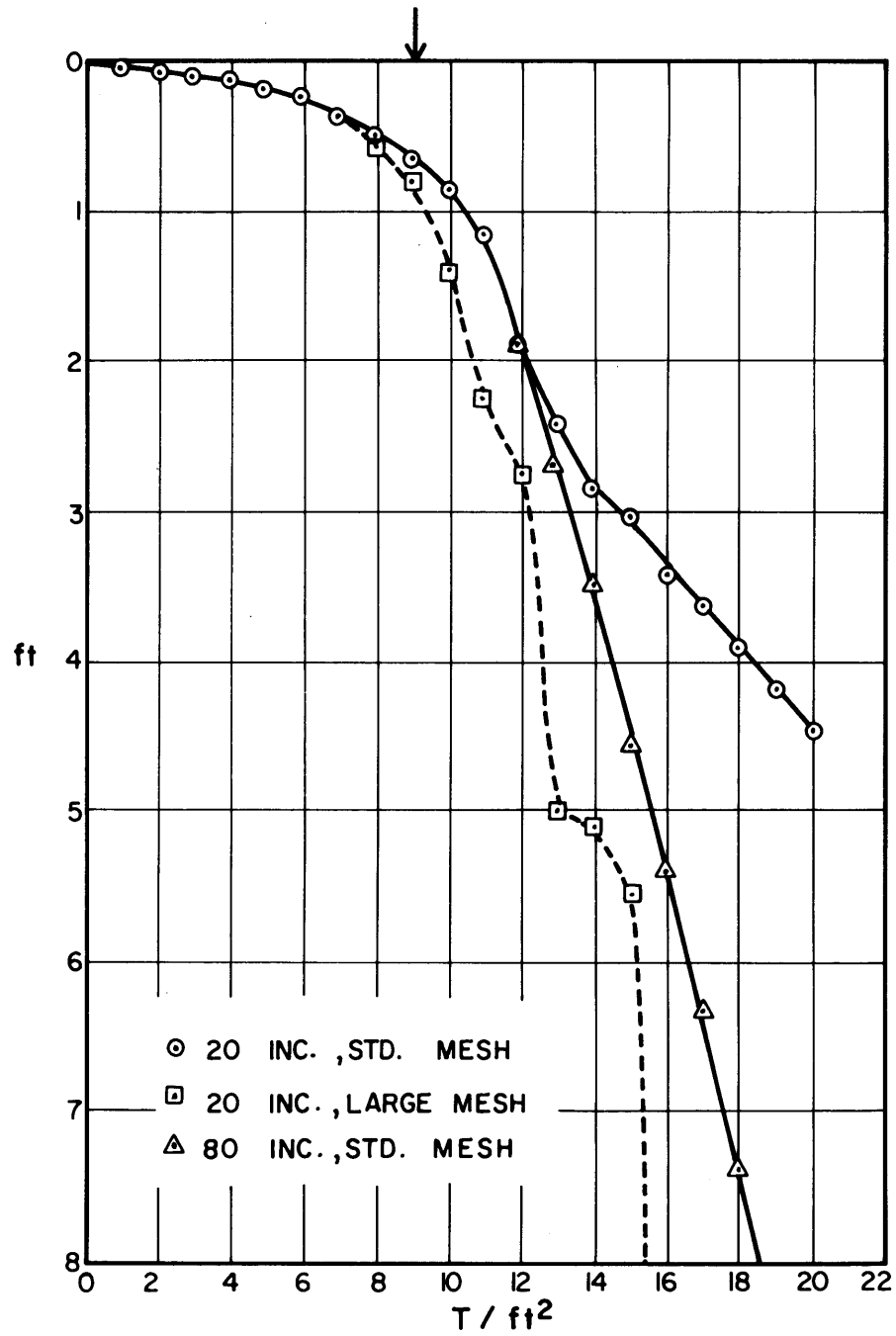


FIGURE 5.6: MESH AND INCREMENT INFLUENCE

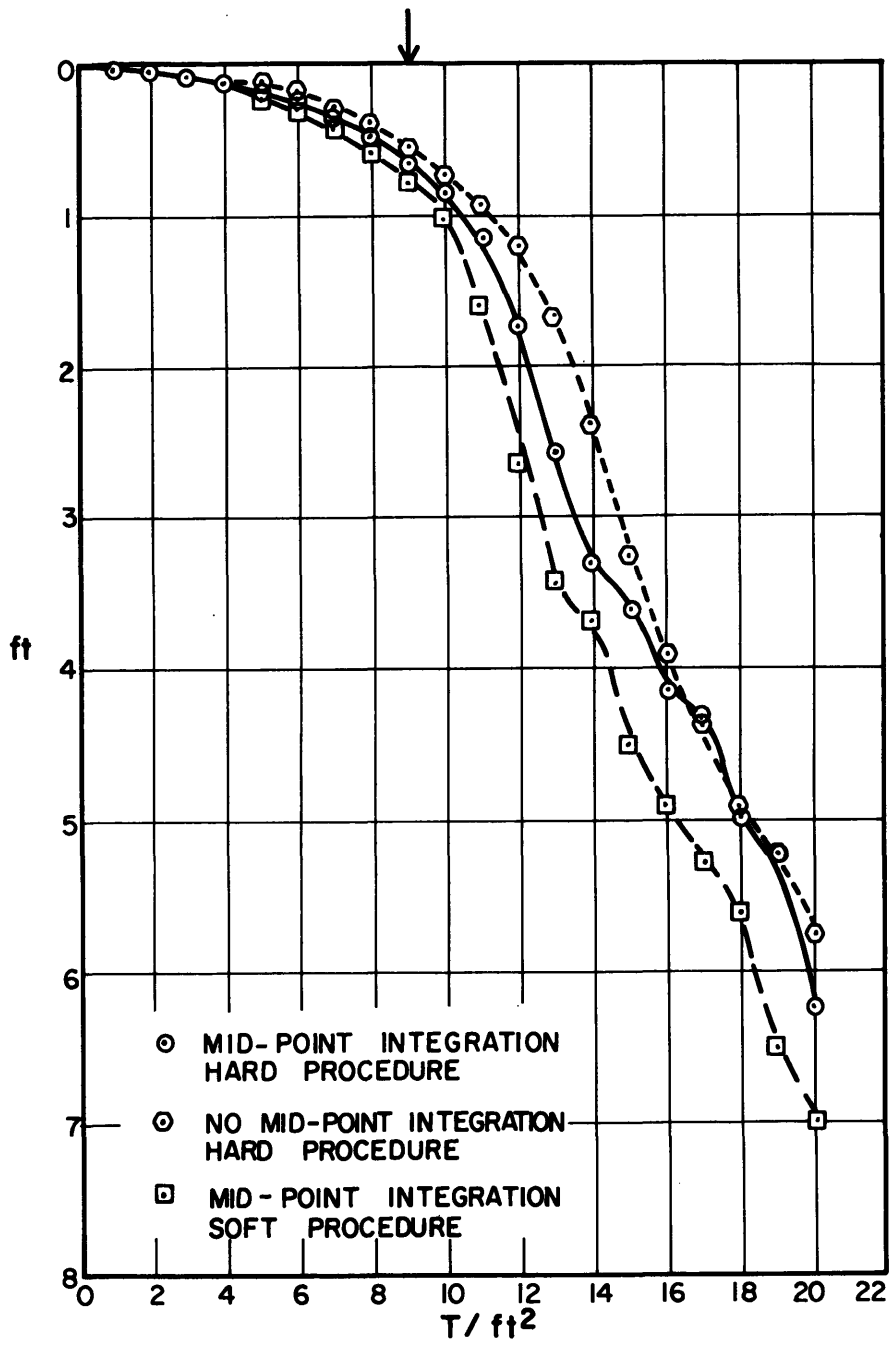


FIGURE 5.7: INTEGRATION PROCEDURE INFLUENCE

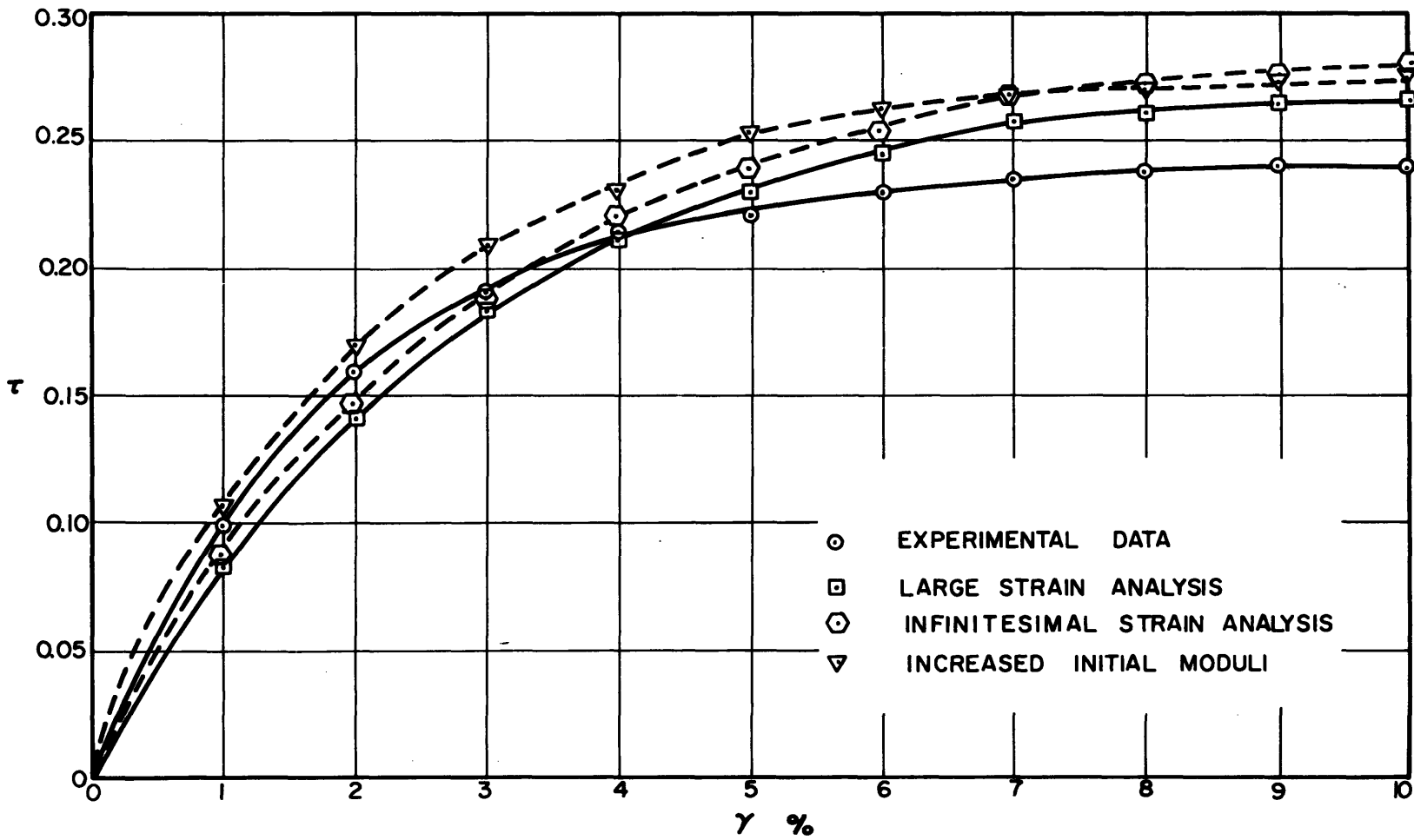


FIGURE 5.8 : SIMPLE SHEAR

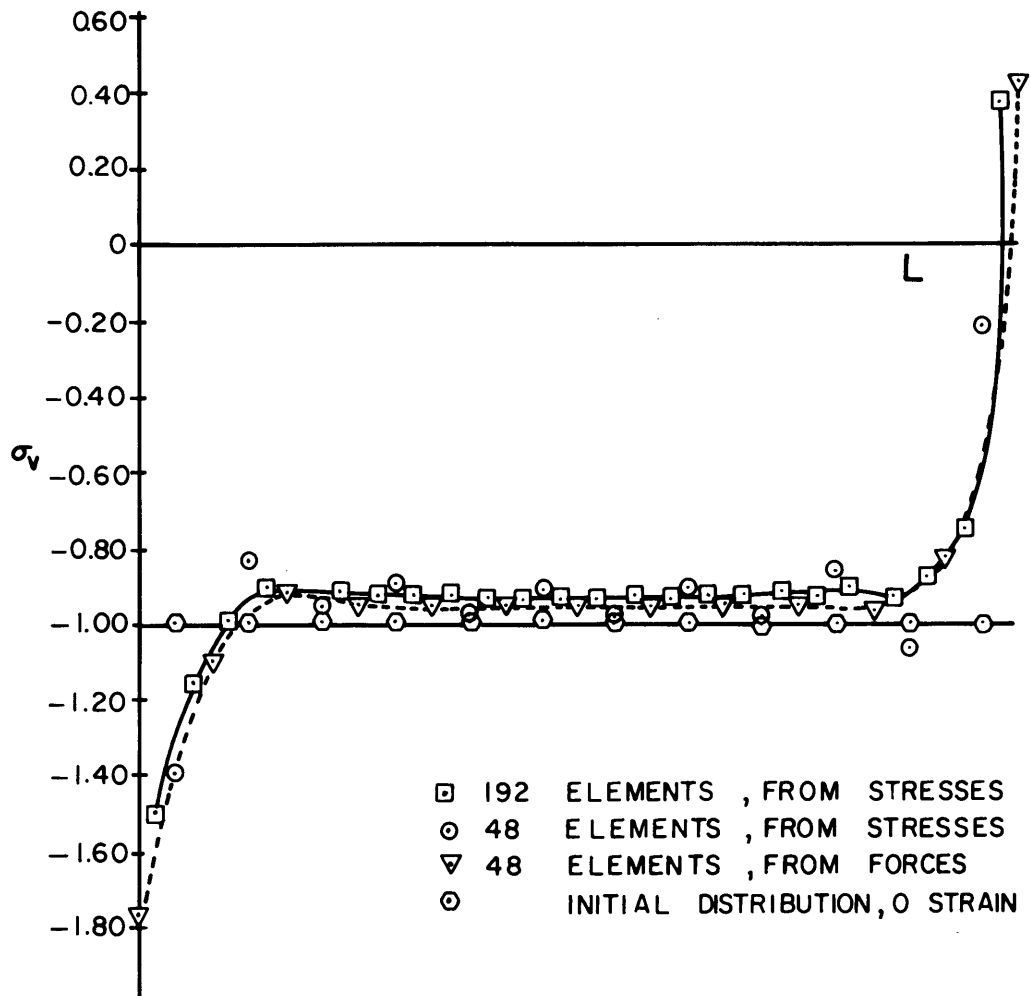


FIGURE 5.9: SIMPLE SHEAR , NORMAL STRESS DISTRIBUTION IN THE UPPER FACE OF THE SAMPLE AT 10% STRAIN

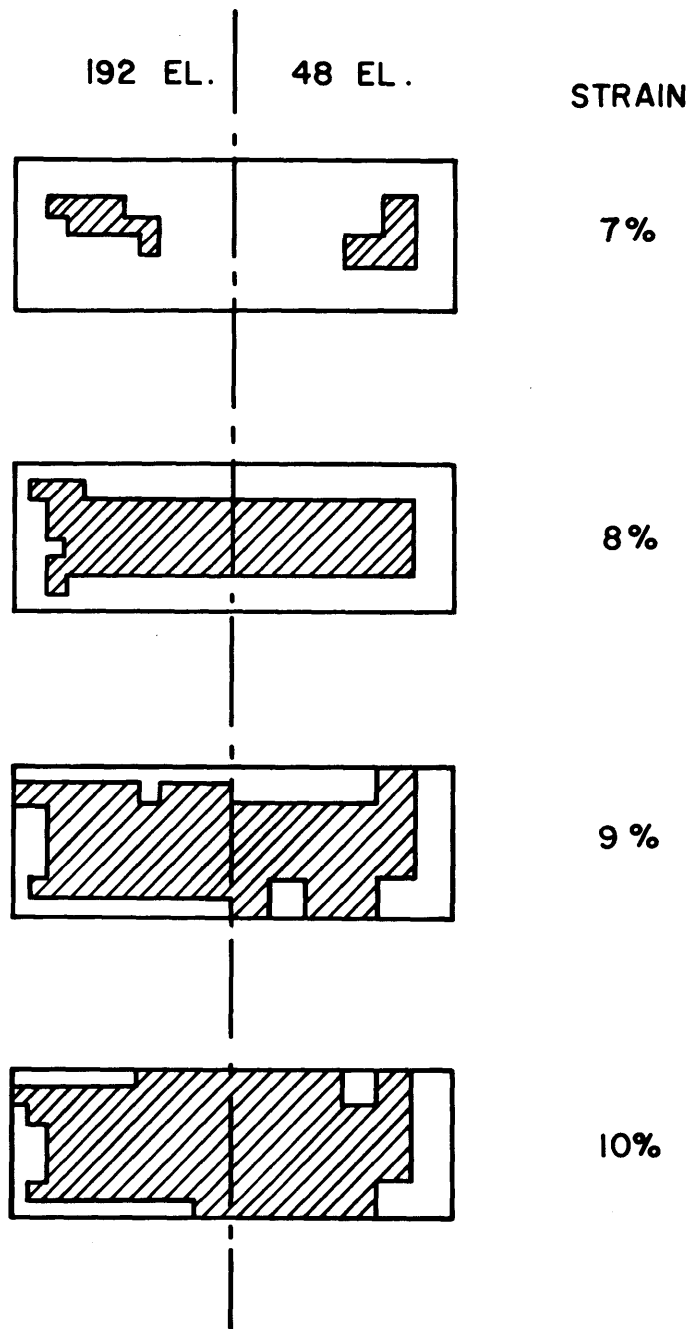


FIGURE 5.10 : SIMPLE SHEAR YIELDED ZONES

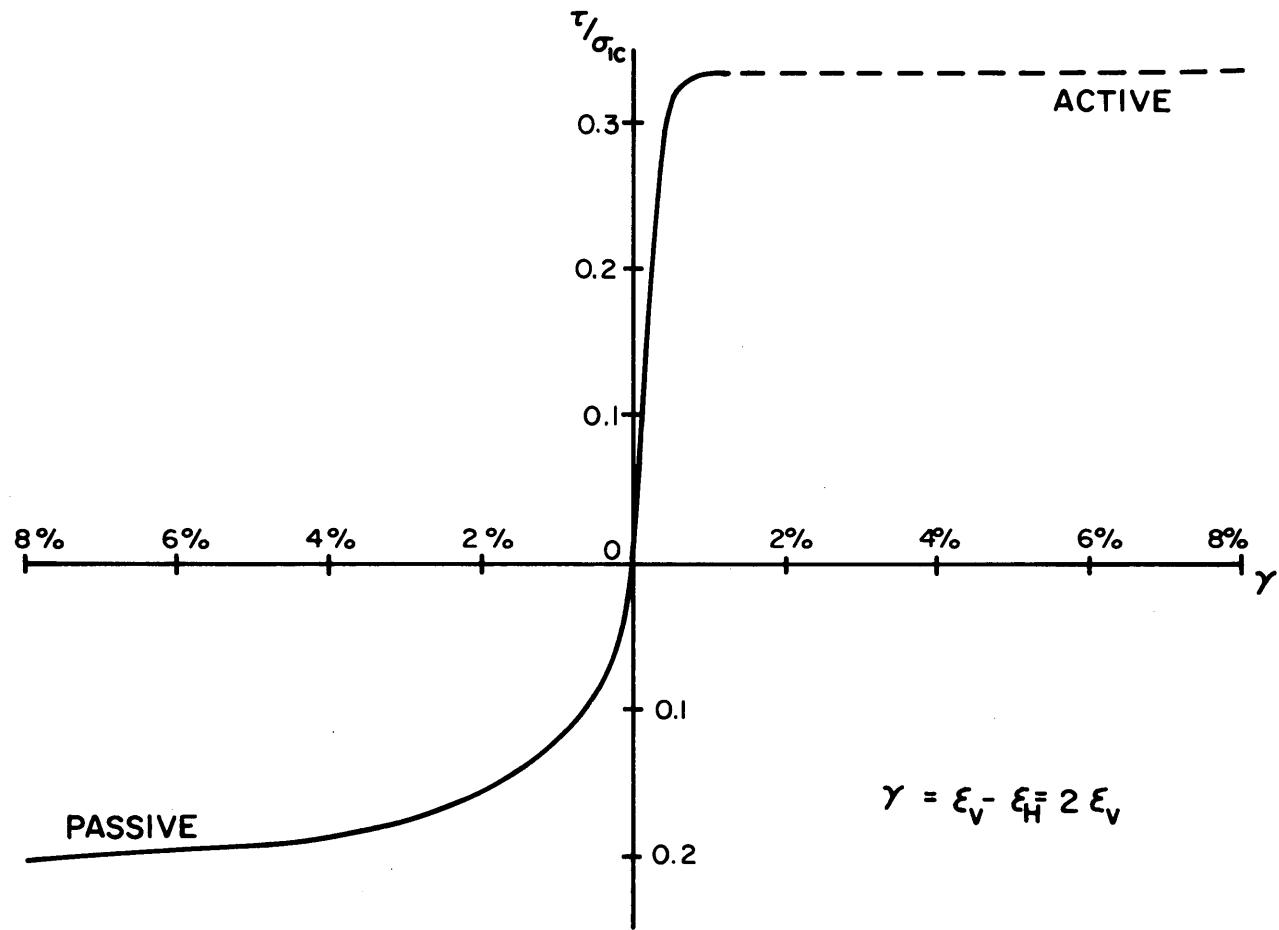


FIGURE 5.11 : STRESS - STRAIN CURVES FOR BOSTON BLUE CLAY

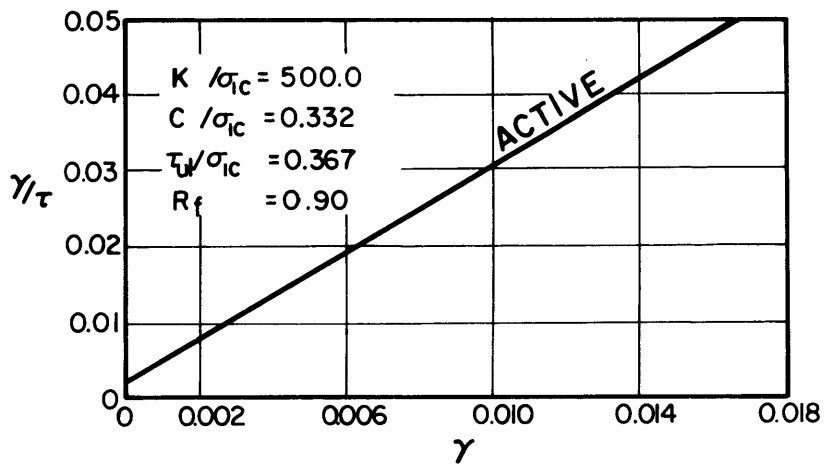
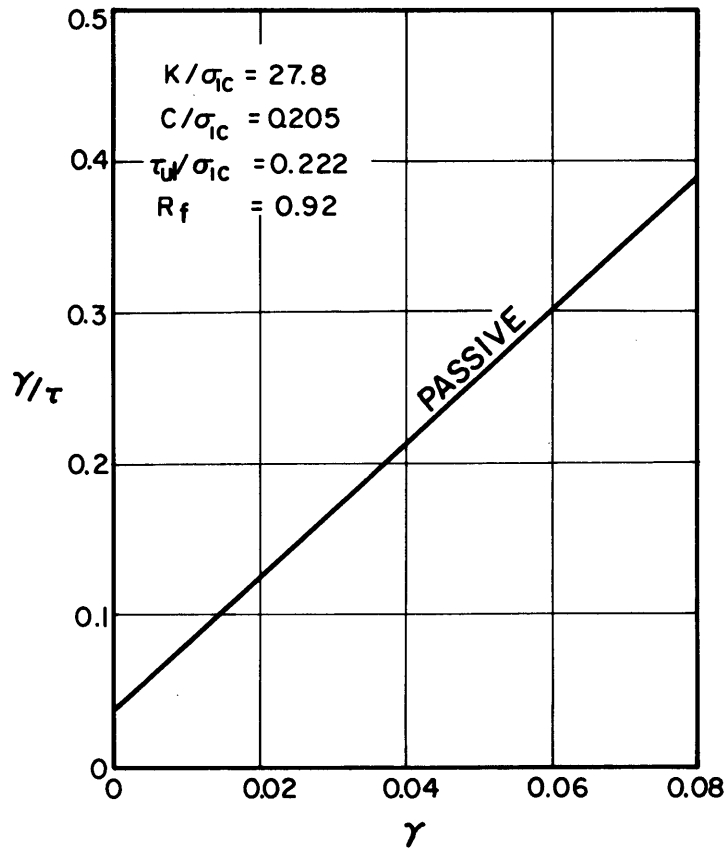


FIGURE 5.12: STRESS - STRAIN PARAMETERS FOR BOSTON BLUE CLAY.

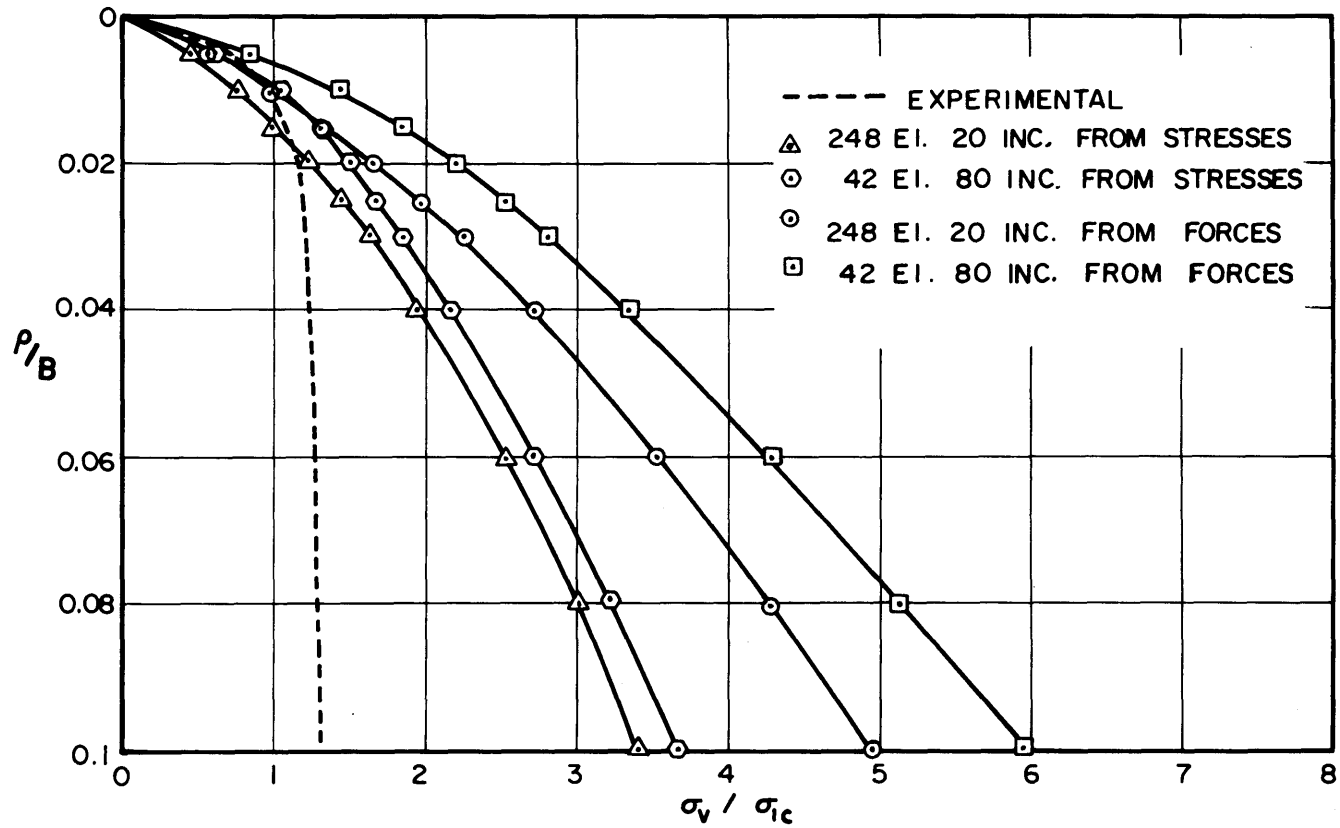


FIGURE 5.13 : MODEL FOOTING , SETTLEMENT CURVES

100

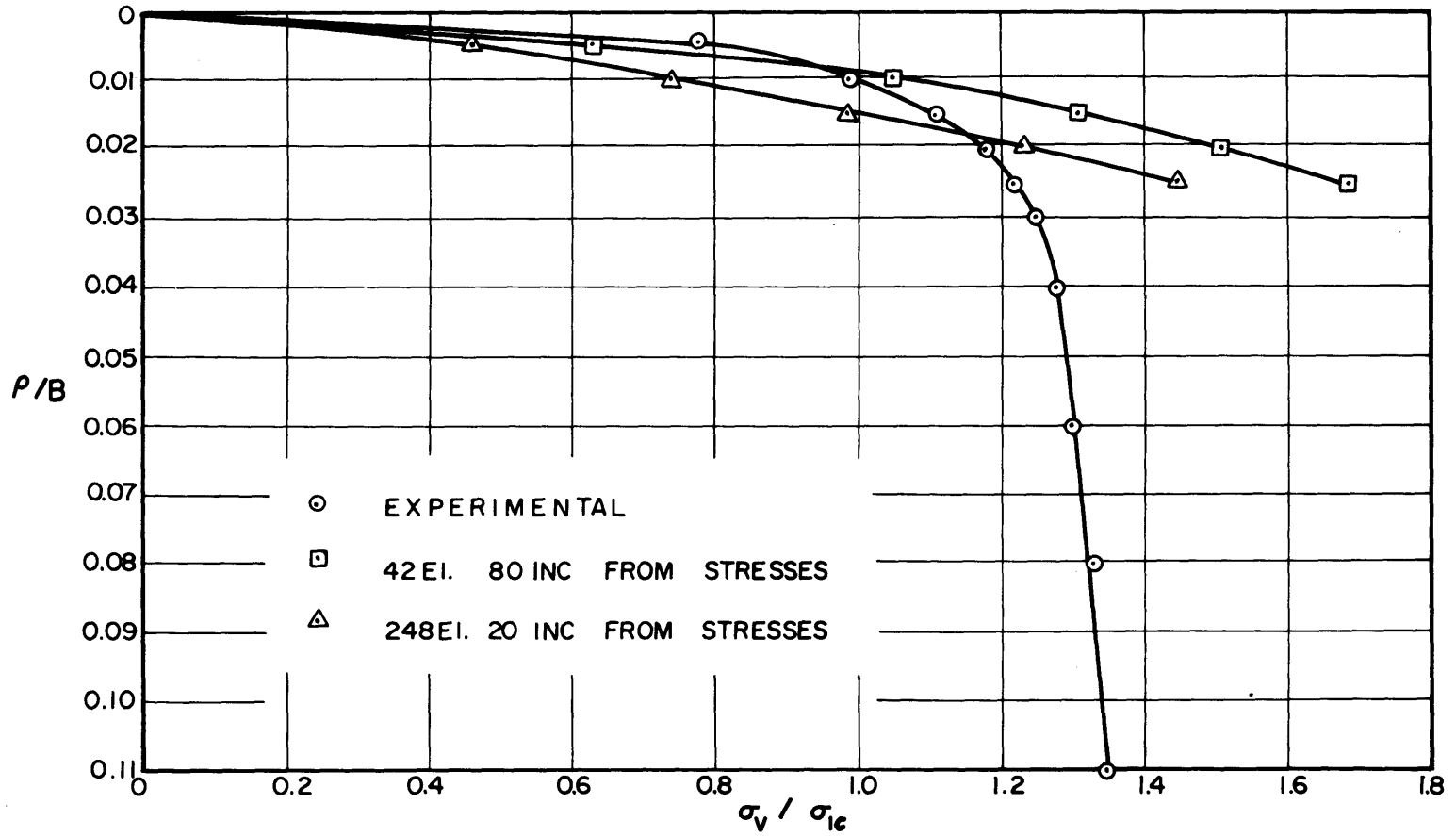


FIGURE 5.14 : MODEL FOOTING ON CLAY . FIRST PART OF SETTLEMENT CURVES

	P = - 1			P = - 2		
	u	v	$\frac{\sigma_z - P/A}{P/A} 100$	u	v	$\frac{\sigma_z - P/A}{P/A} 100$
THEORETICAL	0.1225	- 0.1133	0	0.245	- 0.2039	0
1 Inc. , 1 ft.				0.245	- 0.1982	1.2 %
5 Inc. , 1 ft.	0.1225	- 0.1133	2 %			
10 Inc. , 1 ft.				0.245	- 0.2039	4.8 %
25 Inc. , 1 ft.	0.1225	- 0.1133	2.8 %			
50 Inc. , 1 ft.	0.1225	- 0.1133	2.7 %			
5 Inc. , 0 ft.	0.1225	- 0.1159	0.16 %			
10 Inc. , 0 ft.				0.245	- 0.2081	0.28 %
50 Inc. , 0 ft.	0.1225	- 0.1136	0.02 %			

TABLE 5.1: RESULTS OF UNIT CUBE RUNS

	Passive	Active
S_u	0.31Kg/cm ²	0.405Kg/cm ²
k'	10.42Kg/cm ²	62.5Kg/cm ²
R_f	0.9	0.91
n	1.0	1.0
K_B		100.0Kg/cm ²
P_a		1.0Kg/cm ²
K_0		0.45
A_f		1

Table 5.2 STRESS-STRAIN PARAMETERS

CHAPTER 6

SUMMARY, CONCLUSIONS AND RECOMMENDATIONS

In order to obtain better predictions of the behavior of soils by means of computer modeling, the influence of large deformations has been taken into account. A suitable formulation of the large strain problem for the use of finite element techniques was found. Biot's formulation was used because it is a consistent formulation, and because the separation of physical effects from geometrical effects allows the use of constitutive relations between stresses and strains that can be readily obtained from normal testing procedures in Soil Engineering practice.

Two constitutive relations were used; one for perfectly plastic Tresca Materials, and another one a hyperbolic stress-strain relation described by Kondner (1963). The Tresca Material formulation is valid for undrained conditions; the hyperbolic stress-strain may be used for both drained and undrained conditions. An interpolation procedure was used to handle anisotropy.

Two finite element programs were developed, one with each constitutive relation. Quadrilateral elements were used. The programs have an incremental approach, and in order to improve accuracy a mid-point integration scheme

was employed.

Some test runs were made where some results were predictable either theoretically or experimentally. The results obtained in the runs are inconclusive. While some simple cases are predicted very well the more complicated ones give results that are far from satisfactory.

Although in one of the cases the use of the large strain formulation led to greater accuracy than the use of the infinitesimal formulation, there is not enough evidence to assure that the increase in accuracy is worth the use of the large strain formulation. On the other hand, the drawbacks of the formulation are important:

- 1) There is an increase in computing time when the large strain formulation is used instead of a conventional infinitesimal strain approach.
- 2) Because of the large strains the convergence of iterative procedures can not be established; furthermore normal procedures to determine when an element is loading or unloading do not work properly.
- 3) Instability, that is the existence of more than one solution for equilibrium, creates problems, especially when the elastic parameters are very small, at failure, and when

forces are specified instead of displacements.

- 4) The constitutive equations after yielding are not very well known, and it is at that level when the large strains influence the solutions; therefore what is gained in accuracy using large strain formulation, may be lost in the constitutive equations.

Some conclusions can be obtained about the use of the program:

- 1) In undrained cases the value of B will have to be a low value in order to obtain meaningful results.
- 2) Elements should not be in failure initially, and K_0 conditions should be adjusted so the maximum shear stress is less than the undrained shear strength, or in the case of drained conditions that the K_0 line is always below the failure envelope.
- 3) The use of the mid-point integration procedure gives better results for the displacement field but it also gives more causes for lack of equilibrium among stresses and forces.
- 4) To repeat several times the mid-point inte-

gration for the same increment is not effective.

- 5) An increase in the number of increments is a much more effective way to increase the accuracy in the displacement field than an increase in the number of elements.
- 6) Stress distribution is improved with finer meshes.

Two main problems are encountered in the results of the runs.

- 1) The displacement solution, or the force solution whichever the case is, becomes highly inaccurate after yielding occurs. The cause for this behavior has to be basically the inadequacy of the stress-strain relations. The hyperbolic stress-strain relation can not model the usual strain-softening, and sometimes it can not even model the pre-yielding relation satisfactorily. Of course if very large increments are used the modification of stresses may have some influence, and it is possible that the integration scheme diverges from the theoretical solution if large increments are used.

- 2) The stresses and the forces are not in equilibrium. Several trends are observed:
 - a) If the strains in each increment are fairly large the transformation equations for the stresses are inexact, and the lack of equilibrium increases.
 - b) When the mid-point integration is used, the lack of equilibrium increases.
 - c) The modification of stresses back to the yield surface has an important role in the lack of equilibrium.

The use of more increments reduces the effect of a and c, but b remains.

Several recommendations for future research can be given:

- 1) The influence of every parameter on the lack of equilibrium should be determined, in particular the influence of the mid-point integration; the way the stresses are obtained in the second step of the mid-point integration is the most likely cause of the lack of equilibrium.
- 2) The reasons why the use of unloading laws always gives instability and closed itera-

tion cycles should be determined.

- 3) The development of a strain-softening constitutive relation could be very helpful for post-yielding behavior.
- 4) The extra accuracy obtained with the large strain formulation should be determined in order to judge the effectiveness of the program.
- 5) Some test runs should be made for drained cases to see how the hyperbolic stress-strain relation behaves in such cases.

REFERENCES

- Ang, A.H.S. and Harper,
G.N. (1964) "Analysis of Contained Plastic Flow in Plane Solids", Proc., ASCE, JEMD, Vol. 90, No. EM2, pp. 195-223.
- Biot, M.A. (1965) Mechanics of Incremental Deformations, Wiley, New York.
- Christian, J.T. (1966) "Two Dimensional Analysis of Stress and Strain in Soils", Report 3, U.S. Army Waterways Experiment Station, Contract No. DA-22-079-eng-471.
- Christian, J.T. (1970) Personal communication.
- D'Appolonia, J.D. (1968) "Prediction of Stress and Deformation for Undrained Loading Conditions", Ph.D. Thesis, M.I.T.
- Desai, C.S. (1971) "Non-linear Analyses Using Spline Functions", to be published in the JSMFD, ASCE.
- Duncan, J.M. and Chang,
C.Y. (1970) "Non-linear Analysis of Stress and Strain in Soils", Proc., ASCE, JSMFD, Vol. 96, No. SM5, pp. 1629-1653.
- Duncan, J.M. and
Dunlop, P. (1969) "Behavior of Soils in Simple Shear Tests", Proc. of the 7th International Conference on Soil Mechanics and Foundation Engineering, Mexico, Vol. 1, pp. 101-109.
- Elsgolc, L.E. (1961) Calculus of Variations, Addison-Wesley, Reading, Massachusetts.

- Felippa, C.A. (1966) "Refined Finite Element Analysis of Linear and Non-linear Two-Dimensional Structures", Report to National Science Foundation, NSF Grant GK-75, University of California at Berkeley.
- Fung, Y.C. (1965) Foundations of Solid Mechanics, Prentice-Hall, New Jersey.
- Green, A.E. and Zerna, W. (1954) Theoretical Elasticity, Oxford University Press, London.
- Hagmann, A.J. (1971) "Prediction of Stress and Strain Under Loading Conditions", Research Report R71-3, M.I.T.
- Harper, G.N. (1963) "A Numerical Procedure for the Analysis of Contained Plastic Flow Problems", Ph.D. Thesis, University of Illinois.
- Janbu, N. (1963) "Soil Compressibility as Determined by Oedometer and Triaxial Tests", European Conference on Soil Mechanics and Foundations Engineering, Wiesbaden, Germany, Vol. 1, pp. 19-25.
- Karni, Z. and Reiner, M. (1962) "The General Measure of Deformation" Second Order Effects in Elasticity, Plasticity and Fluid Dynamics, ed. Reiner and Abir, MacMillan, New York, pp. 217-227.
- Kinner, E.B. (1970) "Load-Deformation Behavior of Saturated Clays during Undrained Shear" Ph.D. Thesis, M.I.T.
- Kondner, R.L. (1963) "Hyperbolic Stress-Strain Response: Cohesive Soils", Proc., ASCE, JSMFD, Vol. 89, No. S1, pp. 115-143.

- Kondner, R.L. and
Zelasco, J.S. (1963) "A Hyperbolic Stress-Strain Formulation for Sands", Proc., 2nd Pan-American Conference on Soil Mechanics and Foundation Engineering, Brazil, Vol. 1, pp. 289-324.
- Ladd, C.C. (1964a) "Stress-Strain Modulus of Clay in Undrained Shear", Proc., ASCE, Soil Mechanics and Foundations Division Conference on "The Design of Foundations for Control of Settlements", Evanston, Illinois, pp. 127-156.
- Ladd, C.C. (1964b) "Stress-Strain Behavior of Saturated Clay and Basic Strength Principles", Research Report R64-17, M.I.T.
- Lambe, T.W. and
Whitman, R.V. (1968) Soil Mechanics, Wiley, New York.
- Martin, H.C. (1965) "On the Derivation of Stiffness Matrices for the Analysis of Large Deflections and Stability Problems", Proc., Conference on Matrix Methods in Structural Mechanics, AFIT, Ohio, pp. 697-716.
- Oden, J.T. (1969) "A General Theory of Finite Elements", International Journal for Numerical Methods in Engineering, Vol. 1, pp. 243-261.
- Prager, W. (1961) Introduction to Mechanics of Continua, Ginn and Company, Boston.

- Skempton, A.W. and
Bishop, A.W. (1954) "Soils", Chapter X of Building Materials, their Elasticity and Inelasticity, ed. M. Reines, Interscience, New York.
- Terzaghi, K. (1943) Theoretical Soil Mechanics, Wiley, New York.
- Timoshenko, S. and
Goodier, J.N. (1951) Theory of Elasticity, McGraw-Hill, New York.
- Watt, B.J. (1969) "Analysis of Viscous Behavior in Undrained Soils", Research Report R69-70, M.I.T.
- Whitman, R.V. (1964) "Multidimensional Analysis of Stress and Strain in Soils", Stanford Research Institute Report to the Defense Atomic Support Agency, DASA, No. 1558.
- Wilson, E.L. (1965) "Structural Analysis of Axisymmetric Solids", AIAAJ, Vol. 3112, pp. 2269-2274.
- Wong, I.H. (1971) "Analysis of Braced Excavation", Sc.D. Thesis, M.I.T.
- Zienkiewicz, O.C. and
Cheung, Y.K. (1967) The Finite Element Method in Structural and Continuum Mechanics, McGraw-Hill, New York.

Appendix A

LIST OF SYMBOLS AND NOTATIONS

[]	Denotes matrix, even row and column matrices.
[]'	Inverse of a matrix
a	Cohesion intercept in the Mohr-Coulomb criterion for maximum shear stress.
	Constant in the hyperbola equation, σ vs. ϵ
a'	Constant in the hyperbola equation, τ vs. γ
a _j	Cartesian coordinates of points in a body before deformation, in tensorial formulation
	Horizontal projections of the sides of the triangular elements
a _{ij}	Components of the deformation tensor in Biot's formulation
[a]	Column matrix of values a _j for an element
A	Area of an element
	Skempton's parameter
A _f	Skempton's parameter at failure
A _j	Areas of subtriangles defined by a point in an element
A _{ij}	Areas of triangles formed in an element with the origin and side ij
b	Constant in the hyperbola equation, σ vs. ϵ
b'	Constant in the hyperbola equation, τ vs. γ

b_i	Vertical projections of the sides of the triangular elements
[b]	Column matrix of values b_i for an element
B	Bulk modulus
[B]	Matrix that applied to [U] gives the matrix of Cauchy's strains
c	Cohesion intercept in the Mohr-Coulomb criterion
C_{ijkl}	Constitutive equations parameters
[C]	Matrix of C_{ijkl}
[D]	Matrix obtained in the search for a symmetric matrix formulation for $S_{ij} \delta \eta_{ij}$ (Biot's formulation)
e_{ij}	Almansi strain tensor components in tensorial formulation
	Components of the Cauchy strain tensor in Biot's formulation, (i,j will be x,y)
[e]	Column matrix of the components of Cauchy's strain tensor
E	Young's modulus
E_i	Initial Young's modulus
E_t	Tangent Young's modulus
E_{ij}	Green's strain tensor components
f	Failure law

f_i	Surface tractions referred to original axes and original geometry
F_i	Body forces per unit mass, tensorial formulation. Components of a force vector.
F_{oi}	Body forces per unit mass referred to undeformed geometry.
[F]	Column matrix of nodal forces for each element
[<u>F</u>]	Total nodal force matrix
g_i	Natural coordinates of a triangle
[g]	Column matrix of g_i
G	Shear modulus
G_i	Initial shear modulus
G_u	Unloading shear modulus
G_{ult}	Ultimate shear modulus
G_t	Tangent shear modulus
k	Yielding constant in the Tresca criterion, by extension value of τ at yielding for a given p in the Mohr-Coulomb criterion
K	Modulus number, value of E_i for $\sigma_3 = 1$
K'	Modulus number, value of G_i for $\sigma_3 = 1$
K_0	Coefficient of lateral stress at rest
K_1	Constant
K_u	Modulus number, value of G_t during unloading for $\sigma_3 = 1$.

K_B	Modulus number, value of B for $\sigma_3 = 1$
[K]	Total stiffness matrix for an element
[<u>K</u>]	Overall stiffness matrix
[K_c]	Normal stiffness matrix
[K_g]	Geometric stiffness matrix
l	Final length of sample
l_0	Original length of sample
L	Instantaneous length of sample
n	Variation rate exponent in Janbu's equation for E_i
n'	Variation rate exponent in Janbu's equation for G_i
p	Value of $(\sigma_1 + \sigma_3)/2$
p_a	Atmospheric pressure
P	Point in a body before deformation
P'	Point in a body after deformation
p^*	Modified value of p
R_f	Failure ratio
s'_{ij}	Incremental stress referred to deformed geometry. Components with respect to original axes if i,j are x,y, if i,j are 1,2 the components are with respect to rotated axes.
S	Areas in deformed geometry
S_0	Areas in undeformed geometry

S_u	Undrained strength of soils
S_{ij}	Components of Kirchhoff's stress tensor in tensorial formulation
	Components of the initial stress referred to the original axes in Biot's formulation (the use of x,y or $1,2$ or i,j is immaterial)
[S]	Matrix of combinations of S_{ij} obtained in the search for a symmetric matrix formulation for $S_{ij} \delta \eta_{ij}$ (Biot's formulation)
t_{ij}	Incremental stress components referred to undeformed geometry and rotated axes
T_i	Force components in the deformed geometry
$T_{oi}^{(L)}$	Force components in the undeformed geometry due to a Lagrangian stress tensor
$T_{oi}^{(K)}$	Force components in the undeformed geometry due to a Kirchhoff's stress tensor
ν T_i	Surface traction components referred to the deformed geometry
ν T_{oi}	Initial surface traction components in equilibrium in the undeformed position
ν T_{oi}^*	Surface traction components referred to the undeformed geometry but in the direction of the correspondent T_i
u	Horizontal displacement
	Pore pressure

u_i	Components of displacement
[u]	Column matrix of horizontal nodal displacements
[U]	Column matrix of nodal displacements
[<u>U</u>]	Overall matrix of nodal displacements
v	Vertical displacement
[v]	Column matrix of vertical nodal displacements
V	Volume in deformed geometry
V_0	Volume in undeformed geometry
x	Horizontal coordinate of a point before deformation in Biot's formulation
x_i	Cartesian coordinates of a point after deformation in tensorial formulation
	Horizontal coordinates of the nodal points
$X_i(\xi_j)$	Body forces per unit volume referred to deformed volume, Biot's formulation
$X_i(x_j)$	Body forces, after deformation, per unit volume referred to undeformed geometry, Biot's formulation
y	Vertical coordinate of point before deformation in Biot's formulation
Y_i	Vertical coordinates of the nodal points
α	Pseudo friction angle in the Mohr-Coulomb criterion for maximum shear stress
γ	Maximum engineering pure shear strain

γ_t	Total unit weight of soil
γ_{xy}	Engineering pure shear strain $\gamma_{xy} = 2\epsilon_{xy}$
δ	Variation of... . Virtual... .
δ_{ij}	Kronecker delta
ϵ	Axial strain
ϵ_{ij}	Cauchy's strain tensor components in tensorial formulation
	Components of pure strain in Biot's formulation (where i, j are 1, 2, etc.)
η	Vertical coordinate of deformed point in Biot's formulation
η_{ij}	Second order terms of the Green strain tensor E_{ij} in tensorial formulation
	Second order terms in the expression of pure strain in Biot's formulation
θ	Exact value of local rotation, in two dimensions
ν	Poisson's ratio
ν_i	Components of unit normal vector of an infinitesimal area in deformed geometry
ν_{oi}	Components of unit normal vector of an infinitesimal area in undeformed geometry
ξ	Horizontal coordinate of deformed point in Biot's formulation

ρ	Material density after deformation
ρ	Material density before deformation
σ_1	Major principal stress (remember sign convention)
σ_2	Intermediate principal stress
σ_3	Minor principal stress
σ_c	Consolidation stress, isotropic
σ_{1c}	Vertical consolidation stress for normally consolidated clays
σ_{ij}	Eulerian stress tensor components
σ_{oij}	Initial Eulerian stress tensor components
σ'_{ij}	Total stress referred to deformed geometry. Components with respect to original axes if i, j are x, y , if i, j are $1, 2$, the components are with respect to rotated axes.
σ'^*_{ij}	Modified values of σ'_{ij}
τ	Maximum shear stress
τ_f	Maximum shear stress at failure
τ_{ult}	Asymptotic value of τ in the hyperbolic approximation
τ^*	Modified value of τ
ϕ	Friction angle in the Mohr-Coulomb criterion
ω	Local rotation in two dimensions, to the first order

ω_{ij} Infinitesimal local rotations
 Δ Increment of.....
Value of l/l_0

(blank)

Appendix B

BIOT'S FORMULATION

This is the derivation of Biot's formulation; it follows Biot's own derivation, omitting anything that does not lead to the desired result. This derivation is for Plane Strain.

B.1 STRAINS

Given a point P of initial coordinates (x,y) with respect to a cartesian frame that transforms into a point P' of coordinates (ξ,η) with respect to the original frame,

$$\begin{aligned}\xi &= x + u \\ \eta &= y + v\end{aligned}\tag{B-1}$$

where u and v are the components in the original frame of the displacement vector, that is a function of x and y .

In the vicinity of the point P the continuum undergoes a linear transformation; differentiating Equations (B-1):

$$\begin{aligned}d\xi &= dx\left(1 + \frac{\partial u}{\partial x}\right) + \frac{\partial u}{\partial y} dy \\ d\eta &= dx \frac{\partial v}{\partial x} + \left(1 + \frac{\partial v}{\partial y}\right) dy\end{aligned}\tag{B-2}$$

This transformation is also homogeneous.

If a linear symmetric transformation is defined such that:

$$\begin{aligned}d\xi' &= dx(1+\epsilon_{11}) + dy\epsilon_{12} \\d\eta' &= dx\epsilon_{12} + dy(1+\epsilon_{22})\end{aligned}\tag{B-3}$$

it can be said that this transformation represents a pure deformation, because there are two perpendicular directions in the continuum that remain perpendicular after deformation. This can be proven for any symmetric transformation.

It can be seen that transformation (B-2) can be considered a combination of a rotation and a symmetric transformation (B-3).

If only the infinitesimal region around P is considered, and the values of u and v are made 0 at P, which is always possible with an appropriate translation that does not affect the deformation; given a square of unit side P,A,B,C (Fig. B.1), the symmetric transformation (B-3) will give the transformed parallelogram P,A',B',C'. If the deformed parallelogram is now submitted to a rigid body rotation of angle θ counterclockwise to obtain P, A",B", C", the transformation done is given by

$$\begin{bmatrix}d\xi \\d\eta\end{bmatrix} = \begin{bmatrix}\cos\theta & -\sin\theta \\ \sin\theta & \cos\theta\end{bmatrix} \begin{bmatrix}d\xi' \\d\eta'\end{bmatrix}\tag{B-4}$$

where $d\xi'$ $d\eta'$ are components with respect to the axes 1,2 that rotated with the parallelogram and $d\xi, d\eta$ are components with respect to the dx,dy axes.

From Equations (B-3) and (B-4),

$$\begin{bmatrix} d\xi \\ d\eta \end{bmatrix} = \begin{bmatrix} \cos\theta - \sin\theta \\ \sin\theta \cos\theta \end{bmatrix} \begin{bmatrix} 1 + \epsilon_{11} & \epsilon_{12} \\ \epsilon_{12} & 1 + \epsilon_{22} \end{bmatrix} \begin{bmatrix} dx \\ dy \end{bmatrix} \quad (\text{B-5})$$

This transformation has to be equivalent to (B-2). If, in (B-2)

$$\frac{\partial u}{\partial x} = a_{11}$$

$$\frac{\partial u}{\partial y} = a_{12}$$

$$\frac{\partial v}{\partial x} = a_{21}$$

$$\frac{\partial v}{\partial y} = a_{22}$$

(B-6)

(B-2) becomes

$$\begin{bmatrix} d\xi \\ d\eta \end{bmatrix} = \begin{bmatrix} 1 + a_{11} & a_{12} \\ a_{21} & 1 + a_{22} \end{bmatrix} \begin{bmatrix} dx \\ dy \end{bmatrix} \quad (\text{B-7})$$

Then, from (B-5)

$$1 + a_{11} = (1 + \epsilon_{11}) \cos\theta - \epsilon_{12} \sin\theta$$

$$a_{21} = (1 + \epsilon_{11}) \sin\theta + \epsilon_{12} \cos\theta$$

$$1 + a_{22} = (1 + \epsilon_{22}) \cos\theta + \epsilon_{12} \sin\theta$$

$$a_{12} = -(1 + \epsilon_{22}) \sin\theta + \epsilon_{12} \cos\theta$$

(B-8)

Solving the first two equations for ϵ_{11} and ϵ_{12} and the last two for ϵ_{22} and ϵ_{12}

$$\begin{aligned}
\varepsilon_{11} &= a_{21} \cos\theta - (1+a_{11}) \sin\theta \\
\varepsilon_{12} &= a_{12} \cos\theta + (1+a_{22}) \sin\theta \\
1 + \varepsilon_{11} &= (1+a_{11}) \cos\theta + a_{21} \sin\theta \\
1 + \varepsilon_{22} &= (1+a_{22}) \cos\theta - a_{12} \sin\theta
\end{aligned}
\tag{B-9}$$

From the first pair of equations:

$$\tan\theta = \frac{a_{21} - a_{12}}{2 + a_{11} + a_{22}}
\tag{B-10}$$

So the rotation contained in transformation (B-2) is given by Equation (B-10), and the pure deformation contained in (B-2) is

$$\begin{aligned}
\varepsilon_{12} &= \frac{1}{2}(a_{21} + a_{12}) \cos\theta + \frac{1}{2}(a_{22} - a_{11}) \sin\theta \\
\varepsilon_{11} &= a_{11} \cos\theta + a_{21} \sin\theta + \cos\theta - 1 \\
\varepsilon_{22} &= a_{22} \cos\theta - a_{12} \sin\theta + \cos\theta - 1
\end{aligned}
\tag{B-11}$$

For a general point P where u and $v \neq 0$, the Figure B.2 gives the locally rotated axes 1,2 with respect to which the pure deformation is defined.

So far, the derivations have been exact. If the values of a_{ij} can be considered infinitesimals

$$a_{ij} \ll 1
\tag{B-12}$$

then to the first order:

$$\theta = \frac{1}{2}(a_{21} - a_{12})
\tag{B-13}$$

Defining

$$\begin{aligned}\omega &= \frac{1}{2} (a_{21} - a_{12}) = \frac{1}{2} \left(\frac{\partial v}{\partial x} - \frac{\partial u}{\partial y} \right) \\ e_{xx} &= a_{11} = \frac{\partial u}{\partial x} \\ e_{yy} &= a_{22} = \frac{\partial v}{\partial y} \\ e_{xy} &= \frac{1}{2} (a_{21} + a_{12}) = \frac{1}{2} \left(\frac{\partial v}{\partial x} + \frac{\partial u}{\partial y} \right)\end{aligned}\tag{B-14}$$

to the first order

$$\begin{aligned}\theta &= \omega \\ \sin\theta &= \omega \\ \cos\theta &= 1\end{aligned}\tag{B-15}$$

and to the second order

$$1 - \cos\theta = \frac{1}{2}\omega^2\tag{B-16}$$

Then, substituting in Equations (B-11), to the second order

$$\begin{aligned}\epsilon_{12} &= e_{xy} + \frac{1}{2} (e_{yy} - e_{xx})\omega \\ \epsilon_{11} &= e_{xx} + e_{xy}\omega + \frac{1}{2}\omega^2 \\ \epsilon_{22} &= e_{yy} - e_{xy}\omega + \frac{1}{2}\omega^2\end{aligned}\tag{B-17}$$

To the first order:

$$\begin{aligned}\epsilon_{12} &= e_{xy} \\ \epsilon_{11} &= e_{xx} \\ \epsilon_{22} &= e_{yy}\end{aligned}\tag{B-18}$$

which are the infinitesimal strains.

B.2 INCREMENTAL STRESSES

The two dimensional stress at a point is a second order symmetric tensor with four components

$$\begin{array}{cc} \sigma_{xx} & \sigma_{xy} \\ \sigma_{xy} & \sigma_{yy} \end{array} \quad (\text{B-19})$$

These components are referred to axes x,y , the components referred to a set of axes $1,2$ rotated an angle α counterclockwise would be (Timoshenko and Goodier, 1951)

$$\begin{aligned} \sigma_{11} &= \sigma_{xx} \cos^2 \alpha + \sigma_{yy} \sin^2 \alpha + \sigma_{xy} \sin 2\alpha \\ \sigma_{22} &= \sigma_{xx} \sin^2 \alpha + \sigma_{yy} \cos^2 \alpha - \sigma_{xy} \sin 2\alpha \\ \sigma_{12} &= \frac{1}{2} (\sigma_{yy} - \sigma_{xx}) \sin 2\alpha + \sigma_{xy} \cos 2\alpha \end{aligned} \quad (\text{B-20})$$

The initial stress field referred to axes x,y

(Fig. A.3) is:

$$\begin{array}{cc} S_{xx} & S_{xy} \\ S_{xy} & S_{yy} \end{array} \quad (\text{B-21})$$

these components give the initial value of the stress at point P of coordinates x,y . After deformation, P becomes P' of coordinates ξ,η , and the components of the stress at P' , referred to the same reference frame xy , are

$$\begin{aligned} \sigma'_{xx} &= S_{xx} + s'_{xx} \\ \sigma'_{yy} &= S_{yy} + s'_{yy} \\ \sigma'_{xy} &= S_{xy} + s'_{xy} \end{aligned} \quad (\text{B-22})$$

where the prime denotes values referred to the deformed geometry at point $P'(\xi, \eta)$, and the subindices refer to the axes. s'_{xx} , s'_{yy} , s'_{xy} are therefore the components of the incremental stress.

If the stress is referred to the locally rotated axis 1,2 (Fig. B.3)

$$\begin{aligned}\sigma'_{11} &= S_{xx} + s'_{11} \\ \sigma'_{22} &= S_{yy} + s'_{22} \\ \sigma'_{12} &= S_{xy} + s'_{12}\end{aligned}\tag{B-23}$$

but the Equations (B-20) give a relation between σ'_{12} and σ'_{xy} . Assuming that incremental stresses are infinitesimals of the first order, and that to the first order:

$$\begin{aligned}\alpha &= \omega \\ \cos\alpha &= 1 \\ \sin\alpha &= \omega \\ \cos 2\alpha &= 1 \\ \sin 2\alpha &= 2\omega\end{aligned}\tag{B-24}$$

then the relation between the incremental stresses is

$$\begin{aligned}s'_{xx} &= s'_{11} - 2S_{xy}\omega \\ s'_{yy} &= s'_{22} + 2S_{xy}\omega \\ s'_{xy} &= s'_{12} + (S_{xx} - S_{yy})\omega\end{aligned}$$

These are relations (B-20) where only first order terms have been kept.

So far, the stress in the body has been referred

to the deformed geometry, that is as a function of ξ and η , however, S_{xx} , S_{yy} , S_{xy} is the real stress before deformation when referred to rotated axis and undeformed geometry, and the strains, Equations (B-17) are also referred to the undeformed geometry as can be seen in Equations (B-14); so an expression of the stress after deformation referred to the geometry before deformation will be necessary.

The components of the stress referred to undeformed geometry with respect to rotated axis 1,2 are

$$\begin{aligned}
 T_{11} &= S_{xx} + t_{11} \\
 T_{22} &= S_{yy} + t_{22} \\
 T_{12} &= S_{xy} + t_{12} \\
 T_{21} &= S_{xy} + t_{21}
 \end{aligned}
 \tag{B-26}$$

Remember that S_{xx} , S_{yy} , S_{xy} are the components of the initial stress respect to axis x, y , if a solid body rotation is given to the body the components of the stress with respect to rotated axis are still S_{xx} , S_{yy} , S_{xy} that can be called

$$\begin{aligned}
 S_{xx} &= S_{11} \\
 S_{yy} &= S_{22} \\
 S_{xy} &= S_{12}
 \end{aligned}
 \tag{B-27}$$

Therefore, if no deformations, but only rotations are

imposed in Equations (B-23) and (B-26)

$$t_{ij} = s'_{ij} = 0 \quad (B-28)$$

where both deformed and undeformed geometries are identical. From Equation (B-25)

$$s'_{xy} \neq 0 \quad s'_{xx} \neq 0 \quad s'_{yy} \neq 0 \quad (B-29)$$

The relation between t_{ij} and s'_{ij} can be found from geometric considerations. Considering rotated axes 1,2 and a deformed element $d\xi', d\eta'$ (Fig. B.4); the dF in this element will have components on axes 1,2

$$dF_1 = \sigma'_{11}d\eta' - \sigma'_{12}d\xi' \quad (B-30)$$

$$dF_2 = \sigma'_{12}d\eta' - \sigma'_{22}d\xi'$$

If a unit square is now considered $P'ABC$, and its deformed shape parallelogram $P'A'B'C'$ the forces in the corresponding sides of both figures have to be the same; with Equations (B-30), the force on sides $P'A'$, $P'B'$, etc., can be found. The values of the components of those forces will be the values of the components of the stress T_{ij} , because the undeformed square P',A,B,C is unitarian.

The coordinates of points A',B',C' , relative to P' are

	ξ'	η'	
A	$1+\epsilon_{11}$	ϵ_{12}	
B	$1+\epsilon_{11}+\epsilon_{12}$	$1+\epsilon_{22}+\epsilon_{12}$	(B-31)
C	ϵ_{12}	$1+\epsilon_{22}$	

$$\begin{aligned}
T_{11} &= \int_A^B dF_1 = \int_A^B \sigma'_{11} d\eta' - \int_A^B \sigma'_{12} d\xi' \\
&= \sigma'_{11} \eta' \Big|_A^B - \sigma'_{12} \xi' \Big|_A^B \quad (B-32) \\
&= \sigma'_{11} (1 + \epsilon_{22}) - \sigma'_{12} \epsilon_{12}
\end{aligned}$$

In a similar fashion

$$\begin{aligned}
T_{21}^* &= \sigma'_{12} (1 + \epsilon_{22}) - \sigma'_{22} \epsilon_{12} \\
T_{12}^* &= \sigma'_{12} (1 + \epsilon_{11}) - \sigma'_{11} \epsilon_{12} \quad (B-33) \\
T_{22} &= \sigma'_{22} (1 + \epsilon_{11}) - \sigma'_{12} \epsilon_{12}
\end{aligned}$$

To the first order, and substituting values from Equations (B-23), (B-26) and (B-27)

$$\begin{aligned}
T_{11} &= \sigma'_{11} + S_{11} \epsilon_{22} - S_{12} \epsilon_{12} \\
T_{21}^* &= \sigma'_{12} + S_{12} \epsilon_{22} - S_{22} \epsilon_{12} \\
T_{12}^* &= \sigma'_{12} + S_{12} \epsilon_{11} - S_{11} \epsilon_{12} \\
T_{22} &= \sigma'_{22} + S_{22} \epsilon_{11} - S_{12} \epsilon_{12} \quad (B-34)
\end{aligned}$$

The stress tensor is not symmetric, however, for work principles T_{21}^* and T_{12}^* are of no interest, so the average is used.

$$T_{12} = \sigma'_{12} + \frac{1}{2} S_{12} (\epsilon_{11} + \epsilon_{22}) - \frac{1}{2} (S_{11} + S_{22}) \epsilon_{12} \quad (B-35)$$

If in (B-34) and (B-35), ϵ_{ij} are replaced by their values given by Equations (B-17); to the first order

$$\begin{aligned}
T_{11} &= \sigma'_{11} + S_{11}e_{yy} - S_{12}e_{xy} \\
T_{22} &= \sigma'_{22} + S_{22}e_{xx} - S_{12}e_{xy} \\
T_{12} &= \sigma'_{12} + \frac{1}{2}S_{12}(e_{xx}+e_{yy}) - \frac{1}{2}(S_{11}+S_{22})e_{xy}
\end{aligned} \tag{B-36}$$

Now, from Equations (B-36),

$$\begin{aligned}
\sigma'_{11} &= T_{11} - S_{11}e_{yy} + S_{12}e_{xy} \\
\sigma'_{22} &= T_{22} - S_{22}e_{xx} + S_{12}e_{xy} \\
\sigma'_{12} &= T_{12} - \frac{1}{2}S_{12}(e_{xx}+e_{yy}) + \frac{1}{2}(S_{11}+S_{22})e_{xy}
\end{aligned} \tag{B-37}$$

and from Equations (B-22), (B-23) and (B-25)

$$\begin{aligned}
\sigma'_{xx} &= \sigma'_{11} - 2S_{xy}\omega \\
\sigma'_{yy} &= \sigma'_{22} + 2S_{xy}\omega \\
\sigma'_{xy} &= \sigma'_{12} + (S_{xx}-S_{yy})\omega
\end{aligned} \tag{B-38}$$

and considering (B-27), (B-37) and (B-38)

$$\begin{aligned}
\sigma'_{xx} &= T_{11} - S_{xx}e_{yy} + S_{xy}(e_{xy}-2\omega) \\
\sigma'_{yy} &= T_{22} - S_{yy}e_{xx} + S_{xy}(e_{xy}+2\omega) \\
\sigma'_{xy} &= T_{12} - \frac{1}{2}S_{xy}(e_{xx}+e_{yy}) + \frac{1}{2}S_{xx}(e_{xy}+\omega) \\
&\quad + \frac{1}{2}S_{yy}(e_{xy}-\omega)
\end{aligned} \tag{B-39}$$

with only first order terms.

B.3 CONSTITUTIVE EQUATIONS

Because T_{ij} , ϵ_{ij} and S_{ij} are all referred to rotated axis and undeformed geometry, it can be said that

$t_{ij} = T_{ij} - S_{ij}$ is the real increment of stress, and that for an elastic material

$$t_{ij} = C_{ijkl} \epsilon_{kl} \quad (B-40)$$

if the increment is considered linear, C_{ijkl} are constants. Because in each increment the material is considered linear elastic and isotropic, C_{ijkl} are all functions of two parameters.

The constitutive equations would be the ones in Equations (3-2) or (3-3) where, instead of $\sigma_{xx}, \sigma_{yy}, \sigma_{xy}$ t_{11}, t_{22} and t_{12} would be used.

Considering the equation only to the first order,

$$t_{ij} = C_{ijkl} \epsilon_{kl} \quad (B-41)$$

For the plastic formulation, the constitutive equations would be (3-4) with the same changes in the stresses as before.

B.4 EQUILIBRIUM

If a virtual work formulation is used, because T_{ij} is conjugate of ϵ_{ij} (both referred to the same geometry and to the same axes) for a field of virtual displacements δu_i , the principle of virtual work states that:

$$\int_{V_0} T_{ij} \delta \epsilon_{ij} dV_0 = \int_{V_0} \rho X_i (\xi_\lambda) \delta u_i dV_0 + \int_{S_0} f_i u_i dS_0 \quad (B-42)$$

where ρ is the density of the material after deformation and f_i is the boundary traction referred as everything, except body forces $X_i(\xi_\ell)$, to the undeformed geometry.

$$\rho X_i(\xi_\ell) = \rho_0 X_i^*(x_\ell) \quad (B-43)$$

if $X_i^*(x_\ell)$ are the body forces after deformation referred to undeformed geometry.

Biot (1965) proves that if Equation (B-42) is considered only to the second order, and the equilibrium of the initial stress field is considered, the resulting equation is equivalent to the statement of equilibrium in the deformed position, to the first order.

Because of equilibrium in the initial state:

$$\int_{V_0} S_{ij} \delta e_{ij} dV_0 = \int_{S_0} S_{ij} v_{0j} \delta u_i dS_0 \quad (B-44)$$

where $S_{ij} v_{0j}$ are the surface tractions, because v_{0j} are the components of the normal to the surface in the undeformed geometry.

Body forces are considered 0 in Equation (B-44), such assumption will be made from here on, because they are 0 in this application.

Equation (B-42) to the second order with body forces equal to 0 is

$$\int_{V_0} (t_{ij} \delta e_{ij} + S_{ij} \delta \varepsilon_{ij}) dV_0 = \int_{S_0} f_i \delta u_i dS_0 \quad (B-45)$$

Subtracting (B-44)

$$\begin{aligned} & \int_{V_0} (t_{ij} \delta e_{ij} + S_{ij} \delta \eta_{ij}) dV_0 \\ & = \int_{S_0} (f_i - S_{ij} v_{0j}) \delta u_i dS_0 \end{aligned} \quad (B-46)$$

If surface tractions are conservative, that is, they do not change direction during deformation, then:

$$f_i - S_{ij} v_{0j} = \Delta f_i \quad (B-47)$$

η_{ij} is defined as:

$$\eta_{ij} = \varepsilon_{ij} - e_{ij}$$

From (B-17)

$$\begin{aligned} \eta_{xx} &= \frac{1}{2} \omega^2 + e_{xy} \omega \\ \eta_{yy} &= \frac{1}{2} \omega^2 - e_{xy} \omega \\ \eta_{xy} &= \frac{1}{2} (e_{yy} - e_{xx}) \omega \end{aligned} \quad (B-48)$$

Substituting (B-47) and (B-41) in (B-46)

$$\int_{V_0} (e_{k\ell} C_{ijkl} \delta e_{ij} + S_{ij} \delta \eta_{ij}) dV_0 = \int_{S_0} \Delta f_i \delta u_i dS_0 \quad (B-49)$$

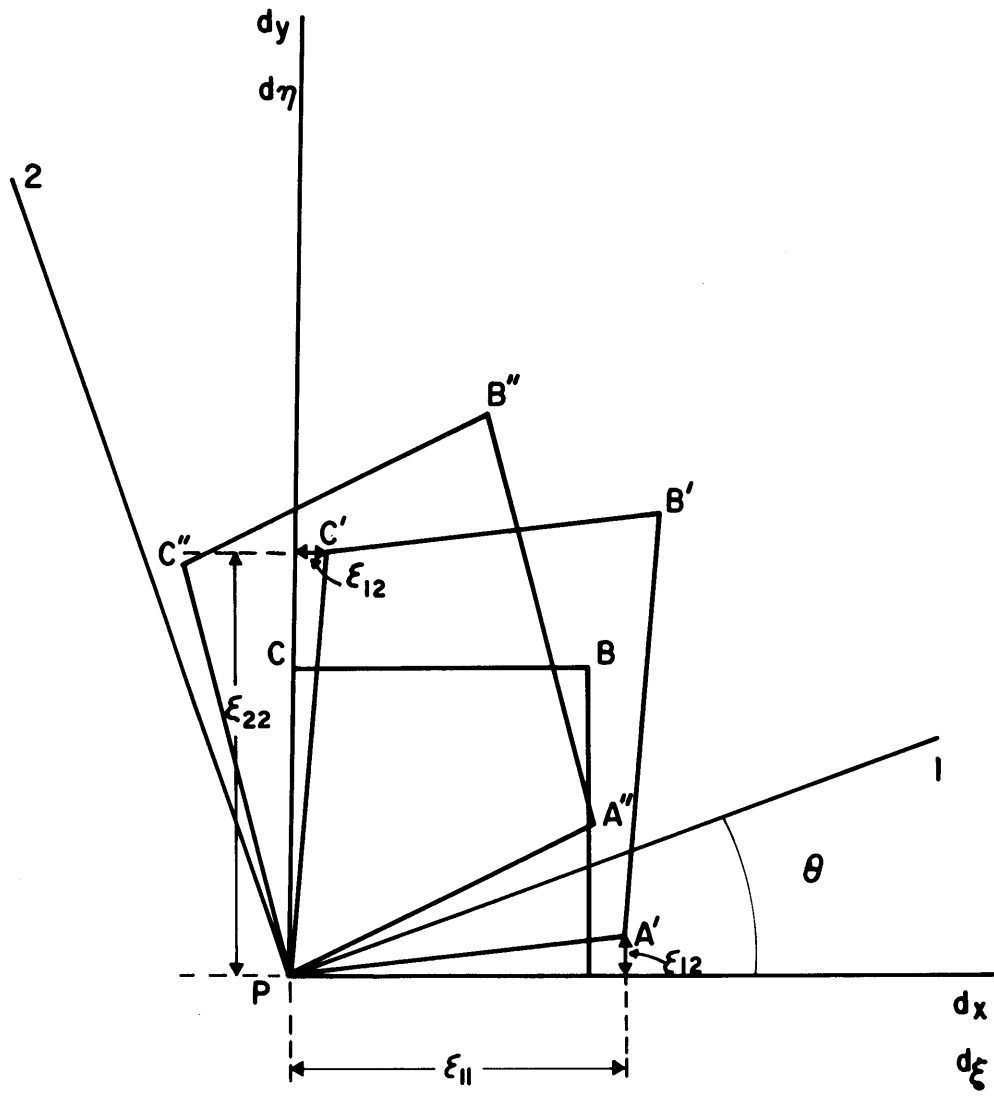


FIGURE B.1 : PURE STRAIN

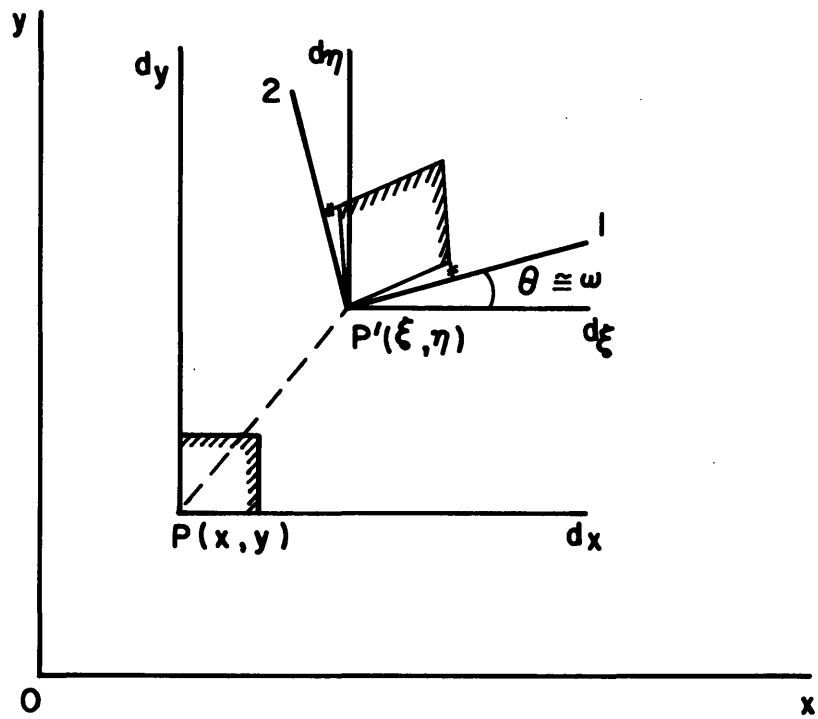


FIGURE B.2 : LOCAL TRANSLATION ,ROTATION AND PURE STRAIN

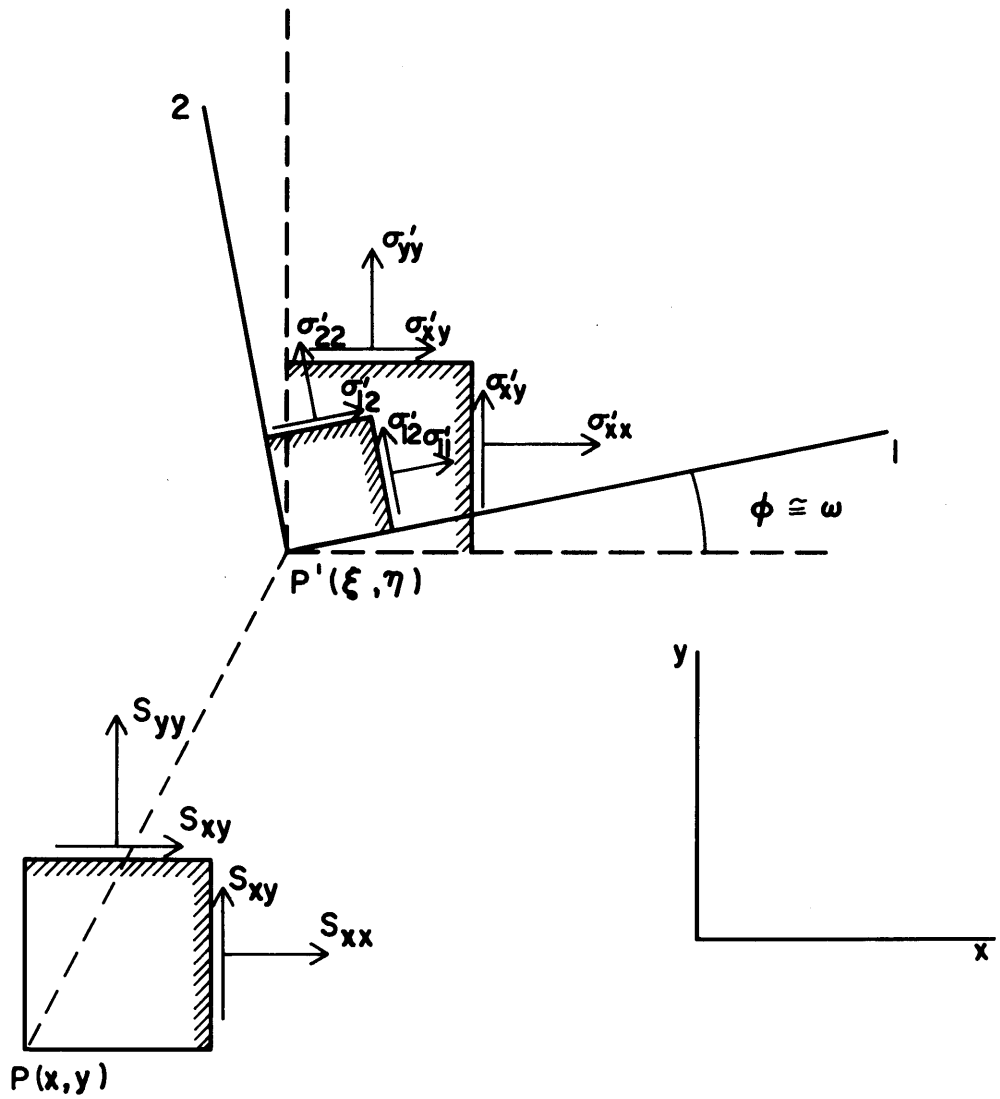


FIGURE B.3 : REPRESENTATION OF THE INITIAL STRESSES S_{xx} , S_{yy} , S_{xy} AND THE FINAL STRESSES WITH RESPECT TO THE TWO SETS OF AXES.

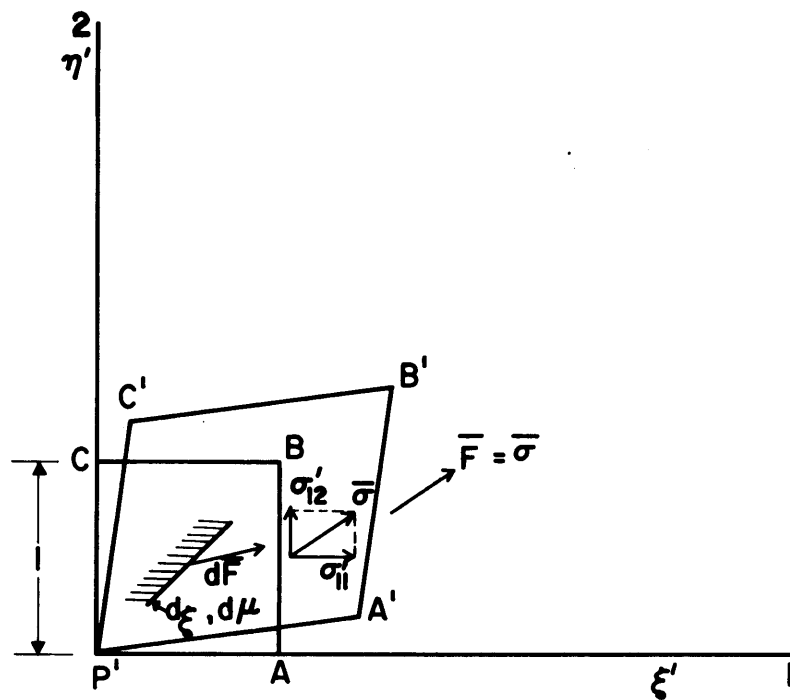


FIGURE B.4 : COMPONENTS OF FORCE IN AN INFINITESIMAL ELEMENT

Appendix C

DERIVATION OF THE STIFFNESS MATRIX

To derive the stiffness matrix equivalent to Equation (4-2), it is necessary to create a coordinate system in each element such that the strains in the element can be expressed as a function of the displacement of the nodal points.

In an effort to obtain symmetry, a natural coordinate system is used. In Figure C.1, x, y represent the global coordinate system, and a_i, b_i are the global dimensions of the triangle; each point in the triangle is represented by three numbers, two of them independent.

The numbers are

$$g_1 = \frac{A_1}{A}, \quad g_2 = \frac{A_2}{A}, \quad g_3 = \frac{A_3}{A} \quad (C-1)$$

where A is the area of the element

$$A = V_0 \quad (C-2)$$

and A_1, A_2, A_3 the areas of the triangles in which the element is divided by the represented point and the nodes.

Of course

$$g_1 + g_2 + g_3 = 1 \quad (C-3)$$

The equations of the sides are

$$\begin{array}{ll}
\text{Side 1 2} & g_3 = 0 \\
\text{Side 2 3} & g_1 = 0 \\
\text{Side 3 1} & g_2 = 0
\end{array} \tag{C-4}$$

and the coordinates of the nodal points are

$$\begin{array}{ll}
\text{N.P. 1:} & g_1 = 1, g_2 = 0, g_3 = 0 \\
\text{N.P. 2:} & g_1 = 0, g_2 = 1, g_3 = 0 \\
\text{N.P. 3:} & g_1 = 0, g_2 = 0, g_3 = 1
\end{array} \tag{C-5}$$

Values of $g_i = \text{constant}$ represent lines parallel to sides jk , etc. The coordinate system is invariant in linear transformations, homogeneous, and dimensionless.

The relation between global coordinates and natural triangular coordinates are (Felippa, 1965)

$$\begin{bmatrix} 1 \\ x \\ y \end{bmatrix} = \begin{bmatrix} 1 & 1 & 1 \\ x_1 & x_2 & x_3 \\ y_1 & y_2 & y_3 \end{bmatrix} \begin{bmatrix} g_1 \\ g_2 \\ g_3 \end{bmatrix} \tag{C-6}$$

$$\begin{aligned}
\begin{bmatrix} g_1 \\ g_2 \\ g_3 \end{bmatrix} &= \frac{1}{2A} \begin{bmatrix} x_2 y_3 - x_3 y_2 & y_2 - y_3 & x_3 - x_2 \\ x_3 y_1 - x_1 y_3 & y_3 - y_1 & x_1 - x_3 \\ x_1 y_2 - x_2 y_1 & y_1 - y_2 & x_2 - x_1 \end{bmatrix} \begin{bmatrix} 1 \\ x \\ y \end{bmatrix} \\
&= \frac{1}{2A} \begin{bmatrix} 2A_{23} & b_1 & a_1 \\ 2A_{31} & b_2 & a_2 \\ 2A_{12} & b_3 & a_3 \end{bmatrix} \begin{bmatrix} 1 \\ x \\ y \end{bmatrix} \tag{C-7}
\end{aligned}$$

where $2A = a_j b_i - b_j a_i$, where j is the next node to i when going counterclockwise around the element. A_{ij} are defined in (C-7).

From Equation (C-7)

$$\frac{\partial g_i}{\partial x} = \frac{b_i}{2A}$$
$$\frac{\partial g_i}{\partial y} = \frac{a_i}{2A}$$
(C-8)

and then

$$\frac{\partial}{\partial x} = \frac{1}{2A} \left(b_1 \frac{\partial}{\partial g_1} + b_2 \frac{\partial}{\partial g_2} + b_3 \frac{\partial}{\partial g_3} \right)$$
$$\frac{\partial}{\partial y} = \frac{1}{2A} \left(a_1 \frac{\partial}{\partial g_1} + a_2 \frac{\partial}{\partial g_2} + a_3 \frac{\partial}{\partial g_3} \right)$$
(C-9)

The displacement of any point in the triangle can be expressed as a linear function of the displacements in the nodes; if u and v are the horizontal and vertical components of the displacement respectively

$$u = u_1 g_1 + u_2 g_2 + u_3 g_3$$
$$v = v_1 g_1 + v_2 g_2 + v_3 g_3$$
(C-10)

if

$$[u] = \begin{bmatrix} u_1 \\ u_2 \\ u_3 \end{bmatrix}$$
$$[v] = \begin{bmatrix} v_1 \\ v_2 \\ v_3 \end{bmatrix}$$
(C-11)

$$[g] = \begin{bmatrix} g_1 \\ g_2 \\ g_3 \end{bmatrix}$$

then

$$u = [g]'[u] = [u]'[g] \quad (C-12)$$

$$v = [g]'[v] = [v]'[g]$$

The same equations are used for virtual displacement if δu is substituted instead of u and δv instead of v .

From Equations (2-43) and (C-9)

$$e_{xx} = \frac{1}{2A} \left(b_1 \frac{\partial u}{\partial g_1} + b_2 \frac{\partial u}{\partial g_2} + b_3 \frac{\partial u}{\partial g_3} \right) \quad (C-13)$$

but the value of u is given by (C-10), then

$$e_{xx} = \frac{1}{2A} (b_1 u_1 + b_2 u_2 + b_3 u_3) \quad (C-14)$$

or, in matricial form

$$e_{xx} = \frac{1}{2A} [u]'[b] = \frac{1}{2A} [b]'[u] \quad (C-15)$$

if

$$[b] = \begin{bmatrix} b_1 \\ b_2 \\ b_3 \end{bmatrix} \quad [a] = \begin{bmatrix} a_1 \\ a_2 \\ a_3 \end{bmatrix} \quad (C-16)$$

In a similar form

$$\begin{aligned} e_{yy} &= \frac{1}{2A} [v]'[a] \\ e_{xy} &= \frac{1}{4A} ([v]'[b] + [u]'[a]) \\ \omega &= \frac{1}{4A} ([v]'[b] - [u]'[a]) \end{aligned} \quad (6-17)$$

Similar expressions with δu , δv would give δe_{ij} .

Always:

$$[v]'[b] = [b]'[v] \quad \text{etc.} \quad (\text{C-18})$$

From equations (B-48)

$$\begin{aligned} \delta \eta_{xx} &= \omega \delta \omega + e_{xy} \delta \omega + \delta e_{xy} \omega \\ \delta \eta_{yy} &= \omega \delta \omega - \delta e_{xy} \delta \omega - \delta e_{xy} \omega \\ \delta \eta_{xy} &= \frac{1}{2} [\delta \omega (e_{yy} - e_{xx}) + \frac{1}{2} \omega (\delta e_{yy} - \delta e_{xx})] \end{aligned} \quad (\text{C-19})$$

If the expressions for e_i , ω , δe_{ij} and $\delta \omega$ from Equations (C-17) are introduced in (C-19), and each $\delta \eta$, multiplied by S_{ij} and all the terms added up to obtain Equation (4-5), then after ordering the terms

$$\begin{aligned} S_{ij} \delta \eta_{ij} &= \frac{1}{16A^2} [(3S_2 - S_1) u'a a' \delta u + 2S_3 u'ba' \delta u \\ &\quad + 2S_3 u'ab' \delta u + (3S_1 - S_2) v'b b' \delta v \\ &\quad + 2S_3 v'ba' \delta v + 2S_3 v'ab' \delta v \\ &\quad - (S_1 + S_2) u'ab' \delta v - 2S_3 u'b b' \delta v \\ &\quad - 2S_3 u'a a' \delta v - (S_1 + S_2) v'ba' \delta u \\ &\quad - 2S_3 v'b b' \delta u - 2S_3 v'a a' \delta u] \end{aligned} \quad (\text{C-20})$$

where v' , u' , v , u , b , b' , a , a' stand for $[u]'$, $[u]'$, $[v]$, etc.; $S_1 = S_{xx}$, $S_2 = S_{yy}$ and $S_3 = S_{xy}$.

The different matrices in Equation (4-3) are

$$[U] = \begin{bmatrix} [u] \\ [v] \end{bmatrix}, \quad [\delta U] = \begin{bmatrix} [\delta u] \\ [\delta v] \end{bmatrix} \quad (\text{C-21})$$

The product $e_{kl} C_{ijkl} \delta e_{ij}$ can be expressed as

$$[e_{xx} \ e_{yy} \ \gamma_{xy}] [C] \begin{bmatrix} \delta e_{xx} \\ \delta e_{yy} \\ \delta \gamma_{xy} \end{bmatrix} \quad (C-22)$$

where $\gamma_{xy} = 2e_{xy}$ and C is a matrix such that

$$[e_{xx} \ e_{yy} \ \gamma_{xy}] [C] = [\sigma_{xx} \ \sigma_{yy} \ \sigma_{xy}] \quad (C-23)$$

From Equation (3-3)

$$[C] = \begin{bmatrix} B + \frac{4}{3}G & B - \frac{2}{3}G & 0 \\ B - \frac{2}{3}G & B + \frac{4}{3}G & 0 \\ 0 & 0 & G \end{bmatrix} \quad (C-24)$$

From Equation (C-17) and (C-21)

$$\begin{matrix} \begin{bmatrix} e_{xx} \\ e_{yy} \\ \gamma_{xy} \end{bmatrix} \\ (3 \times 1) \end{matrix} = \begin{matrix} \begin{bmatrix} [b]' & [0] \\ [0] & [a]' \\ [a]' & [b]' \end{bmatrix} \\ (3 \times 6) \end{matrix} \quad [U] \frac{1}{2A} \quad (C-25)$$

Therefore, the (3x6) matrix is [B] in Equation (4-3),

$$[B] = \begin{bmatrix} b_1 & b_2 & b_3 & 0 & 0 & 0 \\ 0 & 0 & 0 & a_1 & a_2 & a_3 \\ a_1 & a_2 & a_3 & b_1 & b_2 & b_3 \end{bmatrix} \frac{1}{2A} \quad (C-26)$$

Equation (C-20) can be written as

$$\frac{1}{16A^2} [u' \ a' \ b' \ v' \ a' \ v' \ b'] \begin{bmatrix} (3S_{yy} - S_{xx}) & 2S_{xy} & -2S_{xy} & -(S_{xx} + S_{yy}) \\ 2S_{xy} & 0 & 0 & -2S_{xy} \\ -2S_{xy} & 0 & 0 & 2S_{xy} \\ -(S_{xx} + S_{yy}) & -2S_{xy} & 2S_{xy} & (3S_{xx} - S_{yy}) \end{bmatrix} \begin{bmatrix} a' \delta u \\ b' \delta u \\ a' \delta v \\ b' \delta v \end{bmatrix}$$

(1x4) (4x4) (4x1)

(C-27)

So the center (4x4) matrix is [S] in (4-3). The matrix D in (4-3) will be

$$\begin{bmatrix} a' \delta u \\ b' \delta u \\ a' \delta v \\ b' \delta v \end{bmatrix} = \begin{bmatrix} a' & 0 \\ b' & 0 \\ 0 & a' \\ 0 & b' \end{bmatrix} [\delta U]$$

(4x1) (4x6) (6x1)

(C-28)

So

$$[D] = \frac{1}{8A} \begin{bmatrix} a_1 & a_2 & a_3 & 0 & 0 & 0 \\ b_1 & b_2 & b_3 & 0 & 0 & 0 \\ 0 & 0 & 0 & a_1 & a_2 & a_3 \\ 0 & 0 & 0 & b_1 & b_2 & b_3 \end{bmatrix}$$

(C-29)

And $[K_c]$ and $[K_g]$ for each element are given by Equation (4-6).

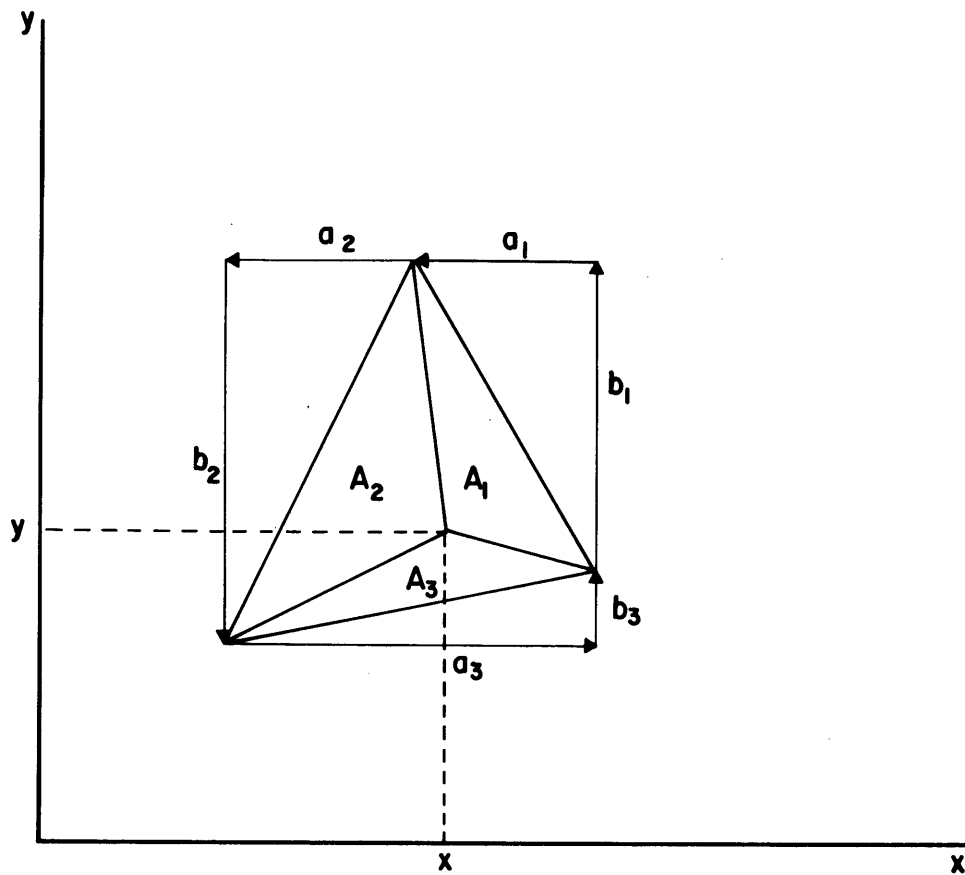


FIGURE C.1 : NATURAL TRIANGULAR COORDINATES

Appendix D

ADJUSTMENT OF STRESSES TO YIELD SURFACE

When the maximum shear stress calculated by the program is larger than the corresponding maximum shear at yielding, the stresses have to be adjusted back to the yield surface.

In two dimensions, the Mohr's circle provides a useful representation of the stress and the yield surface. Instead of the Mohr-Coulomb yield surface, a yield surface defined by the corresponding points of maximum shear stress at yielding is used (Fig. D.1)

$$\begin{aligned} \alpha &= \arctan (\sin \phi) \\ a &= c (\cos \phi) \end{aligned} \tag{D-1}$$

for $\phi = 0$ $c = k$, the Tresca yield surface is obtained. $\alpha = 0$, $a = c = k$, are the corresponding parameters.

So, in the general case, from Figure D.1 and geometric considerations, if the adjustment is made perpendicular to the pseudo yield surface:

$$\begin{aligned} \tau^* &= \tau - (\tau - k) \cos^2 \alpha \\ p^* &= p - (\tau - k) \cos \alpha \sin \alpha \end{aligned} \tag{D-2}$$

where τ^* is the modified maximum shear, k is the corresponding value of the maximum shear at yielding, p^* is the modified value of p , and:

$$p = \frac{\sigma_1 + \sigma_3}{2} = \frac{\sigma'_{xx} + \sigma'_{yy}}{2} \quad (D-3)$$

From the modified values τ^* and p^* , it is impossible to obtain uniquely the modified values of σ'_{xx} , σ'_{yy} , σ'_{xy} , if no further condition is imposed. The other condition is that the principle planes do not rotate.

The angle θ is the angle between the vertical direction and the direction of the minor principal stress, (remember that continuum mechanics convention is being used).

The values of σ'_{xx} , σ'_{yy} , σ'_{xy} , are then

$$\begin{aligned} \sigma'_{xx} &= p^* + \tau^* \cos 2\theta \\ \sigma'_{yy} &= p^* - \tau^* \cos 2\theta \\ \sigma'_{xy} &= \tau^* \sin 2\theta \end{aligned} \quad (D-4)$$

where τ^* is always positive, the sign of the shear stress is always the sign of θ .

If, in Equations (D-2) $\alpha = 0$:

$$\begin{aligned} \tau^* &= k \\ p^* &= p \end{aligned} \quad (D-5)$$

because before modification

$$\tan 2\theta = \frac{\sigma'_{xy}}{\frac{\sigma'_{xx} - \sigma'_{yy}}{2}} \quad (D-6)$$

$$\cos 2\theta = \frac{\frac{\sigma'_{xx} - \sigma'_{yy}}{2}}{\tau} \quad (D-6)$$

$$\sin 2\theta = \frac{\sigma'_{xy}}{\tau}$$

Equation (D-4) becomes, considering (D-3), (D-5), and (D-6)

$$\sigma'_{xx}^* = \frac{\sigma'_{xx}}{2} \left(1 + \frac{\tau^*}{\tau}\right) + \frac{\sigma'_{yy}}{2} \left(1 - \frac{\tau^*}{\tau}\right)$$

$$\sigma'_{yy}^* = \frac{\sigma'_{xx}}{2} \left(1 - \frac{\tau^*}{\tau}\right) + \frac{\sigma'_{yy}}{2} \left(1 + \frac{\tau^*}{\tau}\right) \quad (D-7)$$

$$\sigma'_{xy}^* = \sigma'_{xy} \frac{\tau^*}{\tau}$$

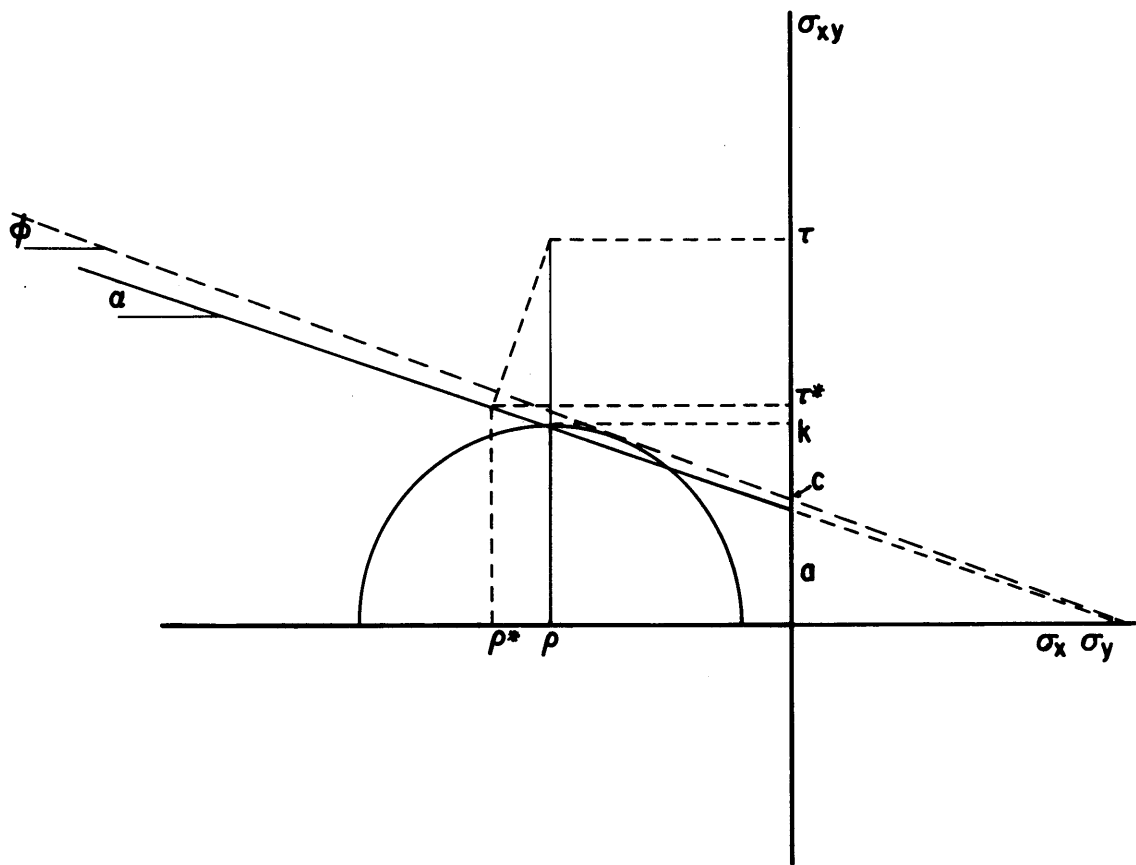


FIGURE D.1 : ADJUSTMENT OF STRESSES

Appendix E

USER'S MANUALS

Computer Programs

FELSP

FELSH

MASSACHUSETTS INSTITUTE OF TECHNOLOGY
DEPARTMENT OF CIVIL ENGINEERING
DIVISION OF SOIL MECHANICS

PROGRAM NAME "FELSH"
"FELSP"
LANGUAGE FORTRAN IV-G LEVEL
DATE JULY 1971
PROGRAMMER RODRIGO MOLINA

DESCRIPTION

These are two Finite Element programs for the analysis of Large Strains in Soils in plane strain loading. FELSH uses an incremental constitutive equation based in a Hyperbolic stress-strain relation, FELSP uses the constitutive equations of a perfectly Plastic Tresca material. FELSH will handle drained or undrained cases, FELSP will handle undrained cases; both programs do a total stress analysis. The procedure is incremental, and a middle point integration is carried in each increment. Although this integration is optional and direct solution in each increment as well as various iterations may be done, the recommended procedure is a single middle point integration.

Elements are constant strain quadrilaterals. No triangular elements can be handled by the program, but two sides of the quadrilateral may be in the same straight line; the resulting initial shape of the element will then be a triangle, while the program will treat it as a quadrilateral. The use of such elements should be avoided if possible, and they should be restricted to low deformation zones, in order to avoid negative areas in the triangular subelements that form the quadrilateral.

The geometry and state of stress is updated after each increment. Because of the updating of post failure stresses, increments should be kept small. Better results are obtained with coarser grids and more increments than with fine grids and less increments for the same computing time.

The sign convention is the continuum mechanics sign convention. Axis X or R is horizontal, positive to the right; axis Y or Z goes in a vertical, positive direction upward. Force, strain and displacement components are positive if they are in the direction of the positive axis when applied to a face whose normal is positive. (That is, tension is positive.) Angles are positive counterclockwise.

Subroutines MODIFY and BANSOL were taken directly from program FEAMOC written by A. Hagmann, and are based

on E.L. Wilson's routines in FEAST-1.

The program operates in double precision.

PROGRAM CAPABILITIES

The program incorporates a data generating facility, whereby the amount of input is reduced. Material properties can be input element by element or as layered systems. The program provides printed and punched output. With the later as input, the program CONTRPLT-ALFRED-M plots the data on a STROMBERG-CARLSON 4020.

Printed output includes:

1. Input and generated data
2. Displacements and forces at the nodal points
3. Stresses and yielding information at the center of the elements
4. Error messages, control information and value of highest residual in the inversion of the stiffness matrix.

Punched output provides:

1. Plots of initial and distorted structure mesh
2. Plots of stress contours
3. Load-deformation curves at specified nodes.

INPUT DATA FORMAT: (Both programs)

- A. Title Card, Format (18A4)

Any information in columns 1 through 72 will be reprinted at the top of the output. This card must be provided.

B. Control Information Card, Format (7I5)

Column	Information
1-5	Number of Nodal Points, (300 max)
6-10	Number of Elements, (250 max)
11-15	Number of Materials (10 max) (Leave this field blank if the material properties are input by layers)
16-20	Number of Horizontal Layers (10 max) (Leave this field blank if the material properties are input by elements)
21-25	Number of Load Increments
26-30	Number of Iterations 1 for normal use 0 for no middle point integration n for n middle point integrations
31-35	Plotting Indicator (NPLOT) NPLOT = 1 output prepared for SC4020 NPLOT = 0 if no plots are required

C. Soil Properties Information

Two options are available

1. Soil Properties Input by Elements

One set of two (or three) cards must be provided for each different material, each set consists of:

C.1.1 Initial Stress Card, Format (I5,2F 10.0)

Column	Information
1-5	Material Identification Number
6-15	Initial Z Stress (vertical)
16-25	Initial R Stress (horizontal)

C.1.2 Material Properties

(see cards C.2.2.2)

2. Soil Properties Input by Layers

One card describes the surface, then a set of two (or three) cards must be provided for each layer.

C.2.1 Surface Card, Format (2F 10.0)

Column	Information
1-10	Z coordinate of Surface
11-20	Initial vertical stress at the surface

(remember the sign convention)

Set of cards for each layer

C.2.2.1 Initial stress card, Format (4F 10.0)

Column	Information
--------	-------------

1-10	Z Coordinate of Base of this Layer
11-20	Total Unit Weight of Soil, γ_t
21-30	Lateral Stress Ratio at Rest, K_0
31-40	Final Value of Skempton's Parameter, A_f if FELSP A_f = blank if drained case A_f = 0 if O.C. clay A_f =0 if N.C. clay and the data comes from anisotropically consolidated tests A_f =1 if N.C. clay and the data comes from isotropically consolidated tests A_f = its measured value.

C.2.2.2 Material Properties

Different information has to be input for FELSP and FELSH.

FELSP Material Properties Card, Format

(4F 10.0)

Column	Information
1-10	Shear Modulus, G
11-20	Bulk Modulus, B

21-30 Yield Constant, $k=c=S_u$

31-40 Poisson's Ratio, ν

FELSH Material Properties Card, 2 cards

Card One Format (7F 10.0)

Column	Information
1-10	Cohesion, c (passive test)
11-20	Cohesion, c (active test)
21-30	Friction Angle, ϕ (in radians)
31-40	Atmospheric Pressure, p_a
41-50	Bulk Modulus Number, K_B
51-60	Poisson's Ratio, ν
61-70	Ultimate Shear Modulus, G_{ult}

Card Two, Format (8F 10.0)

Column	Information
1-10	Modulus Number, K' (passive)
11-20	Modulus Number, K' (active)
21-30	Unloading Modulus Number, K_u (passive)
31-40	Unloading Modulus Number, K_u (active)
41-50	Failure Ratio, R_f (passive)
51-60	Failure Ratio, R_f (active)
61-70	Variation Rate Exponent, n' (passive)

n' (active)

See Chapter 3 and Table E.1 for description of parameters.

D. Nodal Point Cards, (2I5, 4F 10.0)

One card for each nodal point. The cards must be input in increasing order of number of nodal points. If cards are omitted, the omitted nodal points are generated at equal intervals along a straight line between the defined nodal points. All such generated points will have no load on them. All displacements and loads in the positive direction of the axes should be input as positive.

Column	Information
1-5	Nodal Point Number
9	String Information Number J
10	Loading Code (ICODE) indicates whether displacements or forces are to be specified
11-20	X coordinate
21-30	Z coordinate
31-40	UX } These forces/displacements UZ } acting on unit thickness are
41-50	

If ICODE in column 10 is:

- 0 { UX is a force
UZ is a force
- 1 { UX is a X-displacement
UZ is a force
- 2 { UX is a force
UZ is a Z-displacement
- 3 { UX is a X-displacement
UZ is a Z-displacement

If J in column 9 is:

- 0 The string of nodal points that finish in this nodal point will have an ICODE = 0.
- 1 The ICODE in the string will be the same as it is in the last nodal point.

E. Element Cards, Format (6I5)

One card for each element. The cards must be input in order of increasing element number. If cards are omitted, elements will be generated by adding one to each node number of the preceding element. The material numbers are kept constant in the generation. The last element card must always be supplied.

Column	Information
1-5	Element Number
6-10	Node Number I
11-15	Node Number J

16-20	Node Number K
21-25	Node Number L
26-30	Material Number

Number the nodes counterclockwise around the element.

The maximum difference between node numbers for any element must not exceed 24.

If material properties are input in layers, Columns 26-30 are left blank (any information existing in these columns will be ignored).

F. Plotting Information Cards

The following three cards are used only if plots are requested (NPLOT = 1 in Columns 31-35, Card B.)

F.1 Instruction Card, Format (2I5, F 10.0)

The nodes at the ends of straight lines on the boundaries are called Boundary Nodes. All nodal points on the boundaries with ICODE = 0, and any other node that can have displacements out of the initially straight boundary are Boundary Nodes.

Columns	Information
1-5	Number of Boundary Nodes (NUMBN max. 50)
6-10	Load Displacement Plot Code (LODE)
11-20	Maximum Load (TLOAD). This

value must be specified only when the load-deformation plots are to be scaled for larger loads than the maximum applied in the problem. TLOAD will then determine the right hand side of the graph.

If LODE (Card F.1)

= 0 No load displacement plots required
≠ 0 |LODE| is the number of plots required

If LODE is:

> 0 Displacements will be plotted against the value of QNOW (Card G.1)

< 0 If NUMBN :

>0 Displacements will be plotted against the value of the total vertical force acting in any surface with displacements different than 0.

<0 In this case, the total force in the moving surface, against which displacements are plotted is the horizontal force.

F.2 Boundary Cards, Format (16I5)

The numbers of the boundary nodes are listed up to NUMBN nodes (16 nodes per card, max. 53). Numbers of the nodes have to be given in counterclockwise order.

F.3 Load Displacement Plots, Format (8I5)

Only if LODE \neq 0

The number of the nodes at which a load - displacement curve is required (LODEC (I)) have to be input in this card, (max 8).

If LODEC (I) is:

- > 0 the plotted displacement at nodal point
LODEC (I) is the vertical displacement, v.
- < 0 plotted displacements at nodal point
|LODEC(I)| will be the horizontal
displacements, u.

G. Load Increment Cards

Load increment cards must be in the same order in which the load is applied. The program multiplies the incremental load (or displacement)- that is, the difference between successive specified loads (or displacements)- by the UX and UZ figures specified in Card D, and solves for the incremental nodal displacement field caused by this load (or displacement).

One set of two cards must be provided for each increment. If cards are omitted, the information is generated for equal size load increments between two given sets.

G.1 Load Card Format (I5,F 10.0,I3,I2)

Column	Information
1-5	Load Increment Number
6-15	Total Load or Displacement (QNOW). This is not the incremental value but the total value.
18	Generated Data Code, JJ.
19-70	Output Specification Code, NCODE

If NCODE is:

- = 0 only printed output is obtained in this increment.
- = 1 printed and punched output is generated.
- = -1 no output for this load increment

If JJ is:

- = 0 NCODE = 0 in the generated load data
- = 1 NCODE in the generated data is equal to NCODE in this first increment after the generated data.

G.2 Plot Control Card, Format (2F5.0, 6F10.0)

This card is used only if plots are requested for the current load increment (NCODE = 1)

Column	Information
1-5	Distortion factor for displaced mesh, SMSH. Displacements are multiplied by this factor to

	obtain an exaggerated plot.
6-10	Vector scale factor for principal stress plots, STRPLT. Value is length of largest vector in inches.
11-20	Sigma R contour plot code
21-30	Sigma Z contour plot code
31-40	Tau RZ contour plot code
41-50	Sigma Maximum contour plot code
51-60	Sigma Minimum contour plot code
61-70	Tau Maximum contour plot code

For all plots:

0. or blank - no plots desired

Negative value of DMSH;

only distorted mesh will be punched and plotted.

The contour codes are interpreted as:

positive value - is the interval between contours

negative value - is the number of desired

contours. The plotting program
will find a suitable, rounded
interval.

If NCODE = 1, all stress data are punched, even though no stress plots are wanted (because plotting is controlled in CONTRPLT-ALFRED-M). In the case where only the deformed mesh plot is required, this unnecessary punch can be

avoided by putting a negative sign in front of the distortion factor DMSH.

PROGRAM USE

The program has a length of approximately 450 K Bites. External temporary storage is necessary in logical units 1 and 2. In the IBM 360-65/40 under ASP/MVT at the IPC, MIT, the control cards for logical units 1 and 2 are:

```
//G.FT01F001 DD UNIT=SYSDA,SPACE=(3000,(100,50)),
```

```
DCB=BLKSIZE=3000
```

```
//G.FT02F001 DD UNIT=SYSDA,SPACE=(3000,(100,50)),
```

```
DCB=BLKSIZE=3000
```

inserted before the //G.SYSIN DD * card. The source deck has been punched on the 029 Key Punch (EBCDIC).

Any number of problems can be submitted in the same job. If a job is flushed because of errors, the next one will be executed. Problems must be separated by a card with ****(A4) in the first four columns. The last problem should have two consecutive four star cards at the end.

	DRAINED	UNDRAINED	
		N. C. CLAY (1)	O. C. CLAY
C (PASSIVE)	Cohesion, same value for both	S_u / σ_c (pass.)	Average S_u for layer (pass.)
C (ACTIVE)		S_u / σ_c (active)	Average S_u for layer (active)
ϕ	its value	0	0
P_d	Units should be chosen so $P_d = 1$		
K_B	(2)	B / σ_c	Average B for layer
ν	its value	0.5	0.5
σ_{ult}	0.002 $K_B < \sigma_{ult} < \text{Smallest } K(1 - R_f)^2$		
K' (pass. and act.)	(2)	G_i / σ_c	Average G_i for layer
K'_u (pass. and act.)	(2)	G_u / σ_c	Average G_u for layer
R_f	(2)	(2)	(2)
n'	(2)	1.0	1.0

(1) σ_c is the vertical consolidation stress if the data is from anisotropically consolidated tests.

(2) See description of the Hyperbolic Approximation (Chapter 3)

TABLE E - 1

Appendix F

PROGRAM DESCRIPTION, MAIN AND SUBROUTINES

Both programs, FELSP and FELSH, have very similar logic, and many subroutines are common. The descriptions will apply for both programs except where specifically indicated.

MODIFY modifies the general equilibrium equations by introducing the specified displacements and boundary conditions.

It is only called by GESTF.

BANSOL solves the modified system of equilibrium equations for displacements by Gauss elimination.

It is only called by GESTF.

STIFFS assembles the instantaneous stiffness matrix for a triangular element with the expressions of Appendix C. The standard stiffness matrix is calculated first, then the geometric stiffness is calculated and added to obtain the total stiffness matrix.

It is only called by QUAD.

QUAD assembles the quadrilateral stiffness, by calling the subroutines MPROP and STIFFS, for each one of the four triangles. The statically condensed element stiffness is then calculated. Half way through the calculation, there is a logic check. SFLAG is the logical

variable, if it is:

TRUE : QUAD has been called from STRESS, and the result sought is a stage of the static condensation that allows the back-calculation of the center node displacements from the boundary nodal displacements; the displacements are necessary to calculate strains in the triangular elements.

FALSE : QUAD has been called from GESTF, and the static condensation is finished to obtain the statically condensed quadrilateral element stiffness.

GESTF assembles the general stiffness matrix by calling QUAD for each element.

It stores the matrix externally to allow back - calculation of forces.

It modifies the stiffness by calling MODIFY for each imposed displacement.

It stores the modified stiffness externally to allow the calculation of residuals.

It solves the system of equations by calling BANSOL.

It calculates residuals.

It recovers the force vector.

If midpoint integration is being done, logic variable IFLAG will be true for all steps but the one that

gives the final result for the increment.

If IFLAG is true:

no recovery of the force vector is done, and therefore no previous storage of the unmodified matrix is necessary;

values of displacements are halved.

GESTF is only called by MAIN.

MPROP is different for each program.

It calculates the constitutive equations, matrix [C] in Equation (4-3).

It is called by QUAD to calculate stiffness and by STRESS to back-figure stresses from strains.

FELSP MPROP has two parts.

1. Elastic constitutive equations are calculated.
2. If the element has yielded, the plastic terms of the constitutive equations are added to the elastic terms.

FELSH MPROP has also two parts.

1. The values of the two instantaneous elastic constants are calculated.
2. The incremental elastic constitutive equations are assembled.

In part 1, there are six different possibilities:

- a. By means of FI (or ϕ) = 0 or $\neq 0$ the case is classified as drained or undrained

- b. In any case, three situations are possible:
 - b.1 loading : $KSD(NV) = 0$ is the value of the control variable that indicates loading
 - b.2 unloading : $KSD(NV) = 1$ indicates unloading
 - b.3 post yield loading : if TAU is greater than or equal to VM , where TAU is the calculated value of τ , and where VM is the yielding value of the maximum shear stress at that moment.

STRESS

This subroutine is slightly different for each program, although both calculate the same things.

- a. By calling QUAD, it computes the displacements of the center nodal points for each element.
- b. A loop, DO 300, calculates for every element

- 1) The strains from displacements.

- 2) In FELSH, the strains from the middle point geometry to the new geometry are calculated at the same time if $FFLAG = FALSE$. $FFLAG$ is TRUE for the first step in each increment, and FALSE for the next ones.

In FELSP, the same instructions that calculate the normal strains calculate the mid-point to final strains

in a second cycle that is triggered by FFLAG, the control variable is NENA.

3) In FELSP, the control variable APES is made equal to 1 if there has been a change in the sign of the shear strain.

4) Incremental stresses referred to the old or middle point geometry are calculated from the normal strains with the help of MPROP.

5) Total stresses are found by adding the incremental ones to the initial stresses that are recovered in the case of mid-point integration.

6) The transformation of stresses is done and the stresses referred to the new geometry and normal axes are found, by using the strains from mid-point to final geometry if FFLAG = FALSE.

7) In FELSH, the angle that σ_3 forms with the vertical is found.

8) In FELSH, if there is change in the trend of τ (the maximum shear stress) the control variable NAPE is made equal to 1.

9) In both programs, if APES or NAPE are equal 1 and the loading law have been used in the program, the logic variable UFLAG is set as TRUE and PLAST or KSD for the element are set equal to NO or 1, respectively. This is in preparation for repeating the step with

different material properties for the element.

10) If the unloading-reloading law has been used, but the obtained stresses or strains are over the maximum recorded values, the variables PLAST or KSD are given the values YES and 0. In the case of FELSP, UFLAG is put equal to TRUE in order to repeat the step with a softer procedure.

11) In both programs, if the element is in failure, PLAST is made equal to YES and then the stress modification back to the yield surface is done.

12) If UFLAG is FALSE, the principal stresses are found. In FELSP IFLAG has to be FALSE also in order to obtain the principal stresses. The angle between σ_3 and the verticals is also found in FELSP

c. Total forces and displacements are found if UFLAG and IFLAG are FALSE

d. The original geometry is recovered if UFLAG and FFLAG are FALSE.

e. The coordinates of the nodal points are modified if UFLAG is FALSE

f. The coordinates of the center of the elements are found if UFLAG is FALSE.

g. If IFLAG and UFLAG are FALSE and NCODE ≥ 0 ,

1) the displacement and stresses are printed,

2) if NCODE = 1, the information is also punched.

h. If UFLAG is TRUE, the old values of stresses and the sign of the strain are recovered in order to repeat the step.

MAIN

The main program is also a little different for each version.

a. Control information, material properties and nodal point data are read, intermediate data is generated for nodal points. Data is printed.

b. Element data is read; missing data is generated. When the material properties are input in layers, every element is assigned to its corresponding layer. The initial stresses are calculated; in the case of FELSH, the initial principal stresses are also calculated as well as the initial angle of σ_3 with the vertical. In the case of FELSH, the values of the corresponding equivalent consolidation stress are also found. Data is printed.

c. Plotting data is read and printed. The required initial data is punched.

d. The band width is determined.

e. Variables are initialized.

f. A load increment is started by reading load

increment data; if necessary, intermediate data is generated.

- 1) Increment data is output.
 - 2) The initial values of stresses and nodal points coordinates are stored.
 - 3) The first step of the increment is run by calling GESTF and STRESS. If, at the end of STRESS, UFLAG is TRUE, the step is repeated. KAKO in FELSH counts the number of repetitions of the step in order to be able to limit the repetitions by conditioning the UFLAG = TRUE statement in STRESS to a given number of KAKO.
 - 4) If mid-point integration is done, one or several times (one or more iterations), the logical variables are arranged and again GESTF and STRESS are called, etc., as in part 3.
 - 5) When the last step of the increment is done, IFLAG is FALSE, and then, if load deformation plots are required, the information for the plots from the increment is prepared. Depending on the values and signs of the input information, the total incremental force, either horizontal or vertical, or the value of the increment load is given as well as the horizontal or vertical displacements of the selected points.
- g. When the last increment is run, the data

for the load deformation plots is punched.

h. If there are any more decks to be processed, they will be, even if the end of the program has been reached through an error and abnormal termination.

Appendix G

THE UNIT SQUARE

If A is the width of the deformed square and H the height, the incremental strains will be

$$de_x = \frac{du}{A} \quad (G-1)$$

$$de_z = \frac{dv}{H}$$

where

$$A = 1+u \quad (G-2)$$

$$H = 1+v$$

for the unit square.

The incremental stress will be at each moment

$$d\sigma_z = \frac{dP}{A} \quad (G-3)$$

where dP is the increment in the vertical load.

The instantaneous elastic relations will be for plane strain

$$\begin{aligned} de_z &= \frac{1}{E} (d\sigma_z - \nu(d\nu\sigma_z + (1+\nu)d\sigma_x)) \\ de_x &= \frac{1}{E} (d\sigma_x - \nu(1+\nu)d\sigma_z + \nu^2 d\sigma_x) \end{aligned} \quad (G-4)$$

but $d\sigma_x = 0$, so:

$$de_z = \frac{1}{E} (1-\nu^2) d\sigma_z = Y d\sigma_z \quad (G-5)$$

$$de_x = \frac{1}{E} (-\nu-\nu^2) d\sigma_z = X d\sigma_z$$

where

$$Y = \frac{1}{E} (1-\nu^2) \quad (G-6)$$

$$X = \frac{-1}{E} (v+v^2) \quad (G-6)$$

From (G-3), (G-1) and (G-5)

$$\frac{du}{A} = X \frac{dP}{A} \quad (G-7)$$

$$u = XP + C$$

for $P=0$ $u=0$, so $C=0$ and

$$u = XP \quad (G-8)$$

Also from (G-1), (G-3) and (G-5)

$$\frac{dv}{H} = Y \frac{dP}{A} \quad (G-9)$$

with (G-2)

$$\frac{dv}{1+v} = Y \frac{dP}{1+u} = Y \frac{dP}{1+XP} \quad (G-10)$$

and integrating

$$\ln(1+v) = \frac{Y}{X} \ln(1+XP) + C_1 \quad (G-11)$$

for $P=0$ $v=0$ and then $C_1 = 0$ so

$$v = (1+XP)^{Y/X} - 1 \quad (G-12)$$